Ontogenetic Correlation Between Muscle and Nervous System Novelties in a Neritimorph Gastropod

by

Samuel Ferguson
BSc, University of Victoria, 2011

A Thesis Submitted in Partial Fulfillment
of the Requirements for the Degree of

MASTER OF SCIENCE

in the Department of Biology

Supervisory Committee

Ontogenetic Correlation Between Muscle and Nervous System Novelties in a Neritimorph Gastropod

by

Samuel Ferguson
BSc, University of Victoria, 2011

Supervisory Committee

Dr. Louise Page (Department of Biology)
Supervisor

Dr. John Taylor (Department of Biology)
Departmental Member

Dr. Thurston Lacalli (Department of Biology)
Adjunct Departmental Member

Abstract

Supervisory Committee
Dr. Louise Page (Department of Biology)
Supervisor
Dr. John Taylor (Department of Biology)
Departmental Member
Dr. Thurston Lacalli (Department of Biology)
Adjunct Departmental Member

Hatching larvae of neritimorph gastropods have a bilateral set of both larval and pedal retractor muscles, which is unique among gastropod molluscs. Adults also display a novel connection ("shortcut") between the two pleural ganglia. To reconstruct the evolution of the novel shortcut between pleural ganglia and its functional role, I studied the development of the central nervous system and muscle innervation in three distinct larval and one post-metamorphic stages of *Nerita melanotragus* using light and transmission electron microscopy and surface-rendered three-dimensional reconstructions. My results revealed that the novel shortcut is derived from an ancestral nerve connective, which establishes an unconventional link between the ganglia that generate motor output to the bilateral set of larval and pedal retractor muscles to coordinate activity of these muscles. The unique characteristics of the shell, muscles and nervous system in *N. melanotragus* represent secondarily derived characteristics that co-evolved as an integrated functional unit.

Table of Contents

List of Tables

List of Figures

Acknowledgments

I would like to thank my supervisor, Louise Page, first and foremost, for introducing me to the weird and wonderful world of invertebrates and the marine intertidal. The enthusiasm and charisma that Louise displays in the classroom is matched only by her hard work and dedication in the lab. Louise not only shared with me her expertise, patience and dedication throughout both of my degrees, but also remains a personal role model as a scientist and teacher.

I would like to thank the other members of the lab, Hannah Westlake, Alicia Donaldson and Brenda Hookham for their support, ideas, and especially their company, which made every day fun and interesting.

I would like to thank Dorothy Paul whose generosity helped me during an unfortunate situation and allowed me to spend the last part of my degree focused exclusively on my research. I would also like to thank Brent Gowen for teaching me all of the techniques involved in using slot grids and for providing me with his valuable expertise on a daily basis throughout that process. I thank Maria Byrne at the University of Sydney, Australia for facilitating the larval culture work for this project. I would also like to acknowledge my funding through the NSERC discovery grant, NSERC CGS scholarship and the Dr. Arne H. Lane Graduate Fellowship in Marine Sciences.

My parents, Lisa Iannone and Jacques Ferguson, have been a source of unyielding support throughout my life and for that I am forever grateful and indebted. I would also like to thank Leah Mosoff, Gregory Earle, Alex Strong and Tom Iwanicki for they all, in their own way, have had a significant impact on my life throughout this process.

1.0 Introduction

The gastropod nervous system has been exceptionally significant in providing a foundation for pioneering work on the evolution of development (Garstang, 1929) and the neuronal basis of behaviour and learning (Kandel, 1976; Kovac *et al.,* 1985; Chase, 2002; Lorenzetti *et al.,* 2006; Benjamin *et al.,* 2008). A particularly intriguing aspect of gastropod nervous system development and evolution is that the tremendous diversification that has occurred during the evolution of the gastropods (Aktipis *et al.,* 2008), and the magnitude of nervous system variation across taxa (Haszprunar, 1988a, b), has occurred within a complex, biphasic life cycle. Individuals begin life as a planktonic larva that eventually settles and undergoes metamorphosis on the benthos to become a juvenile that grows into an adult. This is significant because the active larval, juvenile and adult stages of the same individual are exposed to different environmental conditions and may evolve different adaptations in response to different selection pressures (Marois and Carew, 1990). Thus, any modifications that are beneficial to the adult gastropod must form within the active, developing planktonic larva without disrupting its functionality. Conversely, any modifications that evolve to benefit the larva must either me modified for the adult phase, be at least neutral overall, or be destroyed at metamorphosis (Marois and Carew, 1990).

However, regardless of which life history stage may benefit from a novel or modified morphological trait, an important larger issue, and the subject of much recent research, is the question of how novel or modified structures arise during evolution. Novel structures can arise *de novo* from major innovations to the developmental program of the organism or from the ectopic activation/expression of pre-existing developmental pathways (Panganiban *et al.,* 1997). Similarly, smaller scale modifications to pre-existing developmental pathways can produce modified and potentially novel derivatives of pre-existing structures (Panganiban *et al.,* 1997). Nevertheless, in order for any trait to become modified or appear *de novo* in a descendant, it must be within the bounds of possibility for the developmental program of the ancestor. If a given characteristic cannot develop, it will not be presented to a selective environment no matter how beneficial the

change would be. For this reason, developmental studies on novel characteristics are a wonderful tool to gain insight into how new structures originated and evolved within a population.

Neritimorph gastropods possess a novel connection within their central nervous system (Bourne, 1908, 1911; Fretter, 1984), as well as two novel attributes within the two sets of shell-anchored muscles that form during development (Page and Ferguson, 2013). I hypothesize that the novel connection in the nervous system is a derived construct of an ancestral gastropod nerve connective and did not evolve *de novo*. I also hypothesize that this novel connection functions to coordinate the two sets of shell-anchored muscles present in the earliest larval stages, and is thus present in the adult as, at the very least, a neutral modification to the configuration of the central nervous system. Finally, I propose that the novel attributes of the shell muscles arose as a result of two documented modifications to the morphology of the shell that occurred over the course of the evolutionary history of the Neritimorpha.

As background to this subject, I provide a description of what is known about the evolutionary history of the neritimorph shell from fossil record data and a summary of current knowledge on the evolution and development of gastropod central nervous systems. I will also review how shell muscle number and morphology is tightly linked with shell morphology and summarize current knowledge on myogenesis in gastropods. A comprehensive understanding of these subjects behooves a preliminary discussion regarding the phylum Gastropoda and the neritimorph subclass in general.

1.1 The Neritimorpha

At 40,000 to 150,000 described species, the Gastropoda stands as the largest Class of molluscs and the second largest Class of Metazoans (Aktipis et al., 2008). They constitute 20% of all species in Recent marine ecosystems, but their peak abundance occurred 65 million years ago (mya)(Lindberg *et al.,* 2004; Frýda *et al.,* 2009). The Neritimorpha is one of the five major gastropod subclasses, although phylogenetic relationships among these subclasses continue to be controversial. Figure 1 shows a recent phylogenetic hypothesis generated from both molecular and morphological data

(Aktipis *et al.,* 2008).

Neritimorphs are distributed among two superfamilies, the Neritoidea and the Neritopsoidea (Fretter, 1965; Ponder, 1998; Bandel and Frýda, 1999). The Neritoidea is comprised of the Hydrocenidae, Helicinidae, Neritiliidae, Phenacolepadidae, and the Neritidae (Ponder, 1998; Kano *et al.*, 2002). The Neritopsoidea consists of only one family, the Neritopsidae (Ponder, 1998), containing the two living genera *Neritopsis* and *Titiscania;* the latter being a relatively recent inclusion based on 28S ribosomal RNA (rRNA) data (Kano *et al.,* 2002). Extant neritimorphs number only 450 species, which makes this a very small clade compared to the Caenogastropoda and Heterobranchia, but neritimorphs have colonized an impressive array of habitats within tropical and subtropical ecosystems (Lindberg, 2008). Many neritimorphs inhabit the marine intertidal and shallow subtidal zones, as well as freshwater lakes, rivers (Neritidae)(Lindberg, 2008) and terrestrial habitats, some even becoming arboreal (Hydrocenidae, Helicinidae) (Kano *et al.,* 2002; Lindberg, 2008). Others occupy more cryptic habitats such as submarine caves, subterranean cavities and deep sea hydrothermal vents and seeps (Neritiliidae, Phenacolepadidae, Neritopsidae)(Kase and Hayami, 1992; Kano *et al.,* 2002; Lindberg, 2008).

Neritimorphs have been exceptionally difficult to place phylogenetically. Traditionally, the Neritimorpha, Patellogastropoda, Vetigastropoda, Cocculiniformia (a small subclass of mostly deep sea gastropods), and Architaenioglossans (now placed within the Caenogastropoda) formed a basal clade known as the Archaeogastropoda (Thiele,1925; Wenz, 1938; Knight *et al.,* 1960; Haszprunar, 1987a). However, the Archaeogastropoda is no longer considered monophyletic (Hickman, 1988; Haszprunar, 1988a, 1993). Although some early authors recognized the Neritimorpha as a distinct lineage from the Archaeogastropoda, based on characteristics such as internal fertilization and a unique female reproductive system (Bourne, 1908; Yonge, 1947), this view was not generally accepted until the late 1980's (Lindberg, 2008). Subsequent morphology-based phylogenetic analyses have placed the Neritimorpha as sister to the Vetigastropoda (Sasaki, 1998; Salvini-Plawen and Haszprunar, 1987b), sister to a sub-clade of the Caenogastropoda (Haszprunar, 1985b), or sister to the rest of the Gastropoda except for the Patellogastropoda (Haszprunar, 1988a; Ponder and Lindberg, 1997; Aktipis *et al*.,

2008). Conversely, still other morphological studies suggest the Neritimorpha are sister to the Apogastropoda (a clade consisting of Caenogastropoda + Heterobranchia) (Bourne, 1908; Younge, 1947).

Phylogenetic analyses based on molecular data have been similarly variable regarding the position of the Neritimorpha within the Gastropoda. However, recent molecular phylogenies place the Neritimorpha as sister to the Apogastropoda (Harasewych *et al.,* 1998; Colgan *et al.,* 2003; Aktipis and Giribet, 2010; Kocot *et al.,* 2011; Castro and Colgan, 2010), a hypothesis also supported by cell lineage data (van den Biggelaar and Haszprunar, 1996; Lindberg and Guralnick, 2003). Furthermore, a sister relationship between Neritimorpha and Apogastropoda was resolved in phylogenetic analyses that combined morphological and molecular data (Fig. 1; McArthur and Harasewych, 2003; Aktipis *et al.,* 2008).

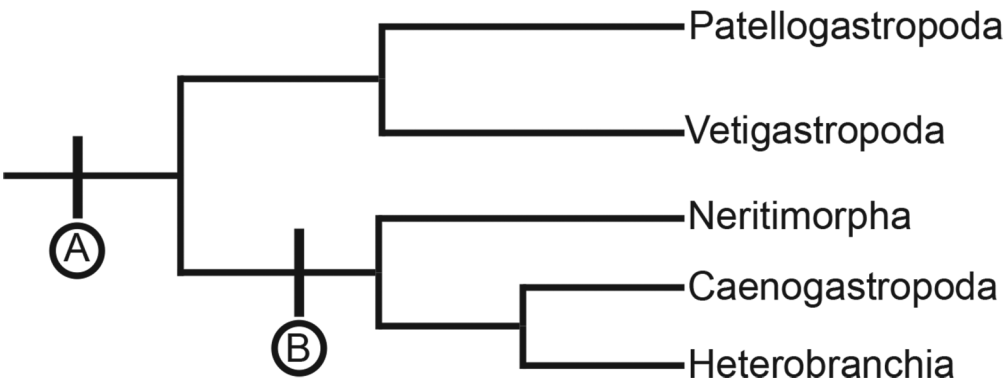

Figure 1. Current phylogeny of major gastropod clades as adapted from Aktipis *et al.* (2008). **A.** Lecithotrophic larva. **B.** Planktotrophic larva.

Much of the contention surrounding the phylogenetic placement of the Neritimorpha relates to the fact that neritimorphs share many anatomical characteristics with patellogastropods and vetigastropods, yet characteristics of reproduction and development are more similar to the caenogastropods (Bandel and Frýda, 1999). Indeed, the Neritimorpha is one of three gastropod sub-classes, along with the Caenogastropoda and Heterobranchia, that exhibit internal fertilization, package their eggs within complex

egg capsules, and undergo planktotrophic development, where small veliger larvae hatch from benthic egg capsules and spend weeks to months feeding in the water column before settling on the benthos and metamorphosing (Strathmann, 1985; Haszprunar *et al.,* 1995; Plaut *et al.,* 1995; Collin, 2001; Kano, 2006). Conversely, patellogastropods and vetigastropods broadcast spawn their gametes and fertilized eggs develop into short-lived, lecithotrophic veligers (Fretter and Graham, 1994; Haszprunar *et al.,* 1995). Consequently, the phylogenetic placement of the Neritimorpha has great implications for understanding gastropod life history evolution. If neritimorphs represent an early offshoot of the gastropod lineage, then planktotrophic development evolved at least two times within the Gastropoda. However, if the Neritimorpha is sister to the Apogastropoda, then planktotrophic development evolved once within the Gastropoda, which represents the more parsimonious hypothesis (Fig. 1).

The perplexing combination of plesiomorphic and synapomorphic anatomical characteristics exhibited by neritimorphs has made this clade exceptionally interesting to malacologists for over one-hundred years. Neritimorph characters that are scored as primitive within morphology-based phylogenetic treatments include: rhipidoglossate radula, a pair of hypobranchial glands (shared with vetigastropods) and a bipectinate ctenidium (shared with patellogastopods and vetigastropods) (Thiele, 1925; Fretter, 1965; Haszprunar, 1988a; Salvini-Plawen and Haszprunar, 1987). On the other hand, neritimorph characters shared with caenogastropods include the presence of only a single ctenidium and osphradium (Yonge, 1947), as well as ultrastructural characteristics of the osphradium (Haszprunar, 1985a).

Neritimorphs also display a number of uniquely derived traits, such as, distinctive sperm ultrastructure, unique buccal musculature and an apomorphic diaulic female reproductive system (Bourne, 1908; Ponder and Lindberg, 1997; Healy, 1988; Kano *et al.,* 2002). However, perhaps the most intriguing aspect of many neritimorphs is their egg-shaped shell, very large and heavily calcified operculum, and paired shell muscles. None of these structures are unique to neritimorphs; however, they coincide with a remarkable novelty involving the configuration of their central nervous system. Modifications in one character are often correlated with accommodating changes to other characters that form an integrated functional unit and thus changes within a single

character can have a substantial effect on the overall morphology of an organism (Darwin, 1859). Indeed, skeletons, muscles and nerves form an integrated functional unit. Therefore clues to understanding the novelty within the neritimorph nervous system may come from study of derived aspects of the neritimorph shell and muscle systems throughout ontogeny.

1.2 Neritimorph shells: morphology and evolution

Neritimorphs display diverse shell morphologies, ranging from tightly coiled with a well-defined spire (Hydrocenidae, Helicinidae) to limpet-shaped (Phenacolepadidae, some Neritiliidae), to completely lacking shells as adults (*Titiscania*) (Knight *et al.*, 1960; Ponder and Lindberg, 1997). However, the plesiomorphic shell condition for the Neritimorpha is one with a low spire, and a high whorl expansion rate, giving them a characteristic egg shape, which is exhibited by most extant neritimorphs, and all of the members of the Neritidae, the largest family (Kano *et al.*, 2002; Nützel *et al.,* 2007). Importantly, all neritoideans resorb the inner-whorls of both the protoconch (embryonic/larval shell) and teleoconch (adult shell), including the internal coiling axis known as the columella (Nützel *et al.,* 2007). Internal shell resorption produces a shell that is a hollow cup. Conversely, members of the Neritopsoidea do not resorb the inner shell whorls of their protoconch and teleoconch and retain their columella (Nützel *et al.,* 2007).

The fossil record of presumed neritimorphs extends back to at least the middle-Devonian (~375MYA) (Knight *et al.,* 1960; Batten, 1984) and possibly even the Ordovician (~500MYA) (Bandel and Frýda, 1999). Extant neritimorphs presumably descended from Palaeozoic naticopsids, an extinct neritimorph clade that possessed smooth, low-spired and non-convolute shells. This assertion is based on similarities in naticopsid shell morphology (Knight, 1933; Knight et al., 1960) and microstructure (Squires, 1976; Bandel *et al.,* 2002; Kaim and Sztajner, 2005; Nützel *et al.,* 2007) to Recent members of the Neritopsidae. Indeed, the Neritopsidae has the oldest fossil record of all the extant neritimorph families (Knight *et al.,* 1960; Batten, 1984; Bandel and Frýda, 1999; Bandel, 2000). Furthermore, protoconchs of both the Palaeozoic naticopsids

(extinct) and extant neritopsids retain the inner whorls of their shell (Nützel *et al.,* 2007; Frýda *et al.,* 2009).

Protoconch morphology may be stable over long time scales, and known patterns of early shell ontogeny in living gastropod groups have been used to infer taxonomic affiliations of fossil gastropod species (Frýda *et al.,* 2009). Protoconchs belonging to all extant neritimorphs exhibit a strongly convolute coiling pattern (Nützel *et al.,* 2007). Convolute coiling is produced when new whorls either partly or completely overgrow previous whorls, resulting in partial or complete internalization of the spire. Analyses of the fossil record suggest that convolute protoconchs characteristic of extant neritimorphs appear around the time of the Palaeozoic-Mesozoic split, most likely in the early Triassic (~250MYA) (Bandel and Frýda, 1999; Bandel 2007).

Protoconchs of both the Palaeozoic naticopsids and extant neritopsids retain the inner shell whorls, thereby suggesting that the convolute protoconch without resorption of internal shell walls exhibited by the Neritopsidae is ancestral for extant neritimorphs (Bandel, 2007; Nützel *et al.,* 2007). This further suggests that the convolute protoconch with resorbed inner-whorls is a relatively recent apomorphy of the neritimorph crown group (all families except for the Neritopsidae), as is the resorption of internal walls of the teleoconch (Frýda *et al.,* 2009).

1.3 Configuration of the gastropod central nervous system

Configuration of the nervous system has been used extensively in morphology-based phylogenetic analyses of gastropods, and at one time nervous system characters were regarded as the most significant for higher-level systematics (Haszprunar, 1988a, b). There are two major regions of the general adult gastropod nervous system, the esophageal nerve ring and the visceral loop (Fretter and Graham, 1962; Bullock and Horridge, 1965). The esophageal nerve ring surrounds the esophagus and, as shown in figure 2, consists of four pairs of interconnected ganglia: the cerebral, buccal, pedal and pleural ganglia. Each pair is connected to the others by cell-free nerve connectives (e.g. cerebro-pleural connective), and like-ganglia are connected to each other via commissures (e.g. cerebral commissure, pedal commissure) (Fig. 2; Fretter and Graham,

1962; Bullock and Horridge, 1965). The pleural ganglia, in contrast to all other ganglionic pairs that make up the esophageal nerve ring, do not have a discrete commissure, but are instead connected to each other by means of a long connective known as the visceral loop that projects posterodorsally and innervates organs of the mantle cavity and visceral mass (Bullock and Horridge, 1965). Two types of ganglia are situated along the visceral loop; two intestinal ganglia (the subintestinal and supraintestinal ganglion) and either one or multiple visceral ganglia (Fig. 2; Bullock and Horridge, 1965). Ganglia are identified by their connections to other ganglia and by their innervation targets, as these characteristics are generally conserved across the Gastropoda (Bullock and Horridge, 1965; Haszprunar, 1985c).

Despite conservation of the basic layout of the nervous system among molluscs, gastropods show more variation in nervous system characters than any other molluscan Class (Haszprunar, 1988a). Two differences in configuration of the central nervous system are considered particularly important for higher-level systematics of gastropods. One involves the configuration of the visceral loop and the other involves relative position of the pleural ganglia within the esophageal nerve ring.

The configuration of the visceral loop among gastropods is described as either streptoneurous or euthyneurous. Streptoneury occurs when the visceral loop has a figure eight conformation as a result of ontogenetic torsion (Fig. 2; Haszprunar, 1988a; Page, 2006). The left limb of a streptoneurous visceral loop is composed of two nerve connectives. The subintestinal connective emanates from the left pleural ganglion, runs underneath the esophagus to the subintestinal ganglion on the right side of the body, then the subintestinal-visceral connective runs posteriorly and to the left, eventually joining the centrally located visceral ganglia (Fig. 2; Bullock and Horridge, 1965). The right limb of the visceral loop is also composed of two nerve connectives. The supraintestinal connective emanates from the right pleural ganglion, runs over the esophagus to the supraintestinal ganglion on the left side of the body, and then the supraintestinal-visceral connective runs posteriorly and to the right to eventually join the visceral ganglia, thereby completing the figure eight circuit (Fig. 2; Bullock and Horridge, 1965).

Euthyneury describes a visceral loop that is not crossed, but instead has a general ‘U’ conformation (Fig. 2; Haszprunar, 1985b, 1988a). Euthyneury occurs by one of three

processes: (1) detorsion, which as the name implies is when certain aspects of the viscera become untwisted to various extents in different species (Haszprunar, 1985b, 1988a; Marois and Carew, 1990); (2) concentration, in which the visceral loop is short and cells of the subintestinal ganglion migrate along the visceral loop connective toward the left cerebral ganglion, effectively concentrating the components of the visceral loop without actually un-twisting it (Page, 1992a); and (3) semidetorsion and concentration, which is a combination of the first two processes (Haszprunar, 1985b, 1988a). All three of these processes result in the intestinal ganglia residing on the same side of the body as the pleural ganglion to which they are connected (Fig. 2). Many heterobranchs with a euthyneuran nervous system also have an additional pair of ganglia along the visceral loop known as the parietal ganglia, producing a pentaganglionate visceral loop (Bullock and Horridge, 1965; Haszrpunar, 1988a; Page, 1992a).

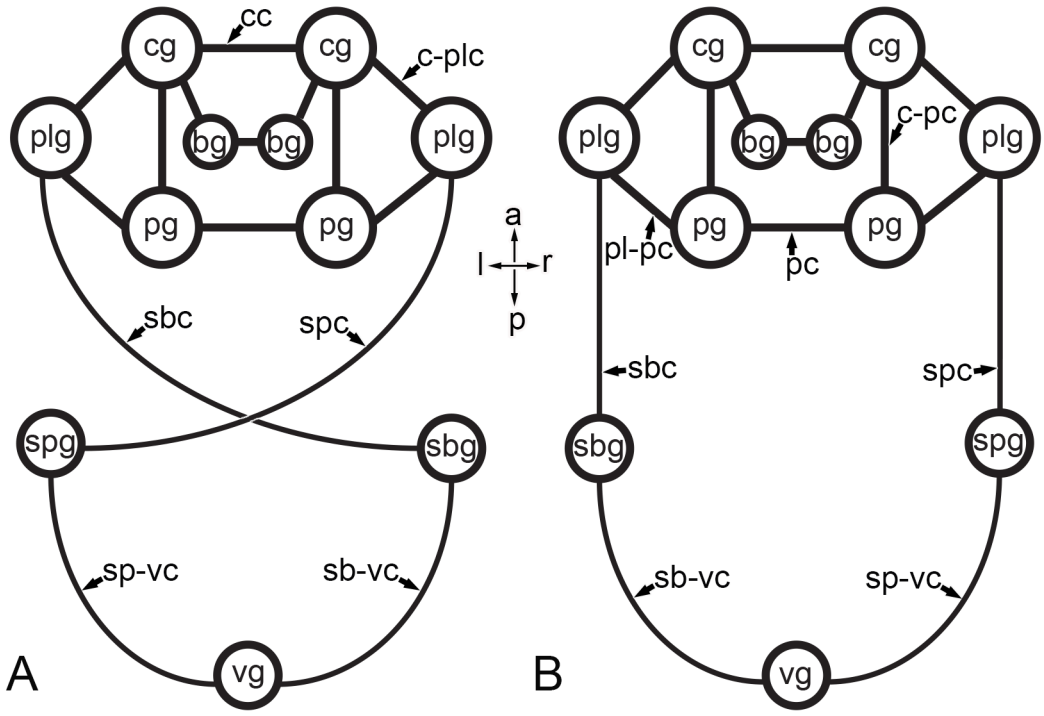

Figure 2. Diagrammatic illustrations of the two major configurations of the gastropod central nervous system in dorsal view; in reality the pleural ganglia sit dorsal to the cerebro-pedal connective (c-pc), but are depicted to the side for clarity and the buccal ganglia (bg) extend dorsally (out of the page) from the cerebral ganglia (cg). **A.** Gastropod central nervous system with a streptoneurous visceral loop. **B.** Gastropod

central nervous system with a euthyneurous visceral loop. Abbreviations: bg= buccal ganglion, cg= cerebral ganglion, c-pc= cerebro-pedal connective, c-plc= cerebro-pleural connective, pc= pedal commissure, pg= pedal ganglion, plg= pleural ganglion, pl-pc= pleuro-pedal connective, sbg= subintestinal ganglion, sbc= subintestinal connective, sb-vc= subintestinal-visceral connective, spg= supraintestinal ganglion, spc= supraintestinal connective, sp-vc= supraintestinal-visceral connective, vg= visceral ganglion. Orientation axes: a= anterior, l= left, p= posterior, r= right.

The other major difference in the configuration of the central nervous system within the Gastropoda is in the relative position of the pleural ganglia within the esophageal nerve ring. The central nervous system is defined as hypoathroid when the pleural ganglia are partially fused with- or closely associated with the pedal ganglia (Fretter and Graham, 1994). The nervous system is defined as epiathroid when the pleural ganglia are at least partially fused with- or are closely associated with the cerebral ganglia (Fretter and Graham, 1994).

There are three general types of central nervous system configurations among gastropods that are characterized by different combinations of the morphological characteristics described above. The Patellogastropoda, Vetigastropoda, Neritimorpha and some basal Caenogastropoda possess streptoneurous-hypoathroid central nervous systems (Salvini-Plawen and Haszprunar, 1987; Haszprunar, 1988a). Most of the Caenogastropoda and some basal Heterobranchia possess streptoneurous-epiathroid central nervous systems (Haszprunar, 1988;a Page, 1992a). The remainder of the Heterobranchia possess euthyneurous-epiathroid central nervous systems that are either triganglionate or pentaganglionate (Haszprunar, 1988a; Page, 1992a). Our current understanding of character trait evolution among gastropods suggests that a streptoneurous-hypoathroid nervous system is the ancestral condition, whereas euthyneury and epiathroidy evolved multiple times independently, as suggested by the three developmental processes that produce euthyneury (Haszprunar, 1985b; Haszprunar, 1988a). These three nervous system configurations represent the basic frameworks on which a tremendous amount of additional variation has been superimposed.

Much of the variation involves anatomical specializations of the visceral loop

(Lin and Leise, 1996). Zygoneuries, defined as secondarily developed connections between a pleural ganglion and the ipsilateral intestinal ganglion (e.g. the left pleural ganglion and the supraintestinal ganglion), are especially common among caenogastropods (Bullock and Horridge, 1965). Anastamoses between nerves emerging from the pleural and intestinal ganglia of the same side, termed dialyneuries, are also scattered among most of the gastropod subclasses (Fretter and Graham, 1962). Moreover, ganglia of the visceral loop may exhibit extensive positional migrations and fusions across gastropod taxa, the intestinal ganglia being the most labile (Bourne, 1908; Bullock and Horridge, 1965; Haszprunar, 1985b, 1988a). Typically the intestinal ganglia will fuse with the visceral ganglion or they will become displaced anteriorly and fuse with the respective pleural ganglion-the subintestinal displacing toward the left pleural ganglion and the supraintestinal toward the right pleural ganglion (Lin and Leise, 1996). Neritimorphs however, show perhaps the most derived condition of their visceral loop among gastropods, as described below.

1.3.1 Configuration of the neritimorph central nervous system

Adult neritimorphs possess a streptoneurous-hypoathroid esophageal nerve ring with elongate pedal ganglia known as pedal cords, elongate buccal ganglia, a long cerebral commissure and a secondary commissure between the anterior most lobes of cerebral ganglia-termed the labial lobes-known as the labial commissure (Bourne, 1908, 1911; Fretter and Graham, 1962; Fretter, 1984). These are considered ancestral characteristics that neritimorphs share with patellogastropods and vetigastropods (Bourne, 1908; Fretter and Graham, 1962). Despite possessing an ancestral esophageal nerve ring configuration, neritimorphs exhibit a remarkably derived visceral loop.

Many early morphologists attempted but failed to correctly describe the nervous system exhibited by members of the Neritidae (Jhering, 1877; Bouvier, 1887; Boutan, 1892; Haller, 1884; Lenssen, 1899). One of the major problems for early neritimorph anatomists was the very thin and reduced supraintestinal connective, which was thus incorrectly described as being absent (Jhering, 1877; Bouvier, 1887; Lenssen, 1899). Haller (1884) was the first to discover the existence of the supraintestinal connective,

however, it was Bourne (1908) who was the first to successfully describe an anatomically accurate model of the neritid nervous system in its entirety. Bourne (1908) showed that although neritids retain a reduced supraintestinal connective with a trajectory typical of streptoneurans, neritimorphs have lost the conventional subintestinal connective of the visceral loop (Fig. 3). Instead the subintestinal ganglion has inconspicuously fused to the right pleural ganglion and there is a direct connection between the two pleural ganglia, forming a pleural commissure, which essentially creates a novel neuroanatomical shortcut in the visceral loop (Fig. 3). Neritimorphs also possess two visceral ganglia at the posterior of the visceral loop (Fig. 3; Bourne, 1908; 1911; Fretter, 1984).

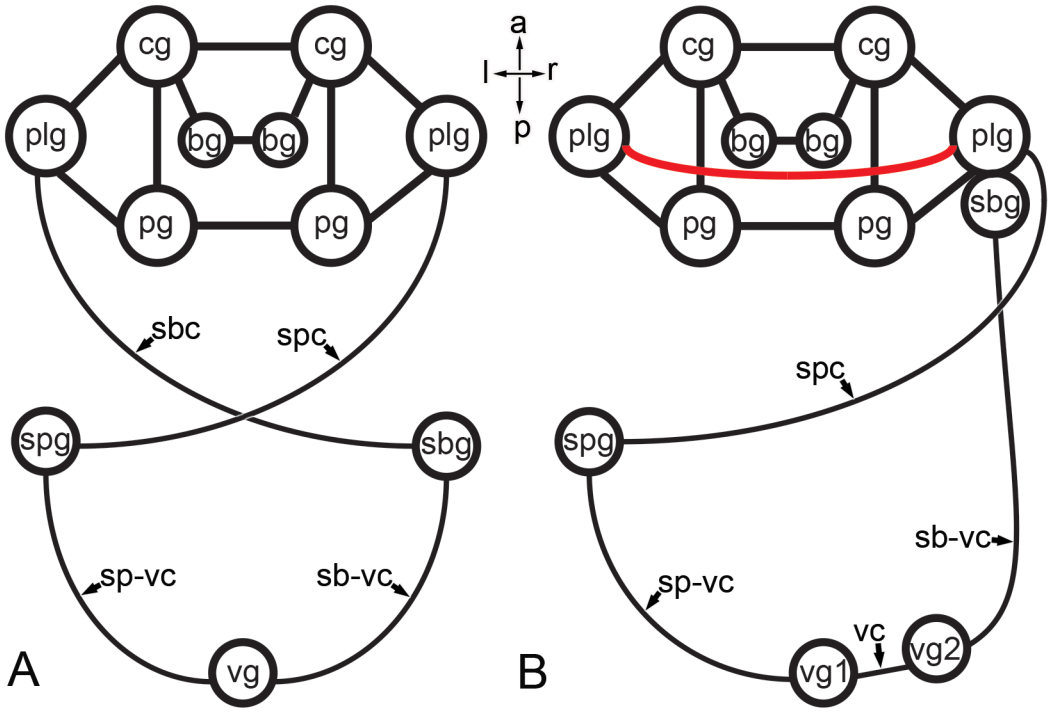

Figure 3. Diagrammatic illustrations of the configuration of the neritimorph central nervous system in comparison with a typical streptoneurous nervous system. **A.** Configuration of the central nervous system of a typical streptoneurous gastropod. **B.** Configuration of the central nervous system in members of the Neritidae; the novel connection between the pleural ganglia forming the neuroanatomical shortcut in the visceral loop is drawn in red. Abbreviations: bg= buccal ganglion, cg= cerebral ganglion, c-pc= cerebro-pedal connective, c-plc= cerebro-pleural connective, pc= pedal

commissure, pg= pedal ganglion, plg= pleural ganglion, pl-pc= pleuro-pedal connective, sbg= subintestinal ganglion, sbc= subintestinal connective, sb-vc= subintestinal-visceral connective, spg= supraintestinal ganglion, spc= supraintestinal connective, sp-vc= supraintestinal-visceral connective, vc= visceral commissure, vg= visceral ganglion, vg1= first visceral ganglion, vg2= second visceral ganglion. Orientation axes: a= anterior, l= left, p= posterior, r= right.

The nervous system in members of adult Helicinidae (Bourne, 1911) and one member of the Phenacolepadidae (Fretter, 1984) have also been described. Their nervous systems are similar to what was observed for members of the Neritidae in the morphology of the esophageal nerve ring, the fusion between the subintestinal ganglion and right pleural ganglion, absence of the subintestinal connective, and the presence of the neuroanatomical shortcut in the visceral loop (Bourne, 1911; Fretter, 1984). This suggests that these derived attributes are characteristic of the neritoideans in general. In contrast to the Neritidae, however, the supraintestinal ganglion has fused to the left pleural ganglion in the Phenacolepadidae, and is completely absent in members of the Helicinidae (Bourne, 1911; Fretter, 1984). Furthermore, the supraintestinal and supraintestinal-visceral connectives are absent in both groups (Bourne, 1911; Fretter, 1984).

As discussed above, the visceral loop is subject to many modifications and specializations across gastropod taxa, however, the presence of a direct connection between the two pleural ganglia represents a significant novelty.

1.4 Gastropod nervous system development

Ancestral gastropods, like most species of extant marine gastropods, had an indirect life cycle that began with a larval stage. The original larval type was probably pelagic but non-feeding, with feeding larvae arising as a derived larval type (Haszprunar et al., 1995; Lindberg and Guralnick, 2003). Nevertheless, the larval body of gastropods is essentially the juvenile body under construction, with additional anatomical

components to allow the larva's swimming lifestyle and, in feeding larval types, to allow capture and ingestion of microalgae (Page, 2009). A nervous system is present in both larval and post-metamorphic gastropods, which are often referred to as the "larval nervous system" and "post-metamorphic (or juvenile/adult or definitive) nervous system", respectively (Croll and Dickinson, 2004). However, much of the nervous system that develops within the larval stage is carried through metamorphosis and thus there is little distinction between the nervous systems of these two life history stages. It is more appropriate, therefore, to define the larval nervous system as those neural components directing exclusively larval behaviours and innervating larval structures that are lost at metamorphosis. Neural components associated with sensory and effector structures that are carried through metamorphosis are technically components of the post-metamorphic (definitive or juvenile/adult) nervous system, even if they develop and begin functioning in the larva. According to these definitions, the nervous system of older larvae will be a composite of exclusively larval neurons and of neurons of the differentiating post-metamorphic nervous system. For the purposes of the present study I will outline the development of the definitive nervous system only.

1.4.1 Development of the definitive nervous system

Ganglia of the definitive (post-metamorphic) gastropod central nervous system begin to develop during embryonic development from specific regions of ectoderm that overlie mesodermal precursors of muscle cells (Schacher *et* al., 1979; Jacob, 1984; Dickinson *et al.,* 2000). Cells within these ectodermal placodes become large and columnar and undergo frequent mitoses to produce multilayered cellular placodes (Jacob, 1984). Cells then migrate from the placodes to regions of ganglia formation (McAllister *et al.,* 1983; Jacob, 1984; Hickmott and Carew, 1991; Page, 1992a,b). Each ganglion is formed by cells from an adjacent and distinct ectodermal proliferative zone (Jacob, 1984; Page 1992a,b). Interestingly, and in contrast to what is observed in the neurogenesis exhibited by other invertebrates and vertebrates, the developing ganglia are devoid of neuroblasts and any mitosis occurring within the ganglia is restricted to the occasional division of glial cells (Jacob, 1984; Hickmott and Carew, 1991). Neurons themselves do

not divide (Jacob, 1984), suggesting that proliferation within the ectodermal placodes generates all neurons within ganglia of the gastropod central nervous system. The lack of cell division within ganglia also suggests that neuronal precursors may begin differentiation sometime before actually joining the ganglion, either within the ectodermal proliferative zone or during migration to the forming ganglion (Kandel *et al.,* 1980; McAllister, 1983; Jacob, 1984).

Many accounts of gangliogenesis report that the ganglia develop in an anterior to posterior sequence, where the cerebral and pedal ganglia are the first to appear, followed by the pleurals, intestinals and visceral ganglion (Raven, 1958; Demian and Yousif, 1975; Kriegstein, 1977; Kandel *et al.,* 1980). However, anlagen of the visceral loop ganglia have also been observed in the earliest stage veligers (Schacher *et al.*, 1979; Croll and Voronezhskaya, 1996; Dickinson *et al.,* 2000; Voronezhskaya and Elekes , 2003), suggesting that gastropods may possess at least anlagen of all of the definitive ganglia at the beginning of the veliger stage, and the subsequent development into functional ganglia is coordinated with the emergence of the anatomical structures that they innervate.

1.4.2 Development of derived nervous system characteristics

Derived aspects of the nervous system configuration of gastropods most often involve fusions between ganglia of the visceral loop or between visceral loop ganglia and the pleural ganglia (Bullock and Horridge, 1965; Haszprunar, 1985b, 1988a; Lin and Leise, 1996). Fusions can make identification of ganglia in the adult nervous system challenging, especially among many members of the Heterobranchia that possess highly consolidated central nervous systems (Kriegstein, 1977; Page, 1992a,b; Carroll and Kempf, 1994). Determining the homology of a ganglionic fusion product requires developmental analyses because studies have shown that the developing central nervous system initially exhibits all ganglionic rudiments in approximately the ancestral configuration, with derived conditions developing gradually during later ontogeny.

Aplysia californica is a species of heterobranch with a euthyneurous and hypoathroid adult central nervous system. The esophageal nerve ring of adults is

composed of discrete cerebral, pedal, pleural and buccal ganglia, but the visceral loop bears only one, seemingly novel ganglion known as the abdominal ganglion (Kandel *et al*., 1980). Developmental analysis by Kriegstein (1977) revealed that the abdominal ganglion is a derived construct of the three, ancestral visceral loop ganglia. At hatching, larvae of *A. californica* possess paired cerebral and pedal ganglia, as well as the visceral loop with three small but separate cell clusters corresponding to the subintestinal, visceral and supraintestinal ganglia (Kriegstein, 1977; Schacher *et al*., 1979). At the onset of metamorphosis, the visceral and subintestinal ganglia fuse, and this fusion product in turn fuses with the supraintestinal ganglion after metamorphosis to form the abdominal ganglion. Furthermore, the pleural ganglia of *A. californica* initially form at the posterolateral surfaces of the cerebral ganglia during the larval stage, but subsequently migrate to a position close to the pedal ganglia. So the hypoathroid condition of adult *A. californica* develops secondarily from an initial epiathroid configuration.

Nudibranchs are heterobranchs that exhibit a rather extreme version of both euthyneury and epiathroidy with a highly condensed visceral loop (Page, 1992a,b; Carroll and Kempf, 1994; Chase, 2002). Detailed analysis of the developing central nervous system in larvae of the nudibranch *Melibe leonina* revealed the pattern of ganglionic fusions and the identity of the ganglia within each of the fusion products (Page, 1992a,b). At hatching, the nervous system in larvae of *M. leonina* consists of interconnected pedal and cerebral ganglia with the visceral loop connective emerging from the posterior of each cerebral ganglion. Around 14 days after hatching, the supraintestinal ganglion begins to form posterodorsally to the right cerebral ganglion, and the subintestinal ganglion begins to form posteroventrally to the left cerebral ganglion shortly after. The visceral ganglion forms late in larval development so that all three ganglia are present along the visceral loop just prior to metamorphosis. Eventually, the supraintestinal ganglion fuses with the right cerebral ganglion and the visceral and subintestinal ganglia fuse with the left cerebral ganglion (Page, 1992a). Similar to *Aplysia* and seemingly all heterobranchs, the pleural ganglia emerge from the cerebral ganglia and so the seemingly novel cerebral ganglionic masses of adult *M. leonina* are actually derived constructs of the ancestral cerebral, pleural, subintestinal and visceral ganglia on the left and cerebral, pleural and supraintestinal ganglia on the right (Page, 1992a,b; Ruthensteiner, 1999).

Development of derived attributes of the central nervous system has also been documented in *Marisa cornuarietis,* a member of the family Ampullariidae (Demian and Yousif, 1973, 1975). The Ampullariidae are members of the order Architaenioglossa, which is now considered a basal group within the Caenogastropoda (Aktipis *et al.,* 2008). Demian and Yousif (1975) described formation of discrete anlagen of the cerebral, pedal, pleural and intestinal ganglia in the ancestral streptoneurous configuration (see Fig. 2) during embryonic development. Later in development, a zygoneury forms between the supraintestinal and left pleural ganglia and the subintestinal ganglion becomes fused to the right pleural ganglion (Demian and Yousif, 1975).

Thus, in these three examples, all ancestral ganglia of the gastropod nervous system appear during development as discrete, individual units that initially develop in their respective plesiomorphic positions. Specific derived attributes form later in ontogeny. This pattern of development suggest that the seemingly novel attributes of the central nervous system in *Aplysia californica, Melibe leonina* and *Marisa cornuarietis* did not evolve *de novo*, but are derived constructs of ancestral attributes of the gastropod central nervous system.

1.5 Gastropod shell muscles

An important behaviour of most gastropods is the ability to retract the body into the shell for protection. This behaviour is executed by the shell muscles, which run from attachments on the inner wall of the shell to insertions into the head and foot. These muscles vary in number and type across gastropod taxa. There are two ontogenetic sets of shell anchored retractor muscles exhibited by all gastropods with an indirect life cycle: the larval retractor muscle and the pedal muscle(s) (Page, 1995, 1997, 1998; Degnan *et al*., 1997; Wanninger *et al.,* 1999a,b; Wollesen *et al.*, 2008; Evans *et al.,* 2009).

The pedal muscles are composed of relatively long myosin filaments that collectively do not form a striation pattern and thus have been described as smooth in appearance (Page, 1997, 1998; Wanninger *et al.*, 1999a; Evans *et al.,* 2009). They attach to the inner wall of the shell via specialized attachment plaques (Tompa and Watabe, 1976) and insert mostly on the epithelium that underlies the operculum on the back of the

foot (Page, 1995, 1997, 1998; Wanninger *et al.,* 1999; Wollesen *et al.*, 2008). Adult gastropods possess either one or two pedal muscles, seemingly dependent on the morphology of the shell. Gastropods with a coiled shell and columella (the central axis of the shell that forms as a result of shell coiling) have one pedal muscle, which has also been termed the columella muscle (Fretter and Graham, 1994). The reason they only require one pedal muscle is because the muscle, which originates on either the left (Page, 1997, 1998; Evans *et al.,* 2009) or right (Wollesen *et al.,* 2008) side of the shell (depending on the direction of shell coiling), becomes centralized over the body of the gastropod as it wraps around the forming columella (Page, 1997, 1998; Wollesen *et al.*, 2008; Evans *et al.,* 2009). A subset of the Vetigastropoda (Trochoidea), the vast majority of the Caenogastropoda (Fretter and Graham, 1994), the majority of the Heterobranchia, and thus the majority of the Gastropoda in general possess one definitive pedal muscle (Haszprunar, 1988a; Fretter and Graham, 1994).

On the other hand, gastropods with left and right pedal muscles tend to have shells in which there is no columella, or the columella is greatly reduced. Therefore, a symmetrical pull on either side of the foot is required to withdraw the foot into the shell interior. Some gastropods with two pedal muscles have cap-shaped shells that are not coiled, such as all of the Patellogastropoda, some members of the Phenacolepadidae, Neritiliidae (Neritimorpha), some members of the Capulidae, *Concholepas* (Caenogastropoda) and the Fissurellidae (Vetigastropoda) (Haszprunar, 1988a; Fretter and Graham, 1994; Lindberg and Ponder, 2001). Other gastropods that have two shell muscles display a shell-coiling pattern in which the body whorl is substantially larger than previous whorls, effectively greatly reducing the columella. This occurs in many of the remaining vetigastropods (Haliotidae, Pleurotomariidae, Scissurellidae, *Tricolia*), and some members of the Velutinidae, Triviidae, Muricidae (Caenogastropoda) and Rissoellidae (Heterobranchia) (Salvini-Plawen and Haszprunar, 1987; Haszprunar, 1988a; Fretter and Graham, 1994). Furthermore, some gastropods resorb the inner-whorls of their shell and thus do not have a columella. This occurs to the greatest extent in members of the Neritimorpha (except for the Neritopsidae)(Solem, 1983).

The larval retractor muscle is also attached to the shell via a specialized attachment plaque, but is composed of shorter myosin filaments that form an oblique

striation pattern (Page, 1995, 1997, 1998, Wanninger *et al.*, 1999a; Evans *et al.,* 2009). The larval retractor muscle originates on the inner postero-lateral wall of the left side of the shell and gives rise to a proximal trunk that splits distally into either discrete bundles, or individual muscle cells that terminate within various structures associated with the head and sometimes the foot of veliger larvae (Page, 1995, 1997, 1998; Degnan *et al*., 1997; Wanninger *et al.,* 1999a,b; Wollesen *et al.,* 2008). The number, and exact insertion sites of the various distal branches of the larval retractor muscle is slightly variable depending on the species, but in general the single larval retractor muscle extends fibres to the anterior esophagus, mantle fold, apical plate, and both the left and right velar lobes (Page, 1995, 1997, 1998; Degnan *et al.,* 1997, Wanninger *et al.,* 1999a, Wollesen *et al.*, 2008). In addition, a pedal branch of the larval retractor muscle that extends into the foot has been reported in *Aplysia californica*, *Aeolidiella stephanieae* (both Heterobranchia) and *Ilyanassa obsoleta* (Caenogastropoda) (Wollesen *et al.*, 2008; Evans *et al.,* 2009; Kristof and Klussmann-Kolb, 2010). Larvae belonging to gastropod representatives of the Patellogastropoda, Vetigastropoda, Caenogastropoda and Heterobranchia in which myogenesis has been studied, all possess one larval retractor muscle anchored on the left side of the shell (Page, 1995, 1997, 1998; Degnan *et al*., 1997; Wanninger *et al.,* 1999a,b; Wollesen *et al.,* 2008; Evans *et al.,* 2009; Kristof and Klussmann-Kolb, 2010). Furthermore, some gastropods such as *H. kamtschatkana* (Vetigastropoda), *Patella vulgata, P. caerulea* (Patellogastropoda), *I. obsoleta* (Caenogastropoda) and *A. californica* (Heterobranchia) possess an additional accessory retractor muscle consisting of fewer muscle cells that originates ventro-medially on the protoconch and inserts on the mantle (Page, 1997, Wanninger *et al.,* 1999a; Wollesen *et al.,* 2008; Evans *et al.,* 2009).

1.5.1 Shell muscle development

Although both the larval retractor muscle and the pedal muscles occupy overlapping morphological and functional space, they are different muscle systems with distinct developmental programmes (Page, 1998). However, evidence indicating a distinction between these two muscle systems did not come to the forefront until relatively recently (Page, 1995, 1997, 1998; Degnan *et al*., 1997; Wanninger *et al.,*

1999a,b). Although earlier studies described developing gastropod shell muscles (Smith, F.G.W., 1935; Crofts, 1937; 1955; Smith, S.T., 1967), prior to the mid-1990's the definitive pedal muscles and the larval retractor muscles were thought to be continuations of the same muscle, which led to many misinterpretations of homologies across gastropod taxa, and incorrect interpretations of shell muscle development (Garstang, 1929; Crofts, 1937, 1955; Fretter and Graham, 1962; Fretter, 1969, Bandel, 1982). Indeed, the evolutionary and developmental homologies of gastropod shell muscles have been at the front of discussions about the origin of the Gastropoda for much of the twentieth century. This is because the early literature implicated the larval shell muscles in the process of ontogenetic torsion (Garstang, 1929; Smith, 1935; Crofts, 1937, 1955), the defining characteristic of gastropods (Haszprunar, 1988a). Much of the misinterpretations in the early studies were due to the relatively low resolution of the available experimental techniques for observing morphogenesis within larval and juvenile gastropods (Page, 1998), and do not represent observational shortcomings of the authors. The emergence of immunolabeling techniques and better techniques for light and transmission electron microscopy provided higher resolution that has led to more robust observations and a clearer depiction of shell muscle development and evolution (Page, 1995, 1997, 1998; Degnan *et al*., 1997; Wanninger *et al.,* 1999a,b; Wollesen *et al.,* 2008), and thus these studies will be the focus of this section.

Despite the variation in number of definitive pedal muscles, and the number of larval retractor muscle tracts and their insertion sites, a relatively conserved pattern of shell muscle development has been observed in studied representatives of the Patellogastropoda (Wanninger *et al*., 1999a,b), Vetigastropoda (Degnan *et al.,* 1997; Page, 1997), Caenogastropoda (Page, 1998; Evans *et al.*, 2009) and Heterobranchia (Page, 1995; Wollesen *et al.*, 2008; Kristof and Klussmann-Kolb, 2010). In general the obliquely striated larval retractor muscle develops first, and is present and functional in hatching planktotrophic (Page, 1995, 1998; Wollesen *et al.,* 2008; Evans *et al.,* 2009) and lecithotrophic (Degnan *et al.*, 1997; Page, 1997; Wanninger *et al*., 1999a; Kristof and Klussmann-Kolb, 2010) veliger larvae. The larval retractor muscle is destroyed either at metamorphosis, or shortly after, and thus does not contribute to the definitive shell musculature (Page, 1997, 1998; Degnan *et al*., 1997; Wanninger *et al.,* 1999a; Wollesen

et al., 2008). The foot is small in the early veliger stages and possesses a thin operculum on the dorsal surface (Page, 1995, 1997, 1998; Wanninger, 1999a). During the early stages of larval development, retraction of the larval retractor muscle functions to bring the entire cephalopodium into the shell (Page, 1995, 1998). As the larvae develop, there is a substantial increase in the size of the foot, and development of the smooth pedal muscle(s) occurs around this same time, midway through larval development (Page, 1995, 1997, 1998; Wanninger, 1999a; Evans *et al.,* 2009). The shell attachment plaques of the left pedal muscle and larval retractor muscle are separate but close to each other in all studied gastropods except for studied representatives of the Patellogastropoda (Wanninger *et al.,* 1999a). For all other gastropods, the two muscles can only be discerned by analyzing their differing trajectories using immunolabeling techniques (Degnan *et al.,* 1997; Evans *et al.,* 2009), and serial analysis of histological sections for light microscopy (Page, 1995, 1997, 1998); or by observing the differing striation patterns using transmission election microscopy (Page, 1995, 1997, 1998). As a general rule, the attachment plaque of the larval retractor muscle is medial to the attachment plaque of the left pedal muscle, and some tracts of the larval retractor muscle are embraced by the cerebro-visceral nerve ring (consisting of the cerebral commissure, cerebral ganglia and visceral loop), whereas no pedal myocytes penetrate through this nerve ring (Page, 1995, 1998). When both a left and right pedal muscle is formed, they differentiate simultaneously, although the attachment sites on the shell are different for the left and right pedal muscles (Page, 1995, 1997; Degnan *et al.,* 1997; Wanninger, 1999a). There is increased complexity in retraction behaviour associated with the development of the pedal muscles (Page, 1995). After the pedal muscles have developed, the velar lobes can be retracted without associated retraction of the foot, and the foot can be extended independently of the velar lobes after full body retraction (Page, 1995). Although the larval retractor muscle is destroyed at metamorphosis, the pedal muscle(s) in more or less their entirety (Page, 1997; Wanninger, 1999a; Wollesen *et al.*, 2008; Evans *et al.,* 2009), or a portion of the left pedal muscle (Page, 1998), survive metamorphosis and are the sole contributors to the post-metamorphic shell muscle.

Together, these observations point to certain defining morphological and developmental characteristics of the two discrete shell muscle systems across the

Gastropoda. The larval retractor muscle is striated, it develops first, the attachment plaque sits medial to that of the left pedal muscle (when present), the ventral muscle tracts of the larval retractor muscle are embraced by the cerebro-visceral nerve ring, distal muscle tracts insert within species specific regions of the head, velar lobes and foot, and the larval retractor muscle is destroyed at metamorphosis. The pedal muscle(s) on the other hand are smooth in appearance, they emerge midway through larval development, the attachment plaque of the left pedal muscle (when present) sits lateral to that of the larval retractor muscle, all of the muscle cells project outside of the cerebro-visceral nerve ring, the majority of the muscle cells insert on epithelium underlying the operculum, and at least a portion of the larval pedal muscles in gastropods that possess an adult shell, survive metamorphosis to become the post-metamorphic shell musculature. These characteristics of myogenesis have been observed in members of the Patellogastropoda (Wanninger, 1999a,b), Vetigastropoda (Degnan *et al.*, 1997; Page, 1997), Caenogastropoda (Page, 1998; Evans *et al.,* 2009) and Heterobranchia (Page, 1995; Wollesen *et al.,* 2008), and thus this general pattern of shell muscle development seems to be relatively conserved across gastropod taxa.

1.5.2 Neritimorph shell muscles

Until recently, analyses of shell muscle systems in neritimorphs have been confined to observations of adult anatomy (Bourne, 1908, 1911; Fretter, 1984; Lindberg and Ponder, 2001). Remarkably, preliminary developmental analysis of myogenesis in *Nerita melanotragus*, a member of the Neritimorpha (family Neritidae), showed that although they do possess an accessory larval retractor muscle similar to what has been described in other gastropod larvae (Page, 1997, Wanninger *et al.,* 1999a; Wollesen *et al.,* 2008; Evans *et al.,* 2009), their shell muscle myogenesis breaks the conserved developmental pattern described above in two ways (Page and Ferguson, 2013).

First, planktotrophic larvae of *N. melanotragus* possess both a left and right larval retractor muscle of similar size (Page and Ferguson, 2013). Nevertheless, the left larval retractor muscle includes more muscle fibres than the right muscle, its distal branches insert within the mantle fold, apical plate, both velar lobes and sites on the larval foregut,

and is embraced by the visceral loop (Page and Ferguson, 2013). The right larval retractor muscle originates from a symmetrical location on the right side of the shell, the trunk projects through the visceral loop and distal branches insert within the right velar lobe only (Page and Ferguson, 2013). The presence of two muscles conforming to the definitive criteria of larval retractor muscles is unprecedented in any other observed gastropod larvae (Page and Ferguson, 2013).

The second deviation in muscle developmental pattern in *N. melanotragus* involves the pedal muscles. Like other extant neritimorphs, *N. melanotragus* possesses left and right pedal muscles; however, unlike what has been observed in all other gastropods to date, fibres of the definitive pedal muscles are fully differentiated and functional within the earliest larval stage (Page and Ferguson, 2013). Observations of shell muscles in juveniles at six days after metamorphosis showed that the paired larval retractor muscles were destroyed at metamorphosis, and the left and right pedal muscles were retained (Page and Ferguson, 2013).

1.6 Hypotheses on the function of the neuroanatomical 'shortcut' in neritimorphs

Bourne (1908) observed that the pedal muscles were each innervated by a nerve emerging from the ipsilateral pleural ganglion in adult neritids. Bourne (1908) therefore speculated that the neuroanatomical shortcut between the two pleural ganglia of adult neritimorphs might function in coordinating the two pedal muscles of these snails. However, the other adult gastropods that possess paired shell muscles do not require new connections in their nervous system in order to coordinate them. This suggests that the paired condition of adult shell muscles may not be enough to justify such a drastic change to the configuration of the central nervous system. However, components of the nervous system tend to develop in coordination with their target tissues and thus it seems reasonable to assume that muscle development would be tightly coordinated with development of the nervous system. Furthermore, Haszprunar (1988a) suggested that each major change that has occurred in the gastropod nervous system is correlated with a major evolutionary novelty. In light of the recent discovery that neritimorph larvae hatch

with the paired adult pedal muscles already present, as well as a pair of larval retractor muscles (Page and Ferguson, 2013), I extend Bourne's (1908) hypothesis to state that the novel neuroanatomical shortcut between the two pleural ganglia in neritimorphs functions to coordinate both pairs of muscles within the larva.

Based on this functional hypothesis one can form a predictive model of development for the neuroanatomical shortcut. The fact that all of the derived attributes of the nervous system discussed previously (Kriegstein, 1977; Page, 1992a,b; Demian and Yousif, 1975) develop late in larval development suggests that their primary function resides within the post-metamorphic stages. On the contrary, I have implicated the neuroanatomical shortcut in *N. melanotragus* in the coordination of the shell muscles present at hatching. Furthermore, we know that the shortcut is present within the adult nervous system (Bourne, 1908, 1911; Fretter, 1984), which assuming that my functional hypothesis is correct, suggests that the shortcut must be either a neutral modification to the adult central nervous system or also serves a beneficial function in post-metamorphic stages. Therefore, I hypothesize that the neuroanatomical shortcut between the two pleural ganglia will have developed by the time of hatching, be present throughout larval development and be subsequently carried through metamorphosis and remain present in the juvenile/adult.

1.7 Hypothesis on the evolutionary origin of the neuroanatomical 'shortcut' in neritimorphs

Previous studies have shown that developmental studies on gastropods can be a powerful tool to explore hypotheses about evolutionary derivation because derived nervous system features are recapitulated during development (Kriegstein, 1977; Page, 1992a,b; Demian and Yousif, 1975).

Although the neuroanatomical shortcut in the neritimorph central nervous system represents a novel connection between the pleural ganglia, it is most likely derived from a pre-existing structure. The subintestinal ganglion is fused to the right pleural ganglion in neritimorphs (Bourne, 1908, 1911; Fretter, 1984), three ampullariid species (Honegger, 1974; Demian and Yousif, 1975; Brown *et al.,* 1990) and a species of *Crepidula*

(Caenogastropoda) (Moritz, 1939). The difference between the other species that possess this fusion product and neritimorphs is that the subintestinal connective remains in the ampulariids and *Crepidula* (Moritz, 1939; Honegger, 1974; Demian and Yousif, 1975; Brown *et al.,* 1990), whereas it appears to be absent in neritimorphs (Bourne, 1908, 1911; Fretter, 1984). Furthermore, in *M. cornuarietis*, the subintestinal ganglion begins development in the ancestral position along the visceral loop, detached from the right pleural ganglion, and then gradually fuses with the right pleural ganglion midway through larval development (Demian and Yousif, 1975). This suggests that this derived fusion product evolved from an ancestor with a typical streptoneurous nervous system (Fig. 4A). The fusion between the subintestinal ganglion and the right pleural ganglion brings the distal end of the subintestinal connective within close proximity to the right pleural ganglion (Fig. 4A). Therefore, it is possible that evolution of the neritimorph nervous system could have proceeded in much the same way as in *M. cornuarietis*, but after the subintestinal ganglion became fused to the right pleural ganglion, the subintestinal connective becomes incorporated into the right pleural ganglion to form the neuroanatomical shortcut between the two pleural ganglia (Fig. 4B). Therefore, I hypothesize that the neuroanatomical shortcut between the left and right pleural ganglia is a derived construct of the ancestral subintestinal connective of the visceral loop.

An alternative, although less likely possibility is that the neuroanatomical shortcut in neritimorphs evolved *de novo*. If this is the case, then the subintestinal connective would be expected to degenerate or never form during development and a completely novel connection between the two pleural ganglia would differentiate.

I further hypothesize that the derived character states of the neritimorph protoconch, shell muscles, and nervous system are functionally linked and therefore evolved in concert.

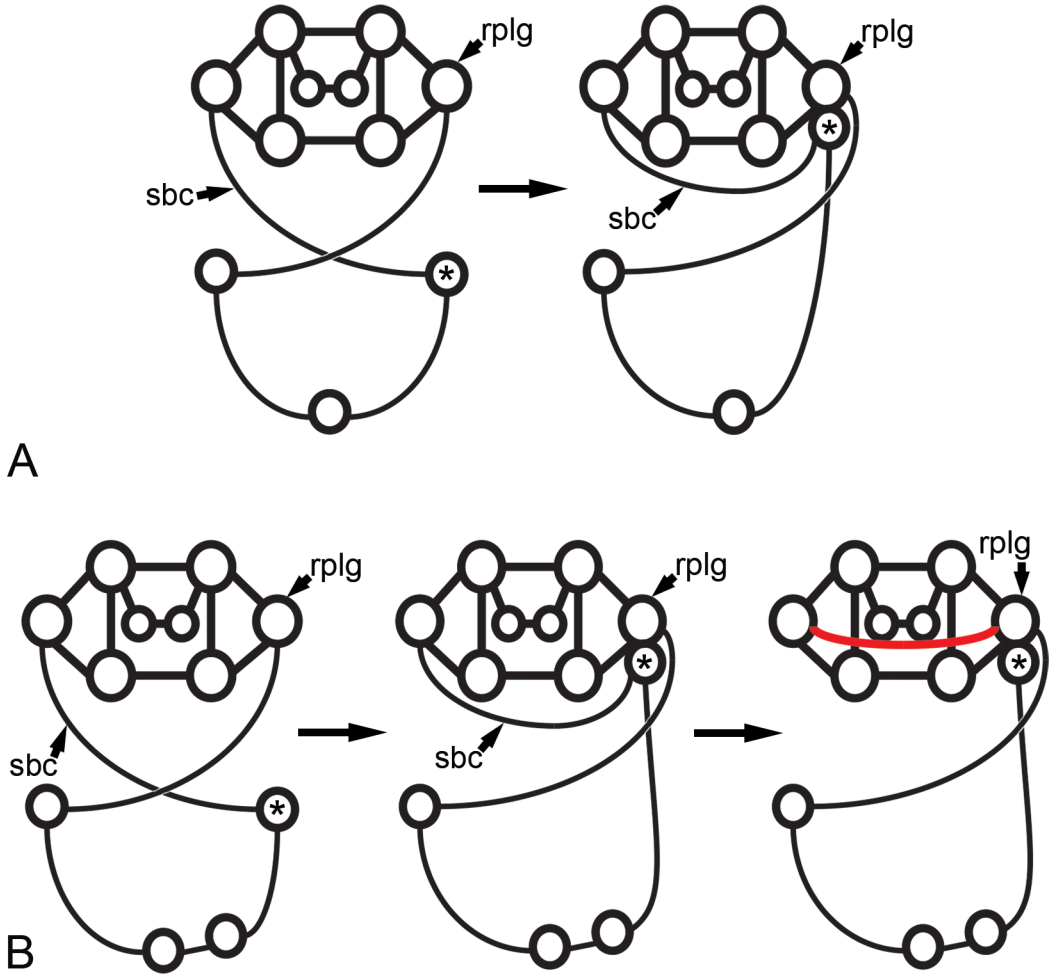

Figure 4. Diagramatic illustration of my hypothesis on the evolutionary origin of the neuroanatomical shortcut in neritimorphs. **A.** Evolution of the derived visceral loop in *Marisa cornuarietis* as suggested by the observed development (Demian and Yousif, 1975); *asterisks* indicate the subintestinal ganglion. **B.** Evolution of the derived visceral loop in neritimorphs based on neurogenesis in *M. cornuarietis*; this evolutionary hypothesis suggests that the neuroanatomical shortcut in neritimorphs is a derived construct of the subintestinal connective; *asterisks* indicate the subintestinal ganglion; neuroanatomical shortcut drawn in red. Abreviation: rplg= right pleural ganglion, sbc= subintestinal connective.

1.8 Objective of present study

I investigated the development of the central nervous system from larval hatching to juveniles at six days after metamorphosis, as well as the innervation of the two sets of shell muscles in a neritimorph gastropod, *Nerita melanotragus* EA SMITH, 1884 (Neritoidea; Neritidae). These snails are herbivorous grazers within the marine intertidal communities along the coast of New Zealand and south-eastern Australia (Przeslawski, 2011). Planktotrophic larvae of *N. melanotragus* hatch from benthic egg capsules and become competent to metamorphose between 45 and 55 days after hatching under laboratory conditions (Page and Ferguson, 2013).

This study represents the first description of neurogenesis for a member of the neritimorph subclass. My objective was to determine how the novel commissure ("shortcut") between the two pleural ganglia may have evolved by analyzing the development of this connection. I sought to determine if the shortcut was a *de novo* neural feature or if it was co-opted from a pre-existing neural tract of the ancestral gastropod nervous system. Furthermore, I analyzed the innervation of the larval retractor muscles and pedal muscles in *N. melanotragus*, to test the hypothesis that the shortcut may serve to coordinate between ganglionic centres that innervate the larval retractor muscles and the pedal muscles on both the left and right sides. Finally, as skeletons, muscles and nerves represent an integrated functional unit, I provide data that are consistent with the hypothesis that the unique characteristics of the shell, muscles and nervous system present in *N. melanotragus* evolved in concert; they represent a suite of derived characteristics that co-evolved as an integrated functional unit.

2.0 Materials and Methods

2.1 Egg collection and larval culture

Egg collection, larval culturing and fixations were done by Dr. Louise Page in 2006, the details of which were described by Page and Ferguson (2013). *Nerita melanotragus* eggs were collected from intertidal rocks in Balmoral Bay, Sydney Harbor, Australia in late October. The egg capsules were maintained in the laboratory within a 20L aquarium containing filtered and aerated seawater held at 19°C.

Larvae did not hatch on their own in the laboratory, so egg capsules were opened with a scalpel and only larvae that appeared fully differentiated and swam vigorously upon release were placed into cultures of 1000 ml sea water at a starting density of approximately 0.3 larvae/ml. Larval cultures were maintained at 20-23°C and fed an algal mixture of *Isochrysis galbana* and *Pavlova lutheri*. Algal cultures were grown in Guillard's f/2 enrichment medium without silicates and were maintained under continuous illumination at approximately 19°C. The larvae were transferred to fresh filtered seawater and fed with the algal mixture every other day.

2.2 Fixation of larval and juvenile specimens for histological sectioning and transmission electron microscopy

N. melanotragus larvae were reared from hatching to 6 days after metamorphic loss of the velar lobes. A subset of the total population was fixed at hatching and at six subsequent larval stages: 6, 9, 18, 27, 35, and 55 days post hatching (dph). Furthermore, one juvenile stage was fixed at 6 days post metamorphosis (dpm).

Larvae and juveniles were anesthetised with artificial seawater containing an increased concentration of Mg^{2+} and a reduced concentration of Ca^{2+} followed by addition of Chloretone (Page, 2002). They were fixed in 2.5% glutaraldehyde in 0.2mol 1^{-1} Millonig's phosphate buffer (pH 7.6) and 0.14mol 1^{-1} sodium chloride (Cloney and Florey, 1968). They were then decalcified in a 1:1 mix of 10% ethylenediamino

tetraacetic acid (disodium salt) and the primary fixative for 3 to 5 hours (Bonar and Hadfield, 1974), rinsed three times in 2.5% sodium bicarbonate buffer (pH 7.2), and postfixed in 2% osmium tetroxide in 1.25% bicarbonate buffer (pH 7.2). The specimens were dehydrated in a graded acetone series and infiltrated and embedded in epoxy resin (Procure 812, ProSciTech, Queensland, Australia).

2.3 Histological sectioning

I examined the development of the central nervous system and shell-anchored muscles by sectioning at least two individuals at all 8 of the fixed larval and juvenile stages in various orientations and analyzing the serial sections using a light microscope. Sections were cut at 750 nm thickness for the newly-hatched larvae and at 1μm for all other developmental stages using a DiATOME histological diamond knife on a Leica Ultracut UCT microtome. The sections were placed on a droplet of water on a glass slide, dried on a hotplate and then stained with a mixture of methylene blue and azure II in sodium borate (Richardson *et al.*, 1960). The serial sections were then viewed using a Zeiss Axioskop compound light microscope and photographs were taken with a mounted Retiga 2000R digital camera using QCapture Pro 5.1 software (QImaging). I identified four developmental stages that best represented the development of the central nervous system and shell-anchored muscles: newly-hatched, 18 dph, 55 dph and 6 dpm. I then made surface-rendered three-dimensional reconstructions of the nervous system and shell-anchored muscles at these 4 major stages of development (See 2.5).

2.4 Transmission electron microscopy (TEM)

Sectioning for transmission electron microscopy was performed to confirm my observations on the conformation and organization of the visceral loop and osphradial innervation in the newly-hatched and 18 dph stages, as many of these nerves were difficult to resolve using light microscopy. I also used transmission electron microscopy to determine the attachment sight of the neuroanatomical shortcut on the right side of the nervous system and the innervation of the shell-anchored muscles at the newly-hatched

stage as these components could not be resolved using light microscopy. Ultrathin serial sections of 75-80 nm were cut through three newly hatched larvae at slightly different orientations and one 18 dph larva using a DiATOME diamond knife for cutting ultrathin sections.

The sections were picked up on copper 2000 μm X 1000 μm single slot grids (Sequetec Limited). The grid slots were covered with a transparent film made from 1.0% formvar in 1,2-dichloroethane. The formvar films were made by standing a glass microscope slide vertically in a chamber filled with the formvar solution and draining the chamber from beneath so as to produce a thin film on the glass slide. The formvar was allowed to dry and then the slide was gently submerged in a bowl of distilled water so that the film detached from the surface of the slide and floated on the surface of the water. Only silver films with a hint of gold were used, as this denoted the appropriate thickness. The copper slot grids were then placed individually on the floating film, which was then gently lifted from the surface of the water using parafilm. The grids were allowed to dry overnight and then carbon coated with an E6700 bench top turbo pumped evaporator loaded with 1/4'' diameter graphite rods.

The sections were stained with a 2% aqueous solution of uranyl acetate for 1 hour followed by a 5-minute wash in distilled water, and then stained with 0.2% solution of lead citrate for 7-minutes, followed by another 5-minute wash. The sections were then imaged with a Hitachi H-7000 transmission electron microscope (TEM) using an AMT digital camera. A surface rendered three-dimensional reconstruction of the neurites innervating the shell-anchored muscles was created by free-hand tracing the detail that was observed in the TEM micrographs onto the 750 nm newly-hatched histological section series using the Reconstruct software.

2.5 Surface-rendered three-dimensional reconstructions

Surface-rendered three-dimensional reconstructions of various components of the central nervous system and shell-anchored muscles for three pre-metamorphic larval stages (newly-hatched, 18 dph and 55 dph) and one post-metamorphic juvenile stage (6 dpm) was accomplished using Reconstruct (version 1.1.0.0) (Fiala, 2005). Photographs of

serial sections were placed in order from anterior to posterior, the contrast and brightness of the images were adjusted with Adobe Photoshop CS3 and the images were then imported into Reconstruct. The image stack was calibrated to represent the appropriate size and thickness of histological sections. Section thickness was set to 750 nm for the newly-hatched specimen and 1 μm for the 18 dph, 55 dph, and 6 dpm specimens. The sections were then aligned manually and specific components of the nervous system and the entirety of the shell-anchored muscles were traced using a Bamboo graphics tablet. Each distinct morphological structure was traced as a separate object so that different colours could be assigned to different structures and traced structures could be edited individually. Distinct and unrelated objects e.g. central nervous system and larval retractor muscles were traced in different colours, whereas distinct but related objects e.g. ganglia of the visceral loop and nerves emanating from the central nervous system were traced in the same colour. The stack of traces making up each object profile was reconstructed and surface rendered using the Boissant surfacing algorithm to make up a three-dimensional representation of the sectioned morphological structures. I created three-dimensional reconstructions of the ganglia, commissures and connectives of the central nervous system, the eyes, the osphradium, the osphradial nerves, pallial nerves and the statocysts for all four of the major developmental stages. I created three-dimensional reconstructions of the shell-anchored muscles for the newly-hatched and 6 dpm stages only. Images of the three-dimensional reconstructions were captured at various orientations and surface smoothing as well as minor adjustments were made using Adobe Photoshop CS3.

3.0 Results

3.1 Development of the central nervous system

3.1.1 Developmental stage 1: Newly hatched stage

3.1.1.1 Esophageal nerve ring

At the newly hatched stage, which is the earliest larval stage, *N. melanotragus* possessed all of the central ganglia, commissures and connectives of the esophageal nerve ring, except for the buccal ganglia (Fig. 5). The protoconchs of newly hatched larvae measured approximately 100 μm across (Page and Ferguson, 2013), and thus all components of the central nervous system were also quite small at this stage. Each cerebral ganglion was roughly 25 μm in diameter and the pair was situated apically within the larva, sitting dorsal to the foregut (Figs. 5A, B; 6A, B). The cerebral commissure was relatively short but broad (Figs. 5A, C; 6B), the cerebro-pedal connectives were thin and extended ventrally from each cerebral ganglion (Fig. 5B, C), the cerebro-pleural connectives were thicker than the cerebro-pedal connectives and extended from the posterior of each cerebral ganglion to the elongate pleural ganglia, which flanked the foregut (Figs. 5A-C; 6C). The pleuro-pedal connective on each side extended from the anteroventral region of the pleural ganglion and passed dorsolaterally over the ipsilateral statocyst (Fig. 7) to merge with the cerebro-pedal connective just before entering the pedal ganglion (Figs. 5C). The pedal ganglia were concentrated and globular and were connected by a single, thin commissure (Figs. 5A, C; 6D).

3.1.1.2 Visceral loop

The visceral loop featured a subintestinal ganglion, supraintestinal ganglion and one visceral ganglion at the newly hatched stage and measured approximately 50 μm in width and length (Fig. 5). The subintestinal and supraintestinal ganglia could be resolved by light microscopy (Fig. 6B, C), but transmission electron microscopy was required to

confirm identity of the visceral ganglion and portions of the supraintestinal-visceral and subintestinal-visceral connectives.

The supraintestinal connective of the visceral loop emerged from the medial-posterior surface of the right pleural ganglion and extended toward the left side of the body by passing dorsally over the foregut to join the medial side of the supraintestinal ganglion (Figs. 5A, B; 8A-E). The supraintestinal ganglion gave rise to a short osphradial nerve (described below), and to the supraintestinal-visceral connective. The latter emerged posterolaterally from the supraintestinal ganglion (Figs. 5A, B; 6B), extended posteriorly between the left hypobranchial gland and the epithelium of the left wall of the mantle cavity (Fig. 6B), and continued posteromedially beneath epithelium of the floor of the mantle cavity until it connected with the single visceral ganglion (Figs. 5A; 9A-D).

At this early larval stage, the subintestinal ganglion was already fused with the right pleural ganglion (Figs. 5A, B, D; 6C), but the shortcut between the two pleural ganglia had not yet formed (Figs 5D; 10). The connective emerged medio-poseteriorly from the left pleural ganglion and extended beneath the esophagus to the right side of the body (Fig. 10A), where it joined the subintestinal ganglion, and was thus the subintestinal connective, by definition (Fig. 10B, D). The subintestinal-visceral connective emerged from the extreme posterior of the subintestinal ganglion (Fig. 5A, B, D); it ran through the larval retractor muscle posteromedially, eventually emerging close to the right hypobranchial gland (Fig. 11A). The subintestinal-visceral connective then travelled posteromedially along the epithelium of the floor of the mantle cavity (Fig. 11B) and joined the visceral ganglion, which was situated just beneath the floor of the mantle cavity, to the left of the anus and to the right of a ciliated tract that runs along the floor of the mantle cavity (Fig. 11C).

3.1.1.3 Sensory organs

Newly hatched larvae of *Nerita melanotragus* had four multicellular sensory structures: the unpaired apical sensory organ (apical ganglion) and a chemosensory osphradium and a pair of eyes and gravity sensing statocysts. The apical sensory organ was previously described by Page and Kempf (2009).

The osphradium of hatching larvae was situated just dorsal to the supraintestinal ganglion, and along the left wall of the mantle cavity (Figs. 5A, B, C; 9A; 12A, C). The osphradium was connected to the supraintestinal ganglion via a short nerve that emerged from the dorsal surface of the supraintestinal ganglion (Figs. 5B, C; 12A, B) and directly innervated the osphradium (Fig. 12C, D). The eyes were directly associated with the anterolateral surface of their respective cerebral ganglion (Figs. 5; 6B).

3.1.1.4 Pallial nerves

Both pallial nerves were present in hatching larvae, although the details of their distal trajectories were not resolved (Figs. 5A; 13A-E). The left pallial nerve exited the left pleural ganglion laterally at the extreme posterior surface (Figs. 5A; 13A). The right pallial nerve emerged laterally from the anterior of the subintestinal ganglion, very close to where the subintestinal ganglion and right pleural ganglion met (Figs. 6C; 13C, D). The right pallial nerve was closely associated with the posterior surface of the right hypobranchial gland as it extended laterally to the mantle fold demarcating the right side of the mantle cavity (Figs. 5A; 13E). The left pallial nerve could be resolved extending dorsally between the outer- and inner-mantle fold epithelium, which lined the roof of the mantle cavity all the way to the dorsal apex of the mantle fold; however, the nerve could not be resolved beyond this point (Figs. 5A; 13B).

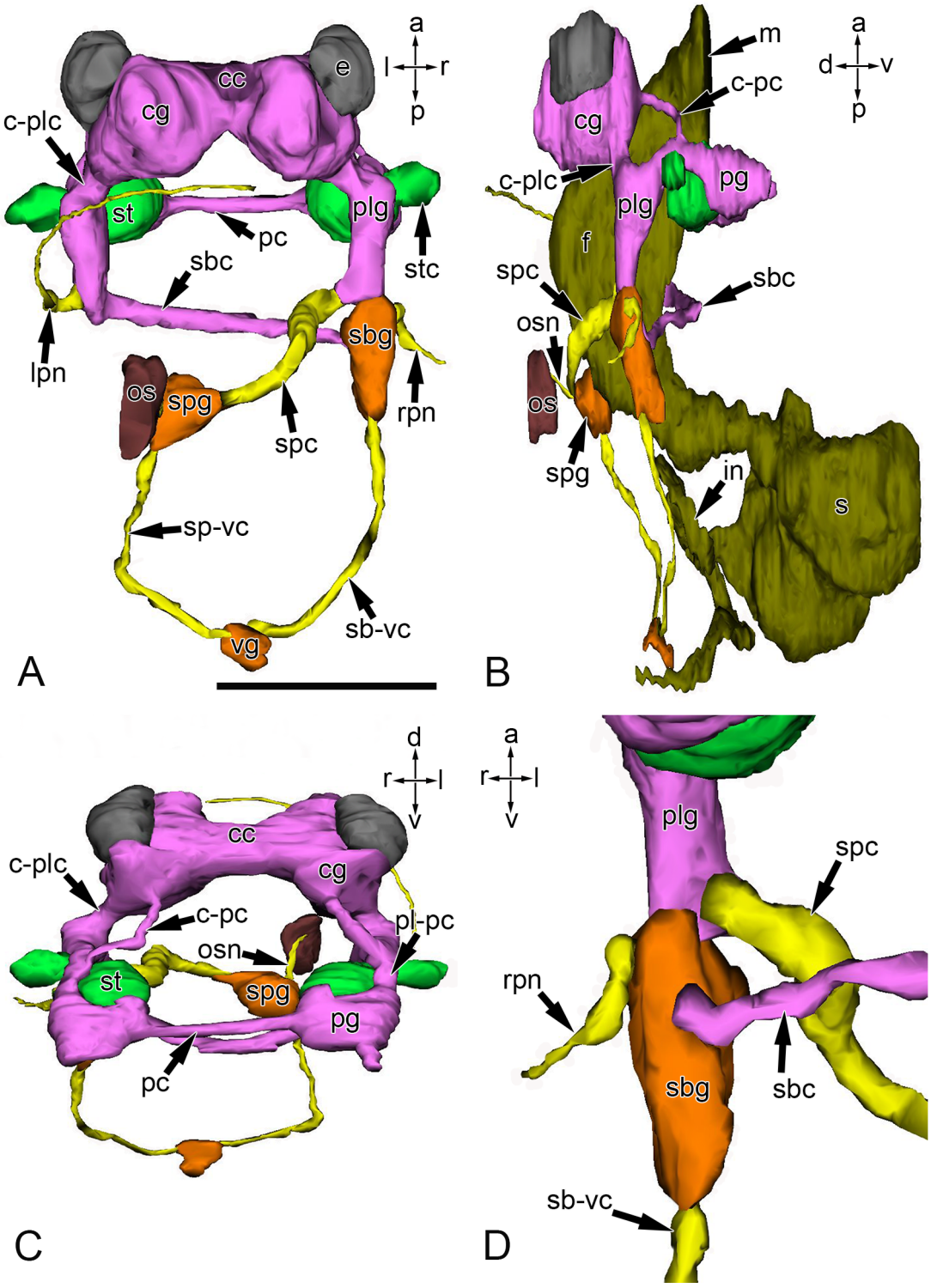

Figure 5. Surface rendered three-dimensional reconstructions showing the components of the central nervous system in newly hatched larvae of *N. melanotragus*. All ganglia of the definitive central nervous system except the buccal ganglia and second visceral ganglion are present, but the neuroanatomical shortcut between the two pleural ganglia is not yet

present. **A.** Dorsal view; scale bar represents 50µm. **B.** Right lateral view of the central nervous system and gut (dark green), showing trajectories of the supraintestinal and subintestinal connectives and the osphradial nerve extending from the supraintestinal ganglion. **C.** Anterior view showing trajectories of the cerebro-pedal connectives, pleuro-pedal connectives, pedal commissure and osphradial nerve. **D.** Enlarged, ventral view of the subintestinal connective connecting with the medial side of the subintestinal ganglion, also note the right pallial nerve emanating from the lateral side of the subintestinal ganglion. Abbreviations: cc= cerebral commissure, cg= cerebral ganglion, c-pc= cerebro-pedal connective, c-plc= cerebro-pleural connective, e= eye, f= foregut, in= intestine, lpn= left pallial nerve, m= mouth, os= osphradium, osn= osphradial nerve, pc= pedal commissure, pg= pedal ganglion, plg= pleural ganglion, pl-pc= pleuro-pedal connective, rpn= right pallial nerve, sbg= subintestinal ganglion, sbc= subintestinal connective, sb-vc= subintestinal-visceral connective, s= stomach, spg= supraintestinal ganglion, spc= supraintestinal connective, sp-vc= supraintestinal-visceral connective, st= statocyst, stc= static canal, vg= visceral ganglion. Orientation axes: a= anterior, d= dorsal, l= left, p= posterior, r= right, v= ventral.

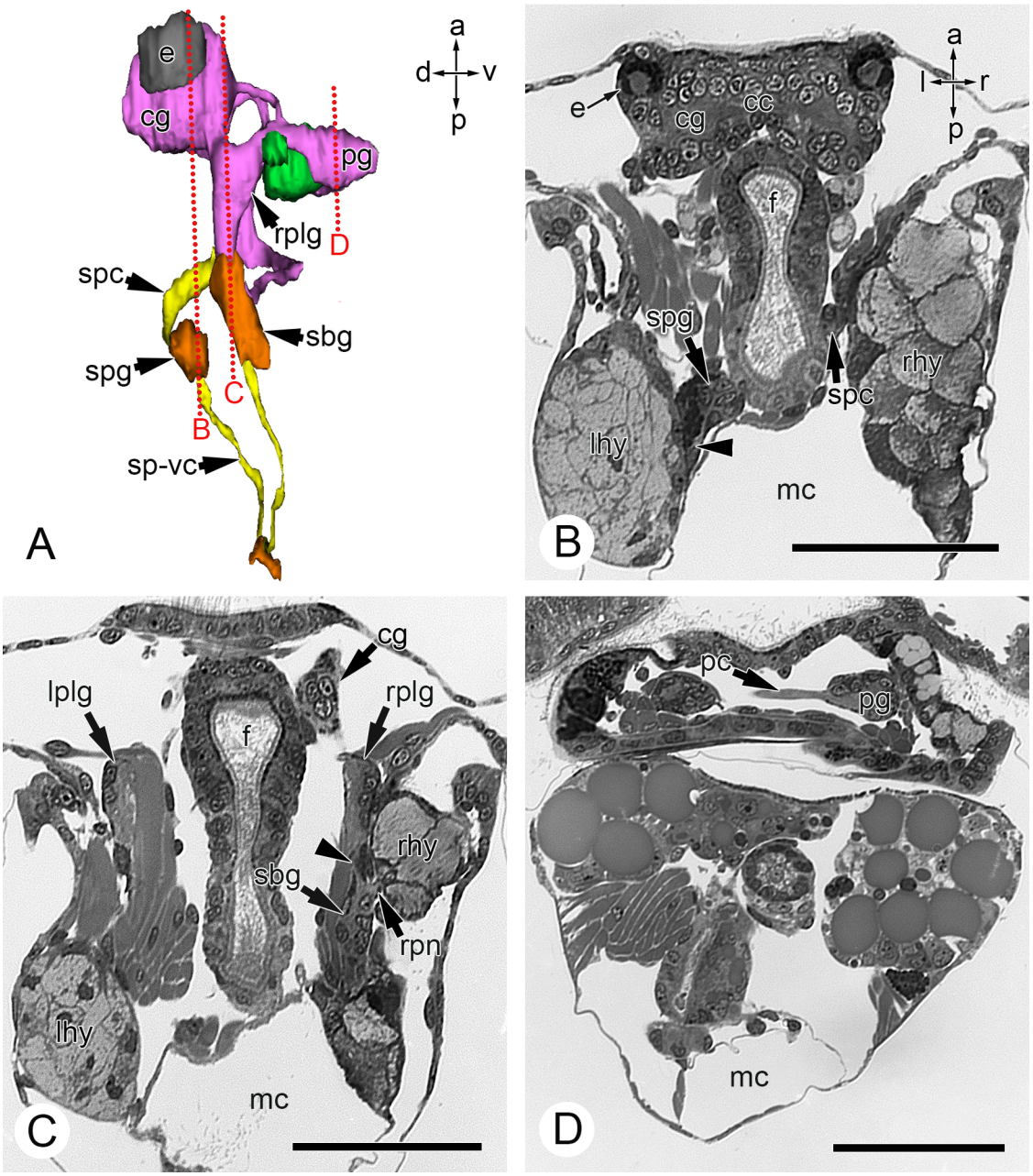

Figure 6. Histological frontal-sections displaying the major ganglia of the central nervous system in newly hatched *N. melanotragus*. All sections displayed in dorsal view; scale bars 50µm. **A.** Right lateral view of a surface rendered three-dimensional reconstruction of the central nervous system; the dotted red lines indicate planes of section for B-D. **B.** Section through the cerebral ganglia, cerebral commissure and eyes; *arrowhead* indicates the supraintestinal-visceral connective emanating from the supraintestinal ganglion; notice the supraintestinal connective on the right side of the foregut. **C.** Section through the elongate pleural ganglia and the connection between the

right pleural ganglion and subintestinal ganglion (*arrowhead*); notice the right pallial nerve emerging from the lateral side of the subintestinal ganglion. **D.** Section passing through the pedal ganglia and the thin pedal commissure. Abbreviations: cc= cerebral commissure, cg= cerebral ganglion, e= eye, f= foregut, lhy= left hypobranchial gland, lplg= left pleural ganglion, mc= mantle cavity, pc= pedal commissure, pg= pedal ganglion, rhy= right hypobranchial gland, rplg= right pleural ganglion, sbg= subintestinal ganglion, sp-vc= supraintestinal-visceral connective, spg= supraintestinal ganglion. Orientation axes: a= anterior, d= dorsal, l= left, p=posterior, r= right, v= ventral.

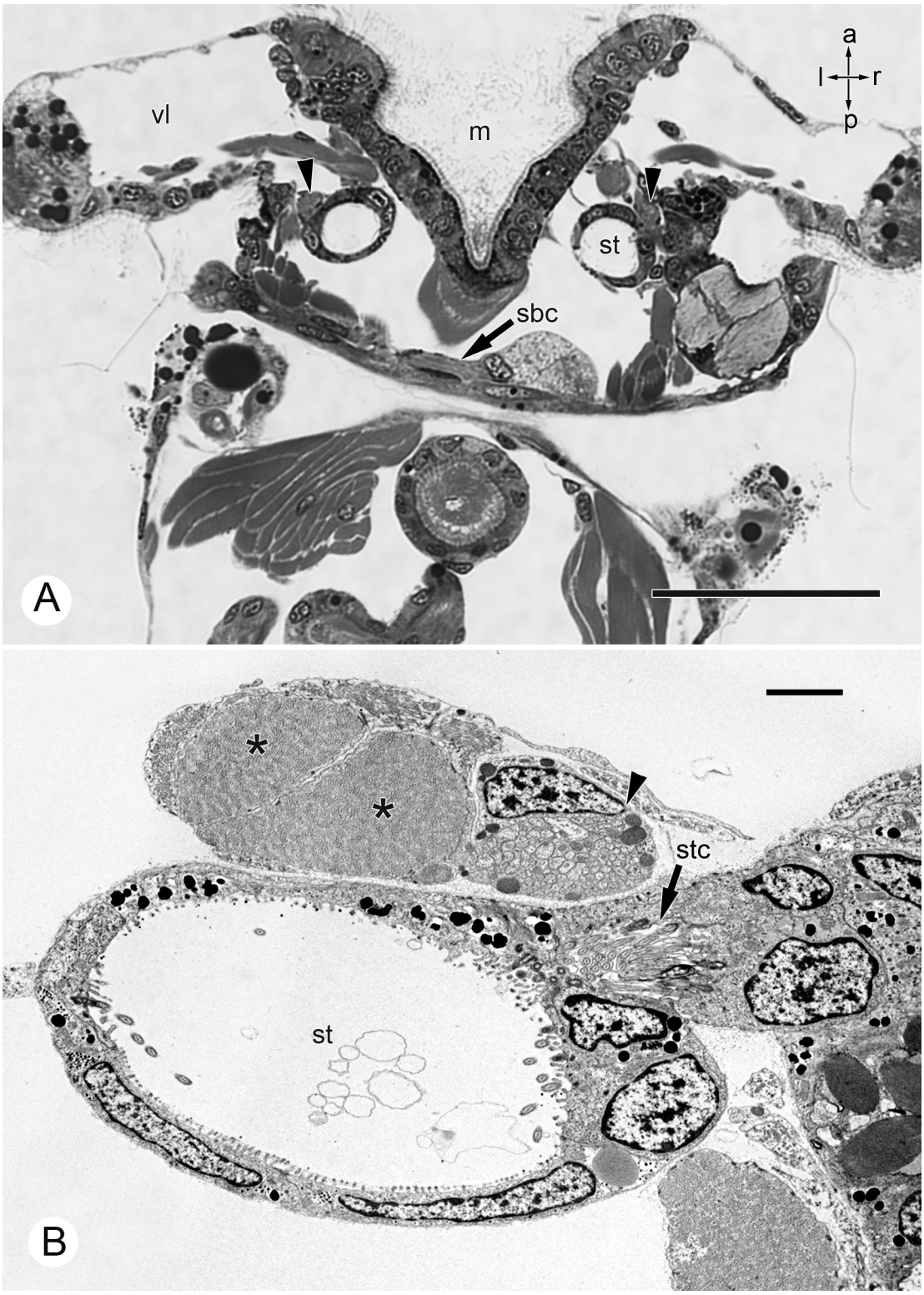

Figure 7. Frontal-sections through the pleuro-pedal and the subintestinal connectives; all sections displayed in dorsal view. **A.** Histological section, showing the anterolateral position of the pleuro-pedal connectives (*arrowheads*) over the statocysts and the ventral

trajectory of the subintestinal connective running beneath the esophagus; scale bar 50µm. **B.** Transmission electron micrograph of a section through the right pleuro-pedal connective (*arrowhead*), the right statocyst and static canal, and two cells of the larval retractor muscle (*asterisks*); scale bar 2 µm. Abbreviations: m= mouth, sbc= subintestinal connective, st= statocyst, stc= static canal, vl=velar lobe. Orientation axes: a= anterior, l= left, p=posterior, r= right.

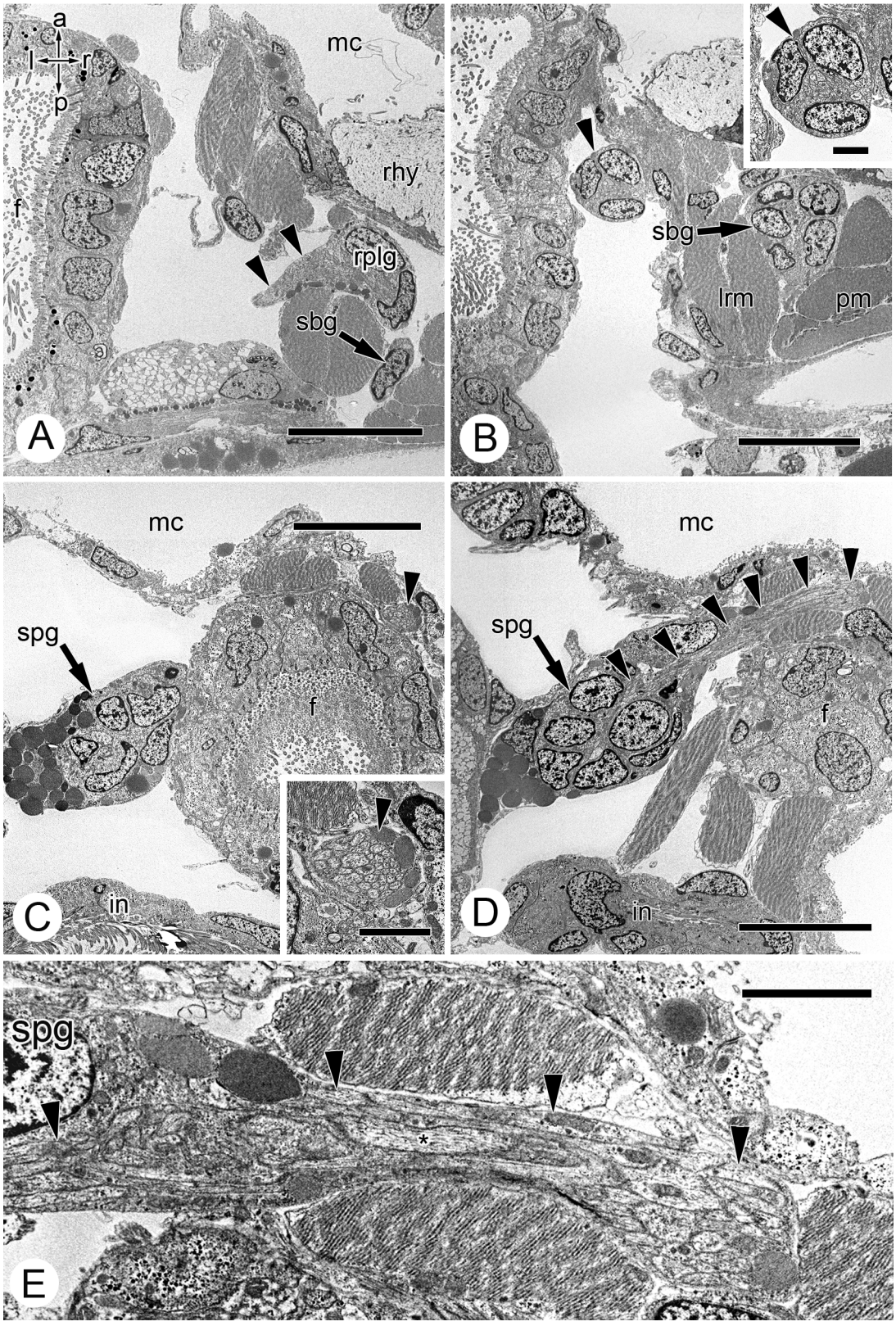

Figure 8. Transmission electron micrographs of frontal-sections showing the trajectory of the supraintestinal connective from the right pleural ganglion, passing dorsally over

the esophagus to the supraintestinal ganglion on the left; all sections displayed in dorsal view. **A.** Supraintestinal connective (*arrowheads*) emerging medially from the dorsal surface of the right pleural ganglion; scale bar 10µm. **B.** Section through a more postero-dorsal region of the supraintestinal connective (*arrowhead*) as it travels leftward from the right pleural ganglion; scale bar 10µm. *Inset*: Higher magnification of the supraintestinal connective; scale bar 2µm. **C.** Section through the supraintestinal connective (*arrowhead*) extending dorsally over the foregut; note the supraintestinal ganglion to the left of the foregut; scale bar 10µm. *Inset*: Higher magnification of the supraintestinal connective; scale bar 2µm. **D.** Supraintestinal connective (*arrowheads*) extending dorsally over the foregut and entering the supraintestinal ganglion on the left; scale bar 10µm. **E.** Higher magnification of the supraintestinal connective joining the supraintestinal ganglion; *asterisk* indicates an individual neurite; scale bar 2µm. Abbreviations: f= foregut, in= intestine, lrm= larval retractor muscle, mc= mantle cavity, pm= pedal muscle, rhy= right hypobranchial gland, rplg= right pleural ganglion, sbg= subintestinal ganglion, spg= supraintestinal ganglion. Orientation axes: a= anterior, l= left, p=posterior, r= right.

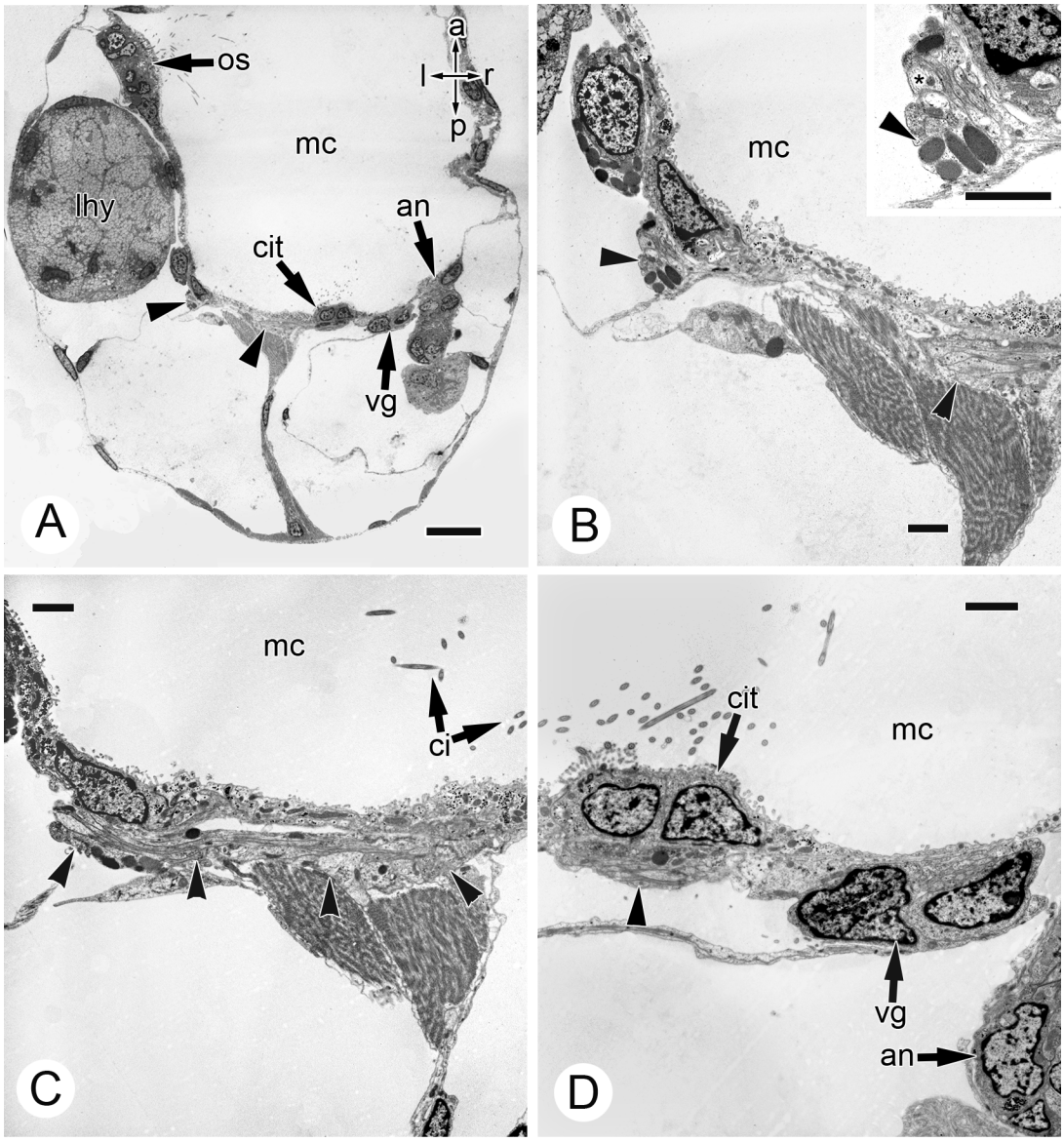

Figure 9. Transmission electron micrographs of frontal-sections showing the trajectory of the supraintestinal-visceral connective; all sections displayed in dorsal view. **A.** Low magnification micrograph through the postero-dorsal region of the mantle cavity showing two portions of the supraintestinal-visceral connective (*arrowheads*) and the visceral ganglion situated beneath the epithelium of the floor of the mantle cavity, between a ciliary tract and the anus; also note the osphradium and the left hypobranchial gland; scale bar 10µm. **B.** Higher magnification of the two portions of the supraintestinal-visceral connective shown in 'A'; scale bar 2µm. *Inset*: Higher magnification of the left portion of the supraintestinal-visceral connective from the same section; *asterisk* indicates an individual neurite; scale bar 2µm. **C.** Section just dorsal to the section

depicted in B; note the two portions of the supraintestinal-visceral connective have joined and it is extending further to the right as denoted by the cilia of the ciliary tract; scale bar 2µm. **D.** Section just dorsal to the section depicted in C; note the supraintestinal-visceral connective is now situated just beneath the ciliated tract of the mantle cavity, and extending towards the visceral ganglion; scale bar 2µm. Abbreviations: an= anus, ci= cilia, cit= ciliated tract, lhy= left hypobranchial gland, mc= mantle cavity, os= osphradium, vg= visceral ganglion. Orientation axes: a= anterior, l= left, p=posterior, r= right.

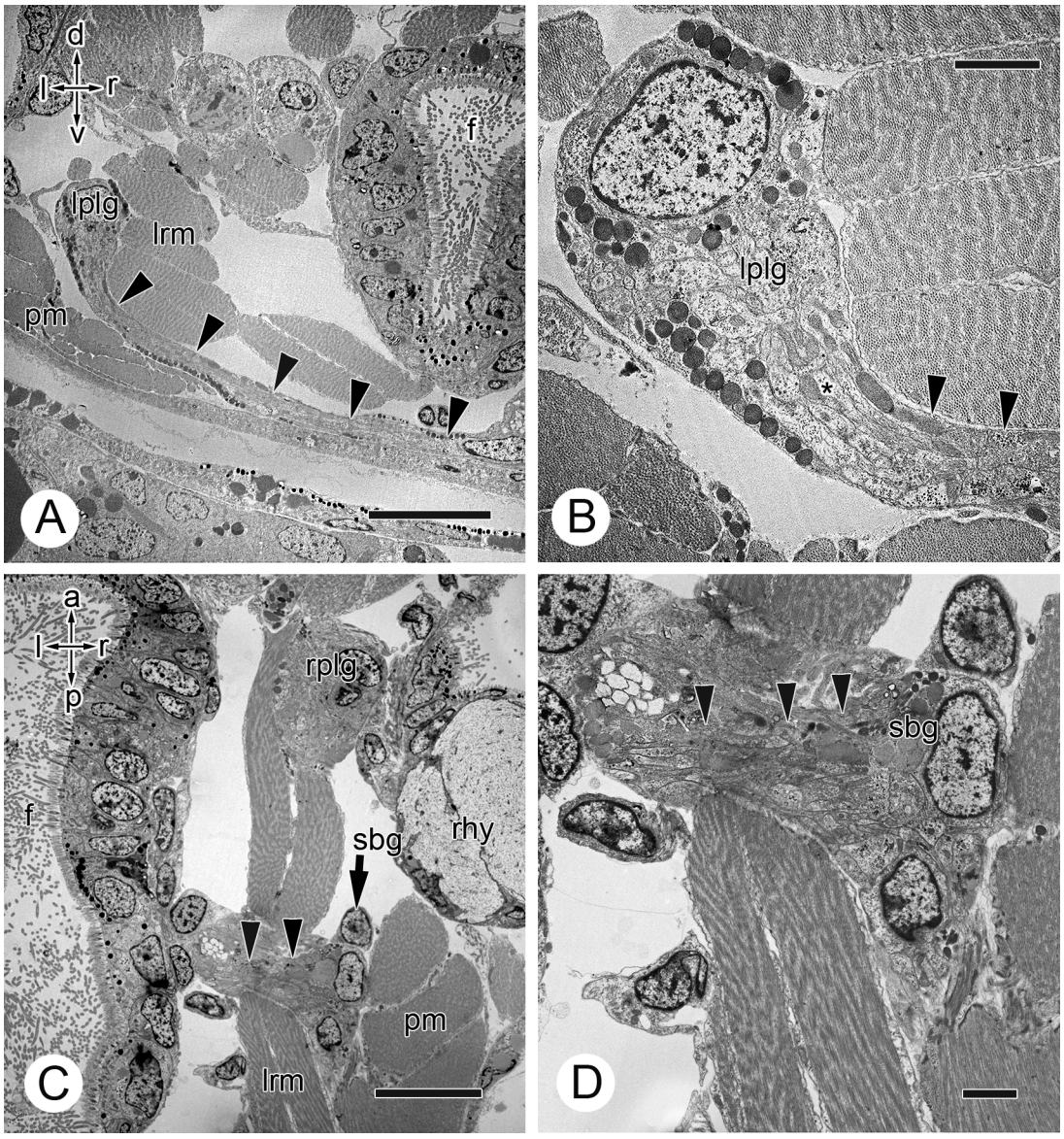

Figure 10. Transmission electron micrographs of transverse- and frontal-sections showing the trajectory of the subintestinal connective from the left pleural ganglion, passing beneath the esophagus ventrally to the subintestinal ganglion on the right; A and B are displayed in posterior view and C and D are displayed in dorsal view. **A.** Transverse-section through the subintestinal connective (*arrowheads*) as it emerges from the left pleural ganglion to travel rightward beneath the foregut; scale bar 10µm. **B.** Higher magnification of the left pleural ganglion giving rise to the subintestinal connective (*arrowheads*); asterisk indicates an individual neurite; scale bar 2µm. **C.** Frontal-section through the right portion of the subintestinal connective (*arrowheads*) where it traverses the right larval retractor muscle to enter the subintestinal ganglion;

scale bar 10µm. **D.** Higher magnification of the subintestinal connective (*arrowheads*) connecting with the subintestinal ganglion; scale bar 2µm. Abbreviations: f= foregut, lplg= left pleural ganglion, lrm= larval retractor muscle, pm= pedal muscle, rhy= right hypobranchial gland, rplg= right pleural ganglion, sbg= subintestinal ganglion. Orientation axes: a= anterior, d= dorsal, l= left, p= posterior, r= right, v= ventral.

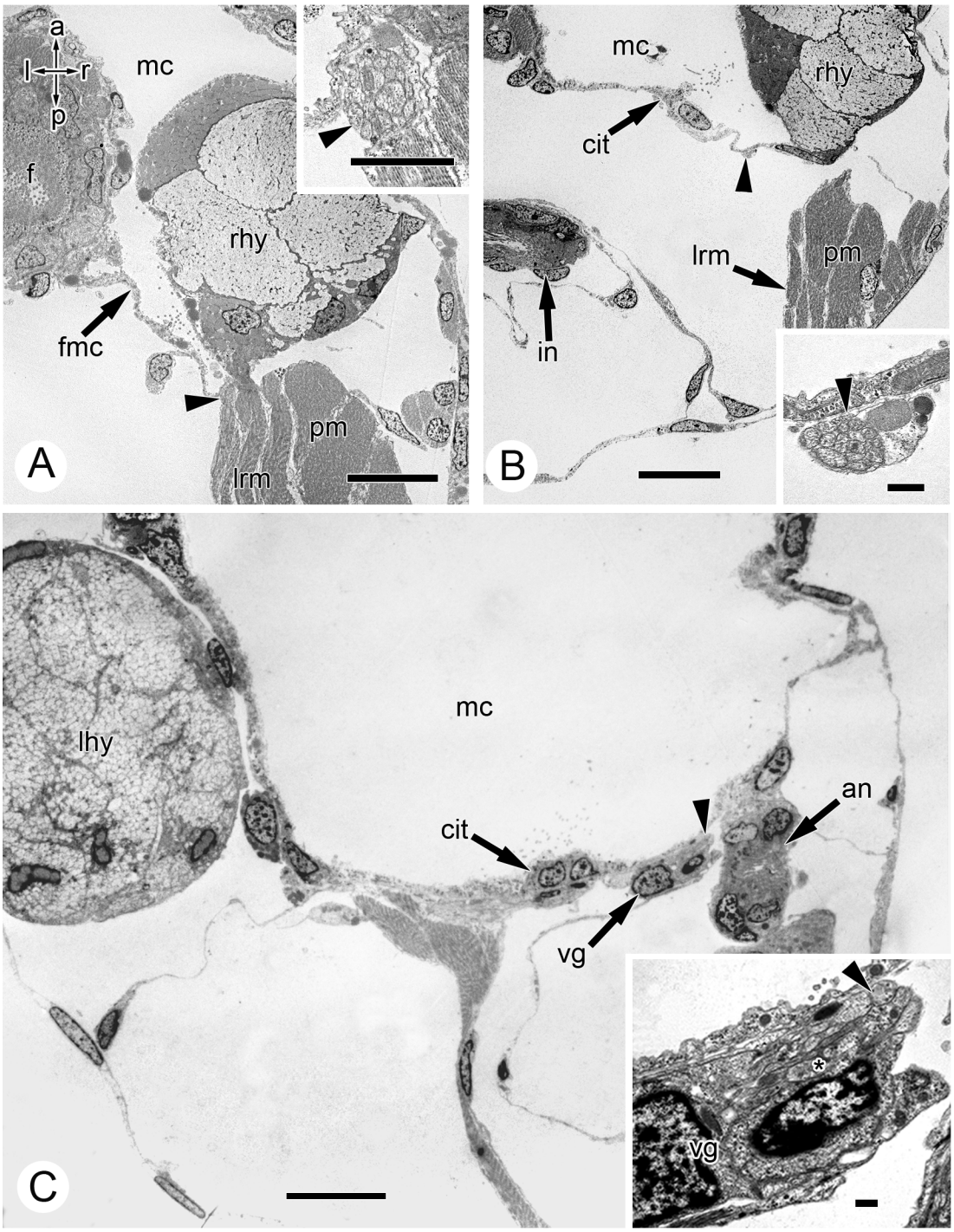

Figure 11. Transmission electron micrographs of frontal-sections showing the trajectory of the subintestinal-visceral connective in newly hatched *N. melanotragus*; all sections displayed in dorsal view. **A.** Section through an anterior portion of the subintestinal-visceral connective (*arrowhead*) where it lies beneath the floor of the mantle cavity adjacent to the right hypobranchial gland; scale bar 10µm. *Inset*: Higher magnification of

the subintestinal-visceral connective (*arrowhead*) from the same section; scale bar represents 2µm. **B.** Section of a more posterior region of the subintestinal-visceral connective (*arrowhead*) as it traverses posteromedially along the floor of the mantle cavity and is situated in close proximity to the right side of the ciliated tract; scale bar 10µm. *Inset*: Higher magnification of the subintestinal-visceral connective (*arrowhead*) from the same section; scale bar 500nm. **C.** Section through the back of the mantle cavity where the subintestinal-visceral connective (*arrowhead*) enters the visceral ganglion adjacent to the anus; scale bar 10µm. *Inset*: Higher magnification of the merger between the subintestinal-visceral connective (*arrowhead*) and the visceral ganglion; *asterisk* indicates an individual neurite; scale bar 500nm. Abbreviations: an= anus, cit= ciliated tract, f= foregut, fmc= floor of the mantle cavity, in= intestine, lhy= left hypobranchial gland, lrm= larval retractor muscle, mc= mantle cavity, pm= pedal muscle, rhy= right hypobranchial gland, vg= visceral ganglion. Orientation axes: a= anterior, l= left, p=posterior, r= right.

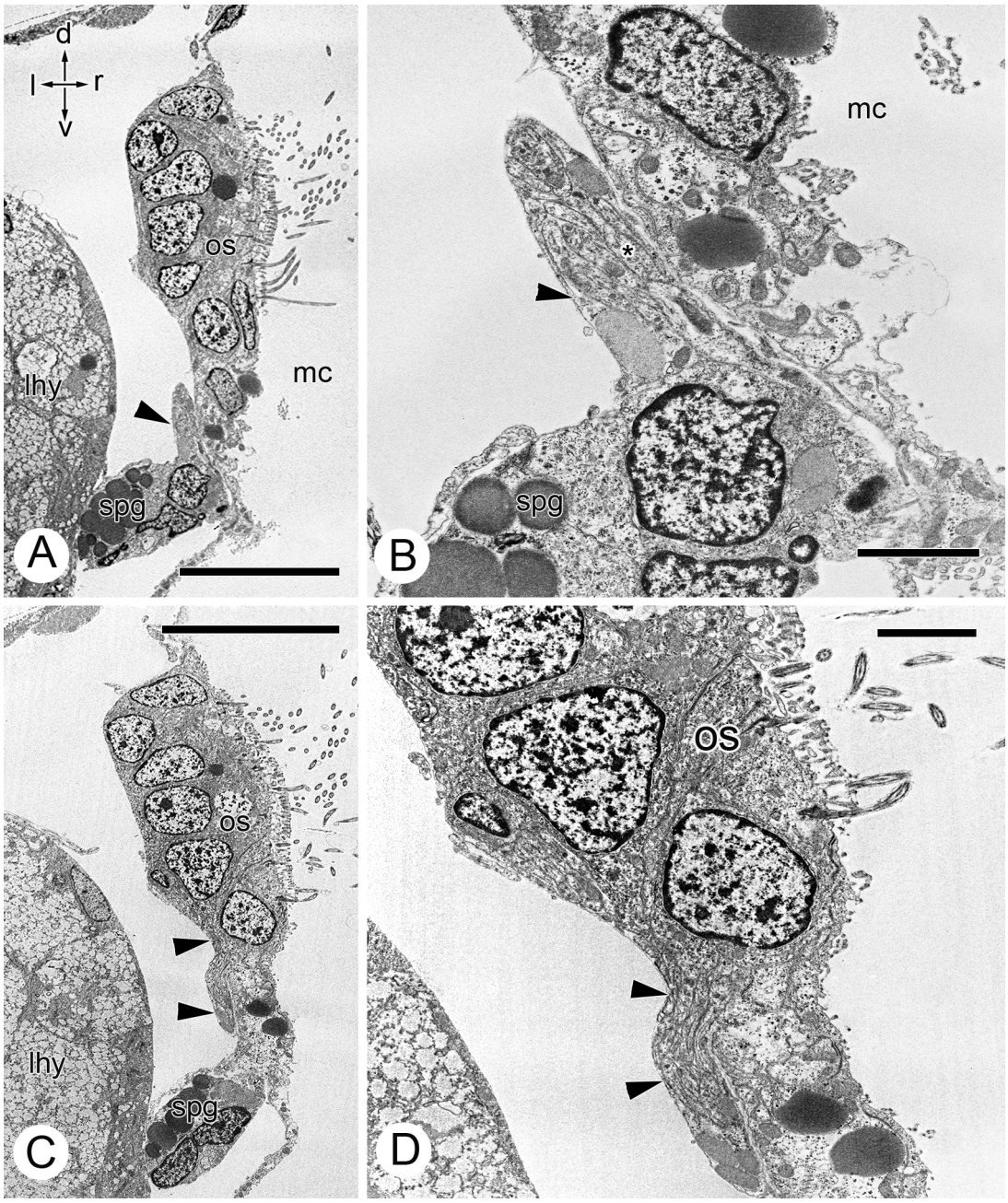

Figure 12. Transmission electron micrographs of transverse-sections showing the trajectory of the osphradial nerve on the left side of the body; all sections are displayed in posterior view. **A.** Osphradial nerve (*arrowhead*) emerging dorsally from the supraintestinal ganglion; scale bar 10µm. **B.** Higher magnification of the osphradial nerve (*arrowhead*) emerging from the supraintestinal ganglion; *asterisk* indicates an individual neurite; scale bar 2µm. **C.** Osphradial nerve (*arrowheads*) innervating the osphradial epithelium; scale bar 10µm. **D.** Higher magnification of the osphradial nerve

(*arrowheads*) innervating the osphradium; scale bar 2µm. Abbreviations: lhy= left hypobranchial gland, mc= mantle cavity, os= osphradium, spg= supraintestinal ganglion. Orientation axes: d= dorsal, l= left, r= right, v= ventral.

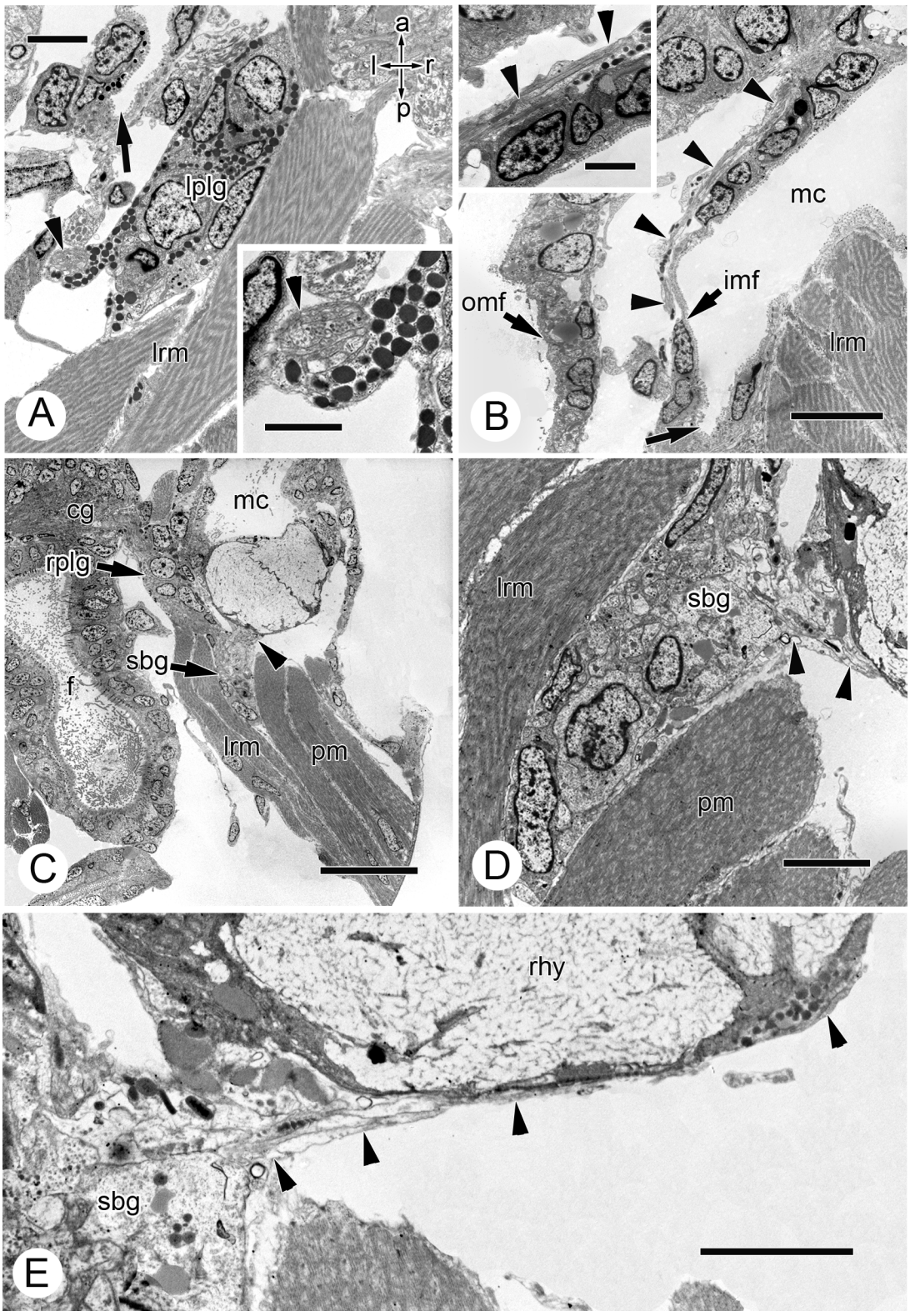

Figure 13. Transmission electron micrographs of frontal-sections showing the trajectories of both the left and right pallial nerves of newly hatched *N. melanotragus*; all

sections are displayed in dorsal view. **A.** Left pallial nerve (*arrowhead*) emerging from the extreme posterolateral surface of the left pleural ganglion; *arrow* indicates the left "corner" of the mantle cavity where the floor and the left wall meet; scale bar 4µm. *Inset*: Higher magnification of the left pallial nerve; scale bar 2µm. **B.** Section through the dorsal-most portion of the left pallial nerve (*arrowheads*) as it extends to the peripheral edge of the mantle fold; *arrow* indicates the left "corner" of the mantle cavity; scale bar 6µm. *Inset*: higher magnification of the left pallial nerve (*arrowheads*); scale bar 2µm. **C.** Right pallial nerve (*arrowhead*) emerging from the subintestinal ganglion at the point where the right pleural ganglion and subintestinal ganglion are connected; scale bar 20µm. **D.** Higher magnification of the right pallial nerve (*arrowheads*) emerging laterally from the anterior of the subintestinal ganglion; scale bar 4µm. **E.** Section through the right pallial nerve slightly more dorsal to the section depicted in C and at higher magnification; note the lateral trajectory of the right pallial nerve (*arrowheads*) and the very close association with the posterior of the right hypobranchial gland; scale bar 4µm. Abbreviations: cg= cerebral ganglion, f= foregut, imf= inner-mantle fold epithelium, lplg= left pleural ganglion, lrm= larval retractor muscle, mc= mantle cavity, omf= outer-mantle fold epithelium, pm= pedal muscle, rhy= right hypobranchial gland, rplg= right pleural ganglion, sbg= subintestinal ganglion. Orientation axes: a= anterior, l= left, p=posterior, r= right.

3.1.2 Developmental stage 2: 18 days post hatching

3.1.2.1 Esophageal nerve ring

By 18 days post hatching (dph), all ganglia, connectives and commissures of the esophageal nerve ring were larger, but were in the same relative configuration (Fig. 14). The cerebral ganglia measured 50µm in diameter, were farther apart and had taken up more lateral positions in relation to the foregut (Figs. 14B); hence the commissure was more elongate but still ran dorsally over the foregut (Fig. 14A, B). The pedal ganglia were less globular and had started to taper into cords that ran ventrally within the foot (Fig. 14B, C). Furthermore, the number of neuronal somata in the medial regions of the each pedal ganglion had increased (not shown), making the pedal commissure appear shorter, although it was still relatively long and slender (Fig. 14B, C). The pleural ganglia were more globular and extended dorsally to a much greater extent than in the newly hatched stage (Figs. 14B, C). The buccal ganglia had not yet developed.

3.1.2.2 Visceral loop

The visceral loop included four ganglia by 18 dph: the subintestinal ganglion, supraintestinal ganglion, the first visceral ganglion, and the second visceral ganglion (Fig. 14). All ganglia and connectives of the visceral loop could be resolved using light microscopy at this stage; however, transmission electron microscopy was used to confirm the trajectory of the posterior portions of the intestinal-visceral connectives and the positions of the visceral ganglia. The ganglia of the visceral loop had increased in size, and the connectives had increased in length. The width of the visceral loop measured approximately 110µm in width and 150µm in length by this stage (Fig. 14A).

Other than size and/or length, no significant changes occurred to the position of the supraintestinal ganglion, or the trajectories of the supraintestinal connective and supraintestinal-visceral connective (Fig. 14). However, some changes occurred within other components of the visceral loop. The position of the first visceral ganglion shifted to a more leftward position, sitting directly beneath the ciliary tract of the mantle cavity (compare Figs. 11C and 15D). The intestine lengthened, which resulted in the anus being

situated in a more dorsal position and was thus no longer within the same plane of section as the first visceral ganglion (compare Figs. 11C and 15D, E). The second visceral ganglion developed at the right-posterior end of the visceral loop (Figs. 14A, B; 16). The origin of the second visceral ganglion occured just after the subintestinal-visceral connective emerged from the medial edge of the right larval retractor muscle and just before the connective looped to the left and extended to the first visceral ganglion (Fig. 16C, D, E).

At 18 dph, the fusion between the subintestinal and the right pleural ganglion became more extensive (Figs. 14A, B, D), but the boundary between the two ganglia was not as easily discernable at this stage. However, the supraintestinal connective consistently emerged medially from the extreme dorsum of the right pleural ganglion (Figs. 5A; 8A; 14A, B, D; 16A) and could thus be used as a landmark for where the right pleural ganglion ended and the subintestinal ganglion began. The subintestinal connective still emerged medially from the posterodorsal surface of the left pleural ganglion and extended ventrally beneath the foregut to the right side of the body (Figs. 14A; 17A). Remarkably, the subintestinal connective no longer connected to the subintestinal ganglion; although it remained close to the subintestinal ganglion at this stage, it directly connected to the right pleural ganglion, forming the characteristic neuroanatomical shortcut between the two pleural ganglia of the Neritimorpha (compare Figs. 5A, D with 14A, D; and Figs. 10C, D with 17B, C, D).

3.1.2.3 Sensory organs

The osphradium was intimately associated with the left wall of the mantle cavity, and as the mantle cavity expanded during development, the osphradium became positioned more anterolaterally, beyond the left cerebral ganglion (Fig. 14A). The osphradial nerve between the osphradium and the supraintestinal ganglion was longer, and the osphradial nerve no longer directly innervated the osphradium (Fig. 18). Instead, the osphradial ganglion had developed by this stage and the osphradial nerve now ran anteroventrally from the supraintestinal ganglion to the osphradial ganglion, which

innervated the osphradium (Fig. 14C; 18). Furthermore, a secondary connective had formed between the osphradial ganglion and the left pleural ganglion (Figs. 14B, C; 19). The pleuro-osphdradial connective exited the left pleural ganglion laterally, posterior to where the left pallial nerve emerges; it traveled anterodorsally between the left pedal muscle and the epithelium of the mantle cavity and connected with the ventral surface of the osphradial ganglion (Figs. 14B, C; Fig. 19).

The eyes sat distally on short optic nerves that had formed by this stage. Each optic nerve extended laterally from their associated cerebral ganglion (Figs. 14C; 20E).

3.1.2.3 Pallial nerves

At 18 dph, the pallial nerves were much more distinct and robust and could be resolved in their entirety using light microscopy. The right pallial nerve no longer emerged from the subintestinal ganglion at this stage, but rather it emerged from the right pleural ganglion, just ventral to where the right pleural ganglion connected with the subintestinal ganglion, and slightly dorsal to the plane in which the shortcut connected to the other side of the right pleural ganglion (compare Figs. 5A, B, D with 14B, D; and 13D, E with 20C). Furthermore, the right pallial nerve remained very closely associated with the posterior surface of the right hypobranchial gland (Fig. 20D).

The trajectories of the left and right pallial nerves formed an anteroventral loop between the two pleural ganglia that extended within the mantle fold roofing the mantle cavity (Figs. 14A; 20F). The left and right pallial nerves exited their respective pleural ganglia laterally, extended to the periphery of either side of the body and then looped up anteriorly between the epithelial layers of the mantle fold where they traveled anteroventrally toward each other and eventually anastomosed apically within the larva (Figs. 14; 20). The pallial nerves gave rise to many peripheral fiber tracts that innervated various aspects of the mantle cavity (not shown).

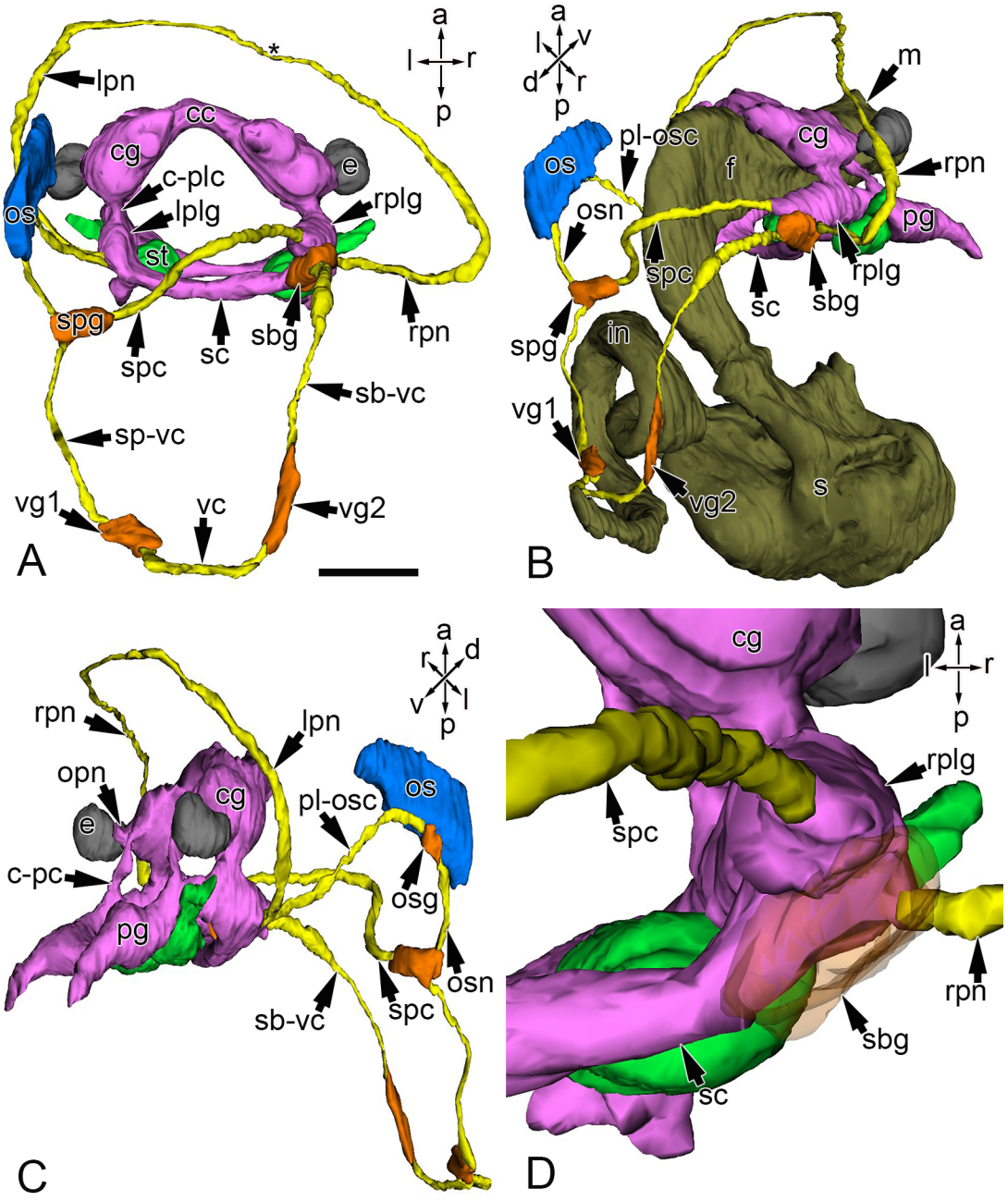

Figure 14. Surface rendered three-dimensional reconstructions showing the components of the central nervous system in 18 dph *N. melanotragus*; notice that the neuroanatomical shortcut between the two pleural ganglia has formed. **A.** Dorsal view; *asterisk* indicates where the two pallial nerves anastomose; scale bar 50µm. **B.** Right dorsolateral view of the central nervous system and gut (dark green), showing the trajectory of the supraintestinal connective, the shortcut and the osphradial nerve. **C.** Left ventrolateral view showing the left optic nerve, osphradial ganglion, osphradial nerve, and the pleuro-

osphradial connective. **D.** Enlarged, dorsal view of the subintestinal connective connecting with the medial side of the right pleural ganglion to form the neuroanatomical shortcut between the two pleural ganglia; note that the subintestinal ganglion has been rendered semi-transparent; also note the right pallial nerve emerging from the lateral side of the right pleural ganglion. Abbreviations: cc= cerebral commissure, cg= cerebral ganglion, c-pc= cerebro-pedal connective, c-plc= cerebro-pleural connective, e= eye, f= foregut, in= intestine, lplg= left pleural ganglion, lpn= left pallial nerve, m= mouth, opn= optic nerve, os= osphradium, osg= osphradial ganglion, osn= osphradial nerve, pg= pedal ganglion, pl-osc= pleuro-osphradial connective, rplg= right pleural ganglion, rpn= right pallial nerve, sbg= subintestinal ganglion, sc= shortcut, sb-vc= subintestinal-visceral connective, s= stomach, spg= supraintestinal ganglion, spc= supraintestinal connective, sp-vc= supraintestinal-visceral connective, st= statocyst, vg1= first visceral ganglion, vg2= second visceral ganglion, vc= visceral commissure. Orientation axes: a= anterior, d= dorsal, l= left, p= posterior, r= right, v= ventral.

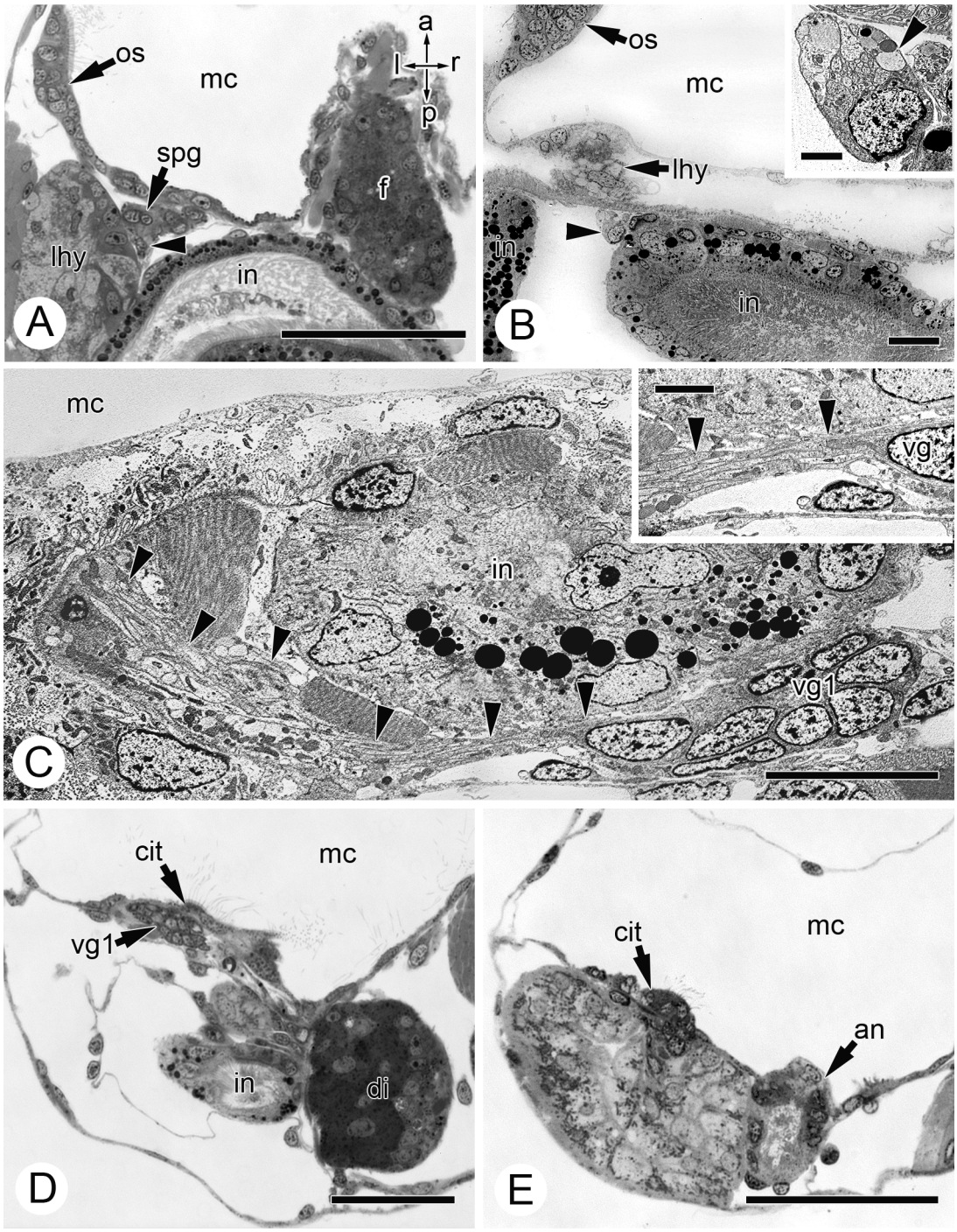

Figure 15. Frontal-sections showing the trajectory of the supraintestinal-visceral connective in 18 dph larvae of *N. melanotragus*; all sections are displayed in dorsal view. **A.** Histological section through the supraintestinal ganglion as the supraintestinal-visceral connective (*arrowhead*) emerges posteriorly and extends between the left hypobranchial gland and the intestine; scale bar 50µm. **B.** Transmision electron micrograph of the

supraintestinal-visceral connective (*arrowhead*) as it is about to pass dorsally over the intestine towards the posterior of the body; note the trajectory of the supraintestinal-visceral connective is akin to what is observed in the newly hatched stage; scale bar 10µm. *Inset*: higher magnification of the supraintestinal-visceral connective from the same section; scale bar 2µm. **C.** Transmission electron micrograph of the supraintestinal-visceral connective (*arrowheads*) entering the first visceral ganglion; scale bar 10µm. *Inset*: higher magnification of the same section, showing the supraintestinal-visceral connective (*arrowheads*) entering the first visceral ganglion; scale bar 2µm. **D.** Histological section of a more dorsal aspect of the first visceral ganglion, showing its shifted position underneath the ciliated tract of the mantle cavity; scale bar 50µm. **E.** Histological section through the dorsal mantle cavity, beyond the posterodorsal extreme of the visceral loop; note that the region where the ciliated tract of the mantle cavity and the anus exist in the same plane occurs more dorsally at the 18 dph stage than it does in the newly hatched stage of development; scale bar represents 50µm. Abbreviations: an= anus, cit= ciliated tract of the mantle cavity, di= digestive gland, f= foregut, in= intestine, lhy= left hypobranchial gland, mc= mantle cavity, os= osphradium, spg= supraintestinal ganglion, vg1= first visceral ganglion. Orientation axes: a= anterior, l= left, p=posterior, r= right.

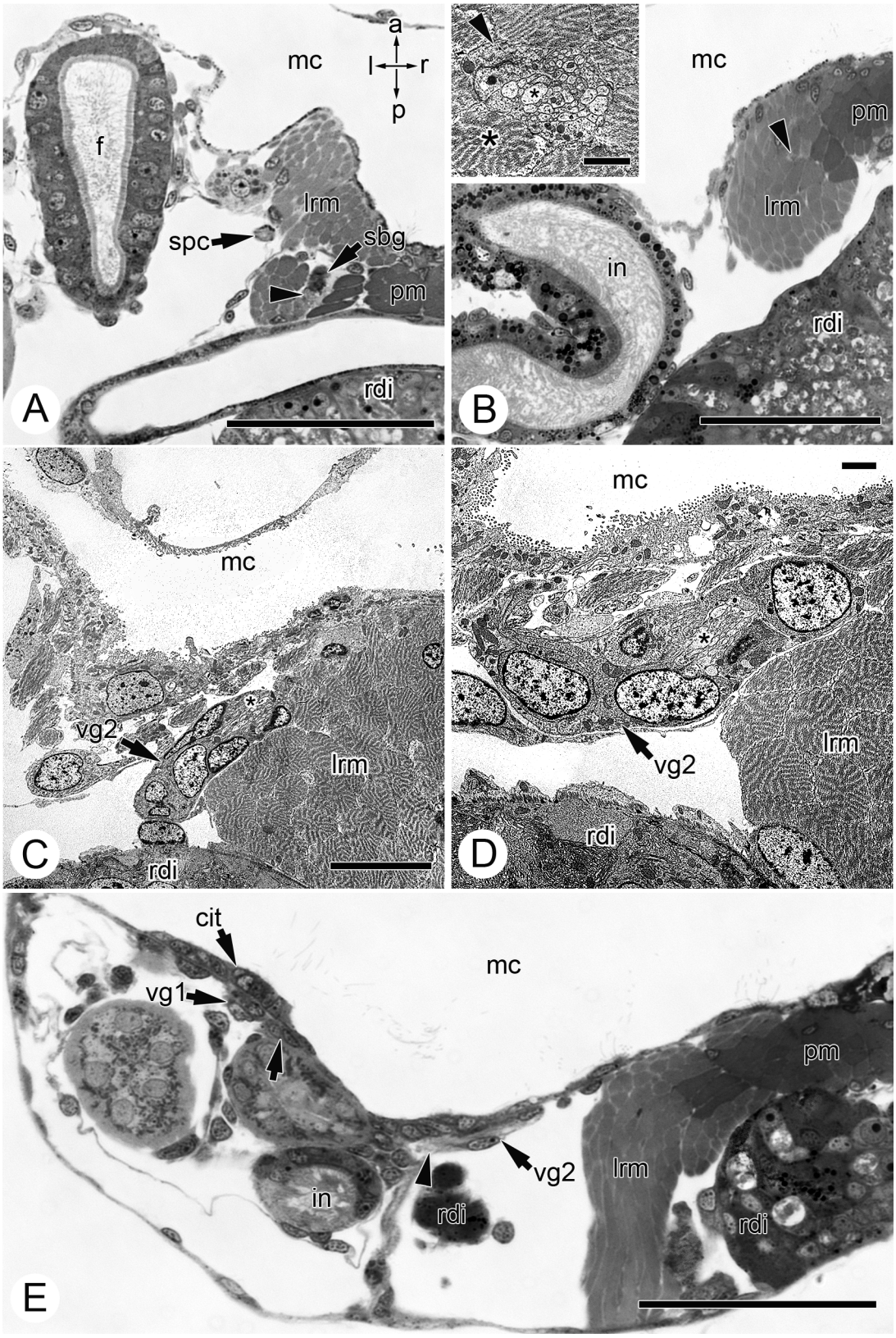
A
mc
a
l
r
p
f
lrm
spc
sbg
pm
rdi
B
mc
pm
lrm
in
rdi
C
mc
vg2
lrm
rdi
D
mc
vg2
lrm
rdi
E
cit
vg1
mc
pm
vg2
lrm
in
rdi
rdi

Figure 16. Frontal-sections displaying the trajectory of the subintestinal-visceral connective and the position of the second visceral ganglion in 18 dph *N. melanotragus*; all sections are displayed in dorsal view; note that the position of the right digestive gland makes a good reference point as it is present in all of the sections. **A.** Histological section through the extreme dorsum of the subintestinal ganglion as the subintestinal-visceral connective (*arrowhead*) is emerging posteriorly in-between the right larval retractor muscle and the right pedal muscle; scale bar 50µm. **B.** Histological section through the subintestinal-visceral connective (*arrowhead*) as it is moving posteromedially through the larval retractor muscle; scale bar 50µm. *Inset*: transmission election micrograph depicting the subintestinal-visceral connective (*arrowhead*) at an equivalent position along its trajectory; the small *asterisk* indicates an individual neurite; large *asterisk* indicates one of the larval retractor muscle cells that is surrounding the connective; scale bar 2µm. **C.** Transmission electron micrograph of the second visceral ganglion; *asterisk* indicates the neuropil; scale bar 10µm. **D.** Higher magnification transmission electron micrograph of a more dorsal region of the second visceral ganglion as it begins to extend leftward toward the first visceral ganglion; *asterisk* indicates the neuropil; scale bar 2µm. **E.** Histological section through the extreme dorsum of both visceral ganglia; *arrow* indicates the visceral commissure emerging medially from the first visceral ganglion; *arrowhead* indicates the visceral commissure emerging medially from the second visceral ganglion; note the position of the first visceral ganglion beneath the ciliated tract of the mantle cavity, and the position of the second visceral ganglion beneath the epithelium of the mantle cavity in close proximity to a portion of the right digestive gland; scale bar 50µm. Abbreviations: cit= ciliated tract of the mantle cavity, f= foregut, in= intestine, lrm= larval retractor muscle, mc= mantle cavity, pm= pedal muscle, rdi= right digestive gland, sbg= subintestinal ganglion, spc= supraintestinal connective, vg1= first visceral ganglion, vg2= second visceral ganglion. Orientation axes: a= anterior, l= left, p=posterior, r= right.

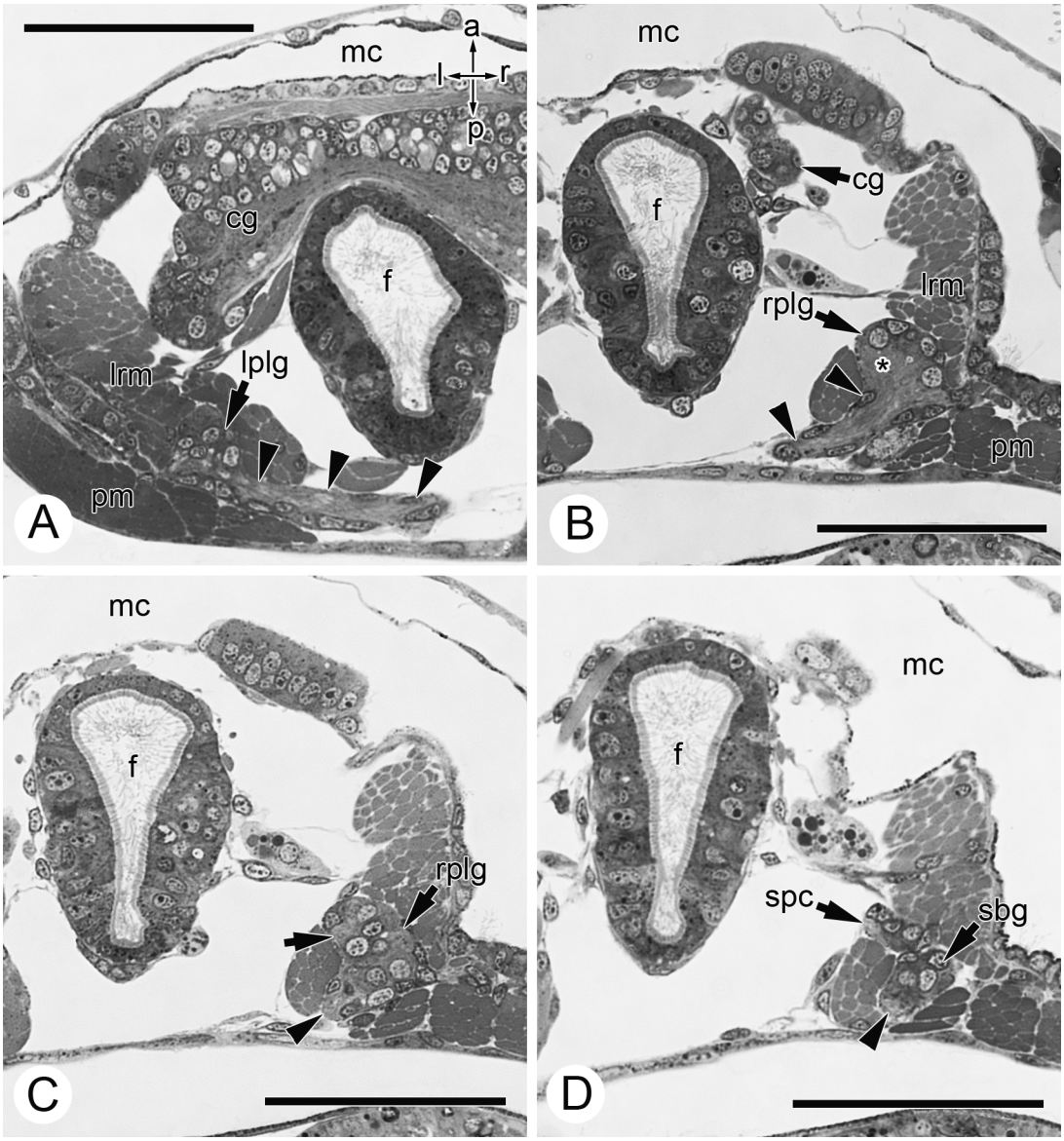

Figure 17. A series of histological frontal-sections showing the subintestinal connective emerging medially from the posterior of the left pleural ganglion, extending to the right side of the body beneath the foregut and connecting directly to the right pleural ganglion, forming the neuroanatomical shortcut between the pleural ganglia; all sections are displayed in dorsal view; scale bars 50µm. **A.** Section through the left pleural ganglia as the shortcut (*arrowheads*) is emerging medially and extending towards the right side of the body, beneath the esophagus. **B.** Section through the right pleural ganglion as the shortcut (*arrowheads*) is connecting directly with the neuropil (*asterisk*) of the right pleural ganglion. **C.** Section through a more dorsal point of the right pleural ganglion where the neuropil has become concentrated at the site of emergence of the

supraintestinal connective (*arrow*) and the site that will connect with the neuropil of the subintestinal ganglion (*arrowhead*). **D.** Section through the point where the right pleural ganglion and the subintestinal ganglion connect as indicated by the emerging supraintestinal connective; note that the connection between the right pleural ganglion and subintestinal ganglion occurs close- but dorsal to where the shortcut connects with the right pleural ganglion; *arrowhead* indicates the neuropil of the subintestinal ganglion. Abbreviations: cg= cerebral ganglion, f= foregut, lplg= left pleural ganglion, lrm= larval retractor muscle, mc= mantle cavity, pm= pedal muscle, rplg= right pleural ganglion, sbg= subintestinal ganglion, spc= supraintestinal connective. Orientation axes: a= anterior, l= left, p=posterior, r= right.

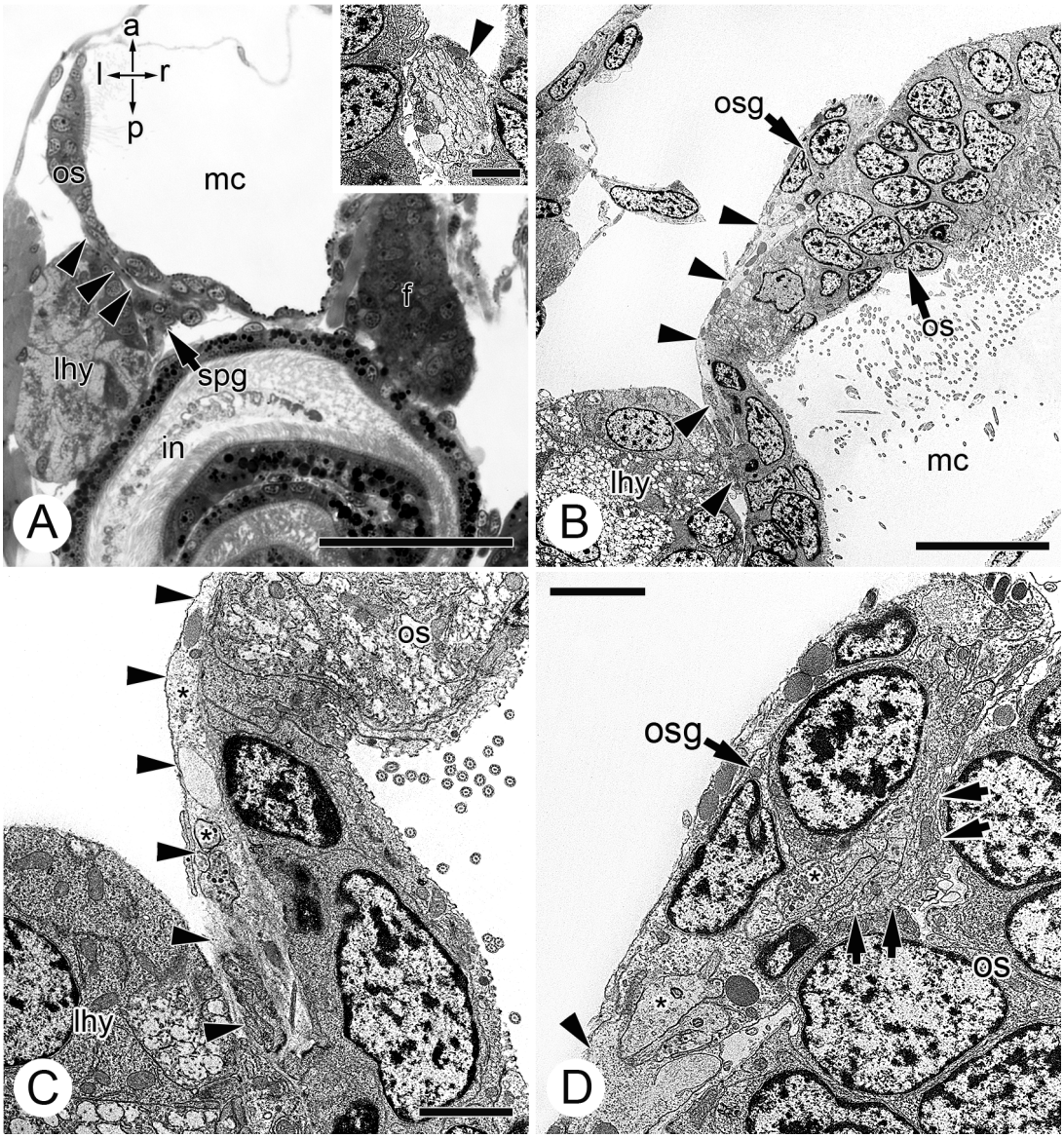

Figure 18. Frontal sections showing the trajectory of the osphradial nerve from the supraintestinal ganglion to the osphradial ganglion and the innervation of the osphradium; all sections shown in dorsal view. **A.** Histological section the supraintestinal ganglion, showing the osphradial nerve (*arrowheads*) emerging anteriorly and extending between the left hypobranchial gland and the epithelium of the mantle cavity towards the osphradium; scale bar 50µm. *Inset*: Transmission electron micrograph of the osphradial nerve at an equivalent position; scale bar 2µm. **B.** Transmission electron micrograph of the osphradial nerve (*arrowheads*) extending from between the left hypobranchial gland and epithelium of the mantle cavity and connecting posteriorly with the osphradial ganglion; scale bar 10µm. **C.** Higher magnification transmission electron micrograph of

the posterior portion of the osphradial nerve (*arrowheads*) depicted in 'B'; *asterisks* indicate individual neurites; scale bar 2µm. **D.** Higher magnification transmission electron micrograph of the anterior portion of the osphradial nerve (*arrowhead*) depicted in 'B' connecting with the osphradial ganglion; *asterisks* indicate individual neurites; *arrows* indicate the region where neurites from the osphradial ganglion are penetrating the epithelium of the osphradium; scale bar represents 2µm. Abbreviations: f= foregut, in= intestine, lhy= left hypobranchial gland; mc= mantle cavity, os= osphradium, osg= osphradial ganglion. Orientation axes: a= anterior, l= left, p=posterior, r= right.

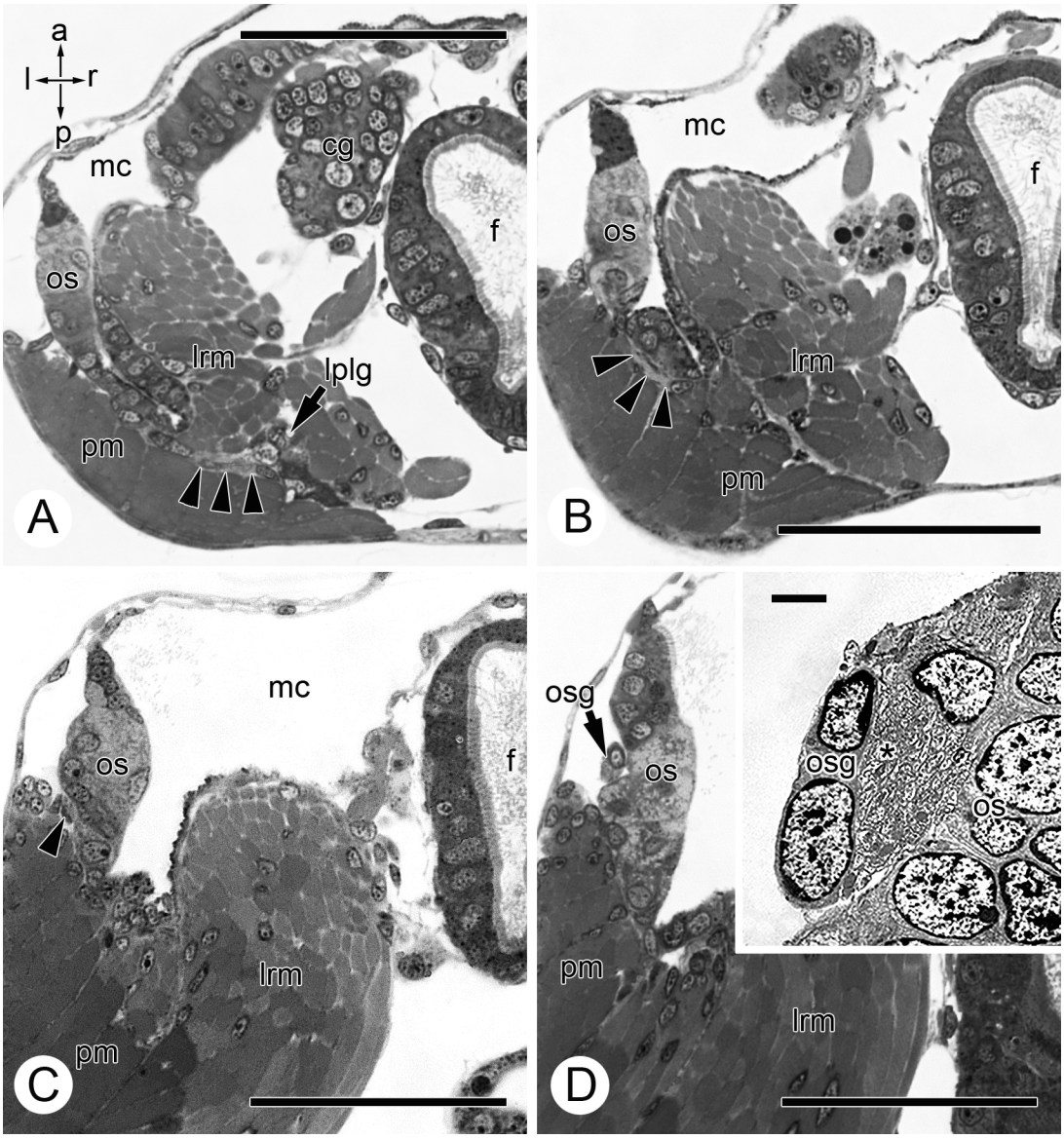

Figure 19. A series of frontal-sections showing key points along the length of the pleuro-osphradial connective; all sections are shown in dorsal view. **A.** Histological section through the left pleural ganglion, showing the pleuro-osphradial connective (*arrowheads*) emerging laterally; scale bar 50µm. **B.** Histological section through the pleuro-osphradial connective (*arrowhead*) as it runs between the pedal muscle and the epithelium of the mantle cavity towards the osphradium; scale bar 50µm. **C.** Histological section through the pleuro-osphradial connective (*arrowhead*) as it is emerging from between the pedal muscle and the epithelium of the mantle cavity to become closely associated with the osphradium; scale bar 50µm. **D.** Histological section through the ventral origin of the osphradial ganglion and thus the connection point between it, and the pleuro-osphradial

connective; scale bar 50µm. *Inset*: Transmission electron micrograph of the osphradial ganglion; *asterisk* indicates the neuropil; scale bar 2µm. Abbreviations: cg= cerebral ganglion, f= foregut, lplg= left pleural ganglion, lrm= larval retractor muscle, mc= mantle cavity, os= osphradium, osg= osphradial ganglion, pm= pedal muscle. Orientation axes: a= anterior, l= left, p=posterior, r= right.

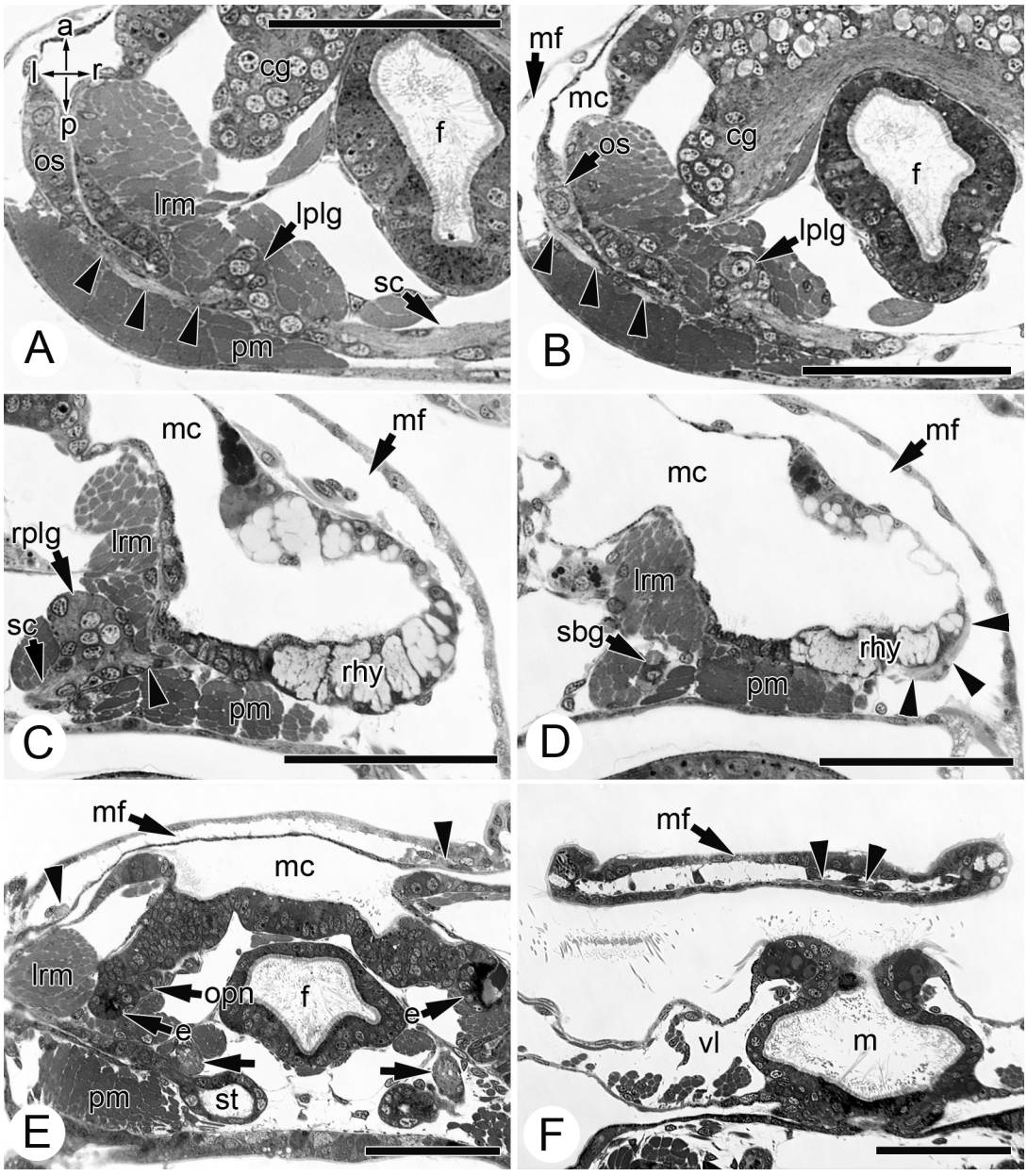

Figure 20. Histological frontal-sections showing the trajectories of left and right pallial nerves in 18 dph *N. melanotragus*; all sections displayed in dorsal view; scale bars 50µm.

A. Left pleural ganglion where the left pallial nerve is extending anterolaterally towards the mantle fold; note that the connection between the left pallial nerve and the left pleural ganglion occurs within the same plane as the connection between the left pleural ganglion and the shortcut. **B.** Left pallial nerve (*arrowheads*) entering the left side of the mantle fold. **C.** Right pleural ganglion where the right pallial nerve (*arrowhead*) is emerging laterally from a point just dorsal to where shortcut joins the right pleural ganglion. **D.** Right pallial nerve (*arrowheads*) extending to the right periphery of the body and looping anteriorly into the right side of the mantle fold. **E.** Section through a more ventral region of the larva that shows the left and right pallial nerves (*arrowheads*) within the left and right anterolateral margins of the mantle fold; the plane of section also passes through both eyes, as well as the left optic nerve. **F.** Section through the point where the left and right pallial nerves (*arrowheads*) anastomose within the anteroventral region of the mantle fold. Abbreviations: cg= cerebral ganglion, e= eye, f= foregut, lplg= left pleural ganglion, lrm= larval retractor muscle, m= mouth, mc= mantle cavity, mf= mantle fold, opn= optic nerve, os= osphradium, pm= pedal muscle, rhy= right hypobranchial gland, rplg= right pleural ganglion, sbg= subintestinal ganglion, sc= shortcut, st= statocyst, vl= velar lobe. Orientation axes: a= anterior, l= left, p=posterior, r= right.

3.1.3 Developmental stage 3: 55 days post hatching

3.1.3.1 Esophageal nerve ring

By 55 dph, the esophageal nerve ring became much more concentrated as a result of a substantial enlargement of ganglia (Fig. 21). By 55 dph, *N. melanotragus* larvae had either reached- or were close to reaching metamorphic competence (Page and Ferguson, 2013). Consequently, many definitive anatomical characteristics had formed, and thus coinciding changes had occurred to the nervous system. Notably, the definitive buccal mass began to develop after 18 dph, and the tentacles began developing at 27dph (Page and Ferguson, 2013) and were both fully formed by 55 dph. The cerebral ganglia were involved in innervating aspects of both of these structures and each cerebral ganglion formed four distinct lobes (Fig. 21C). The largest and most dorsal lobe represented the cerebral lobe, the lobe situated ventrolaterally to the cerebral lobe represented the ocular lobe, which connected to the eyes, the lobe directly medial to the ocular lobe represented the tentacular lobe, which innervated the tentacles, and the ventral-most lobe represented the labial lobe (Figs. 21C; 22; 23A). The labial lobes were involved in innervating the ventral lips of the mouth and the muscles of the buccal mass (Fretter and Graham, 1994), and were also connected to each other forming a second cerebral commissure, known as the labial commissure (Figs. 21C; 22A; 23). The cerebral commissure proper occurred between the two cerebral lobes and it had become more elongate, making the esophageal nerve ring wider at the level of the cerebral ganglia relative to the rest of the esophageal nerve ring (Figs. 21A; 22B, C, D). Development of the buccal ganglia had occurred by this stage; they innervated the buccal mass and were connected to each other by a short, concentrated, commissure (Figs. 21A, D; 24A). The cerebro-buccal connectives exited the labial lobes of the cerebral ganglia dorsally, ran dorsally along the lateral sides of the radular sac and odontophoral cartilages and connected ventrolaterally with the buccal ganglia, which sat between the forgut and the radular sac, just dorsal to where the radular sac opens into the foregut (Figs. 21B; 24). The buccal ganglia were not directly connected to any other ganglia.

Continued growth of the pedal ganglia brought them closer together so that the pedal commissure looked more like a mere narrowing between two interconnected lobes

instead of a long, thin strand (Fig. 23B-D). A similar size increase in the medial aspects of the pleural ganglia had occurred as well, making them more closely associated with each other (Figs. 21A, D; 22C). The neuroanatomical shortcut between the two pleural ganglia became more robust and more direct (Figs. 21A, D; 25B; 26A). At 18 dph, the shortcut connected to the right pleural ganglion immediately ventral to where the subintestinal ganglion and the right pleural ganglion connected (Fig. 25A). At 55 dph, the region where the shortcut connected to the right pleural ganglion was situated at a more ventral position relative to where the right pleural ganglion connected with the subintestinal ganglion (Figs. 21D; 25B; 26). Thus, the shortcut was no longer as closely associated with the subintestinal ganglion by this stage (Figs. 25; 26).

3.1.3.2 Visceral loop

The four ganglia of the visceral loop had all grown larger and the connectives of the visceral loop had all lengthened and become more robust by 55 dph (Fig. 21). At this stage the visceral loop measured approximately 200μm in width and 270μm in length (Fig. 21A), and could be resolved in its entirety using light microscopy. There was been no significant changes to the trajectory of the supraintestinal connective, emerging from the extreme dorsal surface of the right pleural ganglion, running posterodorsally over the foregut and joining the medial side of the supraintestinal ganglion (Fig. 21A, B). The supraintestinal ganglion maintained the same relative position being situated between the epithelium of the mantle cavity and the anterior loop of the intestine (Fig. 21A, B). The supraintestinal-visceral connective had lengthened to a greater extent than the other visceral-loop connectives, running posteriorly along the epithelium of the expanded mantle cavity and eventually looping to the right and connecting medially with the first visceral ganglion (Fig. 21A).

The position of the first visceral ganglion had shifted to be at the right-posterior extent of the visceral loop (Figs. 21A), just anteromedial to the ciliated tract of the mantle cavity. The trajectory of the visceral commissure became anterior-posterior as a result of disproportionate growth of the supraintestinal connective (Figs. 21). The second visceral ganglion maintained the same relative position at this stage (Fig. 21A, B), being situated

along the epithelium of the mantle cavity in close proximity to the dorsal extent of the right digestive gland.

There were no significant changes to the trajectory of the subintestinal-visceral connective, which emerged from the posterodorsal surface of the subintestinal ganglion, extended posterodorsally and joined the second visceral ganglion anteriorly (Fig. 21A).

3.1.3.3 Sensory organs

The osphradium had increased in overall size and length, running anterior-posterior as a part of the wall of the inner-mantlefold on the left side of the mantle cavity (Fig. 21C). The osphradial ganglion had increased in size and length dramatically and ran almost the entire length of the lateral side of the osphradium, within the mantle fold (Figs. 21C). No significant changes occurred to the trajectory of the osphradial nerve; however, due to the lengthening of the osphradial ganglion the nerve became connected with the osphradial ganglion ventrally (Fig. 21C). Furthermore, no significant changes occurred to the trajectory of the pleural-osphradial connective, which emerged from the left pleural ganglion concurrently, but posterior to the left pallial nerve, extended laterally into the mantle fold and then traveled anterodorsally to join with the osphradial ganglion ventrally (Figs. 21C; 25B).

Other than the previously described development of the ocular lobe, no significant changes pertaining to the eyes occurred.

3.1.3.4 Pallial Nerves

The trajectory of the pallial nerves remained virtually unchanged from the 18 dph stage in which they formed an anteroventral loop between the two pleural ganglia that extended above the mantle cavity (Fig. 21). The right pallial nerve however, like the shortcut, became less associated with the subintestinal ganglion and emerged laterally from a more ventral region of the right pleural ganglion in 55 dph larvae (Figs. 21B, D;

25). Both pallial nerves and the shortcut connected to the respective pleural ganglia within the same plane in frontal sections (Fig. 26A).

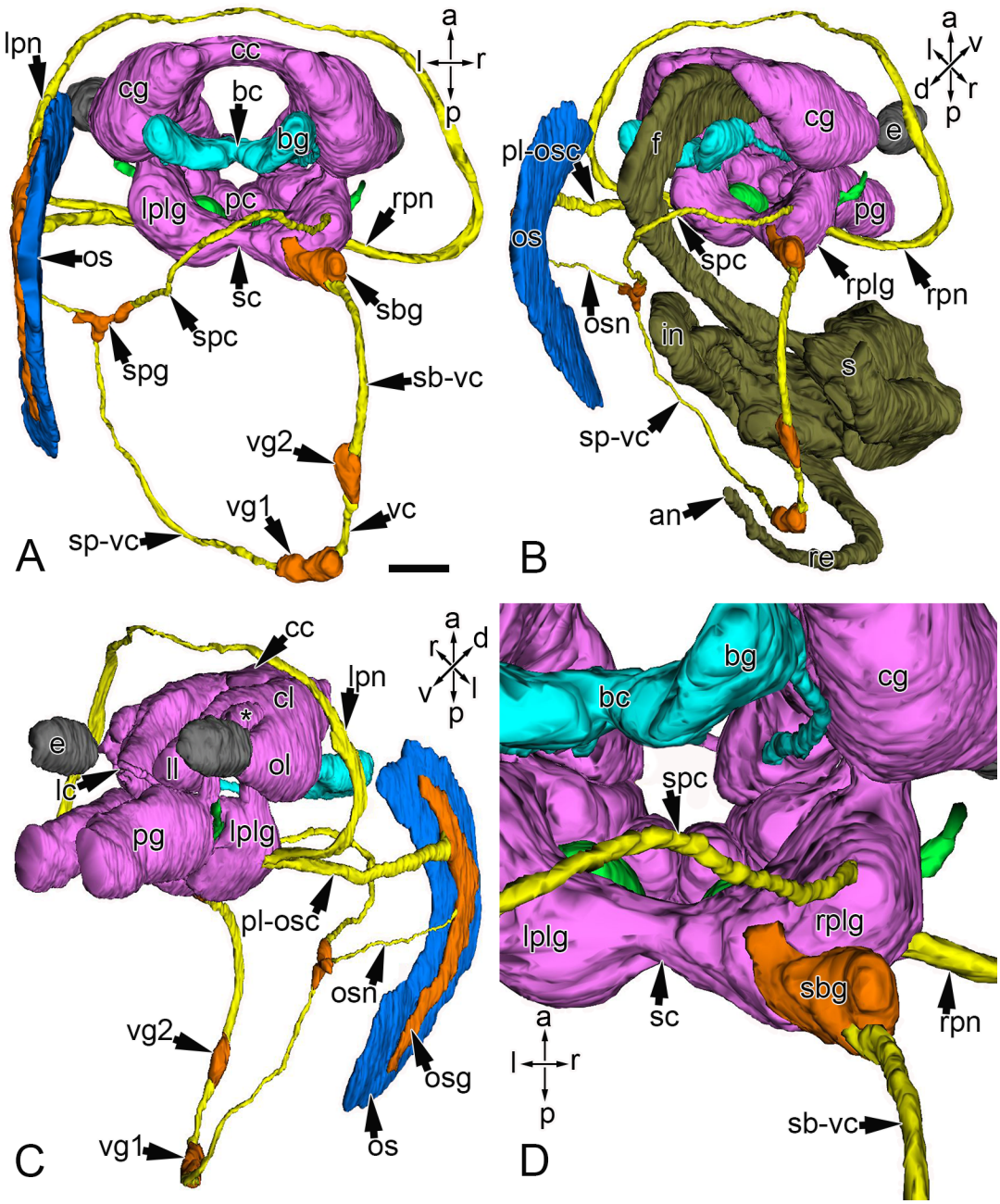

Figure 21. Surface rendered three-dimensional reconstructions showing the components of the central nervous system in a 55 dph larva of *N. melanotragus*; notice the overall size increase, the elongation of the cerebral commissure and the development of the buccal

ganglia. **A.** Dorsal view; scale bar 50µm. **B.** Right dorsolateral view of the central nervous system and gut (dark green), highlighting the trajectory of the supraintestinal connective, the shortcut, and of the osphradial nerve. **C.** Left ventrolateral view showing the pedal ganglia, the four lobes that make up the cerebral ganglia, as well as the osphradial nerve and pleuro-osphradial connective joining with the elongate osphradial ganglion; *asterisk* indicates the tentacular lobe of the left cerebral ganglion; the tentacles were not included in the reconstruction. **D.** Enlarged, dorsal view of the neuroanatomical shortcut between the two pleural ganglia; the shortcut and the right pallial nerve are no longer closely associated with the subintestinal ganglion and both emerge from the right pleural ganglion at more ventral positions. Abbreviations: an= anus, bc= buccal commissure, bg= buccal ganglion, cc= cerebral commissure, cg= cerebral ganglion, cl= cerebral lobe, c-pc= cerebro-pedal connective, c-plc= cerebro-pleural connective, e= eye, es= eye stock, f= foregut, in= intestine, lc= labial commissure, ll= labial lobe, lplg= left pleural ganglion, lpn= left pallial nerve, m= mouth, ol= ocular lobe, os= osphradium, osg= osphradial ganglion, osn= osphradial nerve, pg= pedal ganglion, pl-osc= pleuro-osphradial connective, re= rectum, rplg= right pleural ganglion, rpn= right pallial nerve, sbg= subintestinal ganglion, sc= shortcut, sb-vc= subintestinal-visceral connective, s= stomach, spg= supraintestinal ganglion, spc= supraintestinal connective, sp-vc= supraintestinal-visceral connective, st= statocyst, vg1= first visceral ganglion, vg2= second visceral ganglion, vc= visceral commissure. Orientation axes: a= anterior, d= dorsal, l= left, p= posterior, r= right, v= ventral.

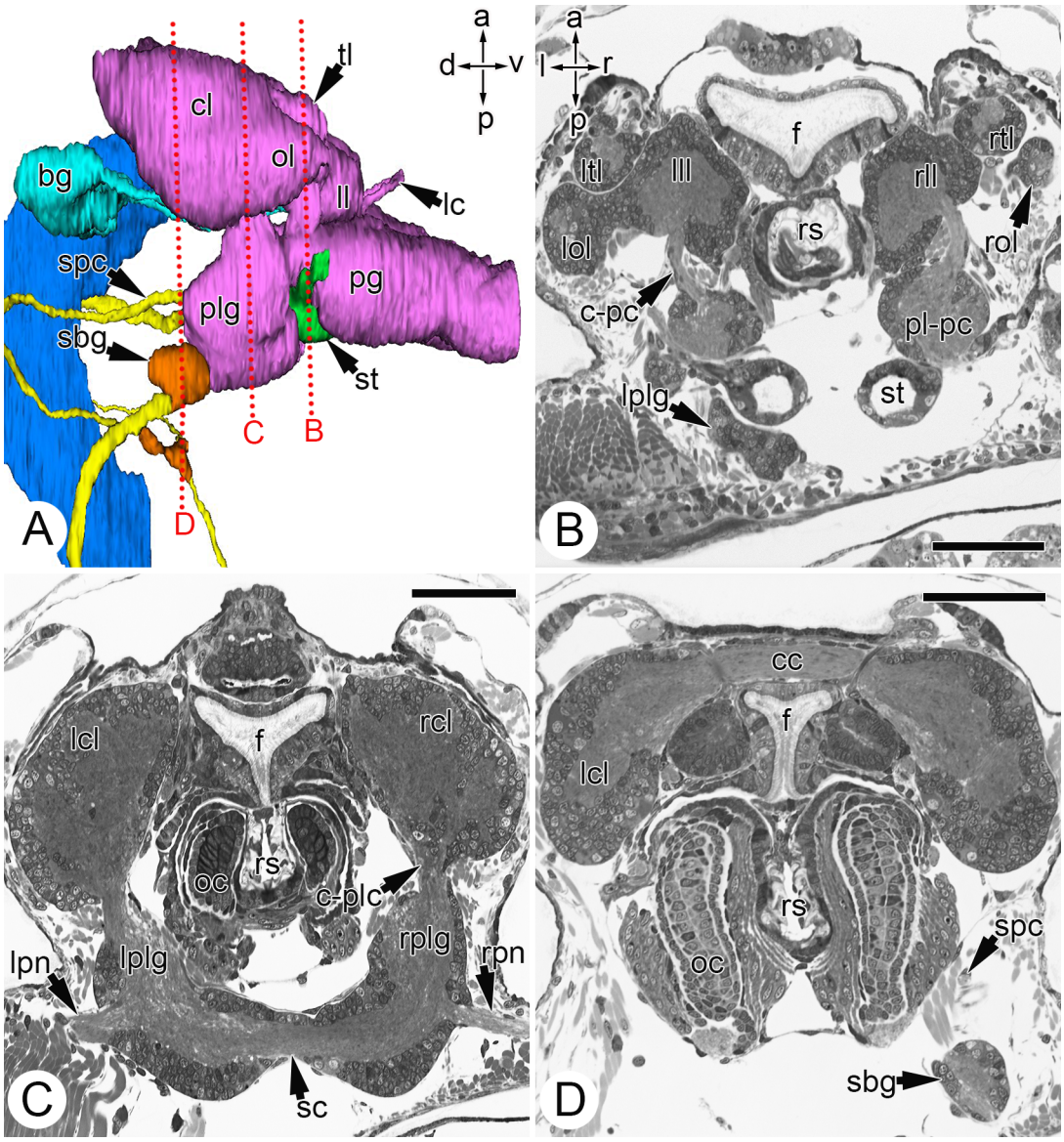

Figure 22. Histological frontal-sections through the ganglia of the central nervous system in 55 dph larva of *N. melanotragus*; all sections displayed in dorsal view; scale bars 50µm. **A.** Surface rendered three-dimensional reconstruction of ganglia of the esophageal nerve ring and the intestinal ganglia of the visceral loop in right lateral view; the eyes and pallial nerves have been omitted for clarity; the red dotted lines indicate planes of section for B-D. **B.** Section through the ocular, tentacular and labial lobes of the cerebral ganglia, the cerebro-pedal connectives, the dorsal portion of the pleuro-pedal connectives passing anterolaterally over the statocysts and the ventral most portion of the left pleural ganglion; also note the radular sac of the definitive buccal mass beneath the foregut. **C.** Section through cerebral lobes of the cerebral ganglia and the pleural ganglia; the

cerebro-pleural connectives are emerging from the cerebral lobes and connecting with the ipsilateral pleural ganglion; the left and right pallial nerves are emerging from their respective pleural ganglion and the neuroanatomical shortcut is running between the pleural ganglia. **D.** Section through the cerebral commissure extending between the two cerebral lobes of the cerebral ganglia; note the subintestinal ganglion and the supraintestinal connective just after it has emerged from the dorsal surface of the right pleural ganglion; also note the definitve buccal mass consisting of odontophoral cartilages and the radular sac beneath the foregut. Abbreviations: bg= buccal ganglion, cc= cerebral commissure, cl= cerebral lobe, c-pc= cerebro-pedal connective, c-plc= cerebro-pleural connective, f= foregut, lc= labial commissure, lcl= left cerebral lobe, ll= labial lobe, lll= left labial lobe, lol= left ocular lobe, lplg= left pleural ganglion, ltl= left tentacular lobe, oc= odontophoral cartilage, pg= pedal ganglion, pl-pc= pleuro-pedal connective, plg= pleural ganglion, rcl= right cerebral lobe, rol= right ocular lobe, rplg, right pleural ganglion, rs= radular sac, rtl= right tentacular lobe, sbg= subintestinal ganglion, sc= shortcut, spc= supraintestinal connective, st= statocyst. Orientation axes: a= anterior, l= left, p=posterior, r= right.

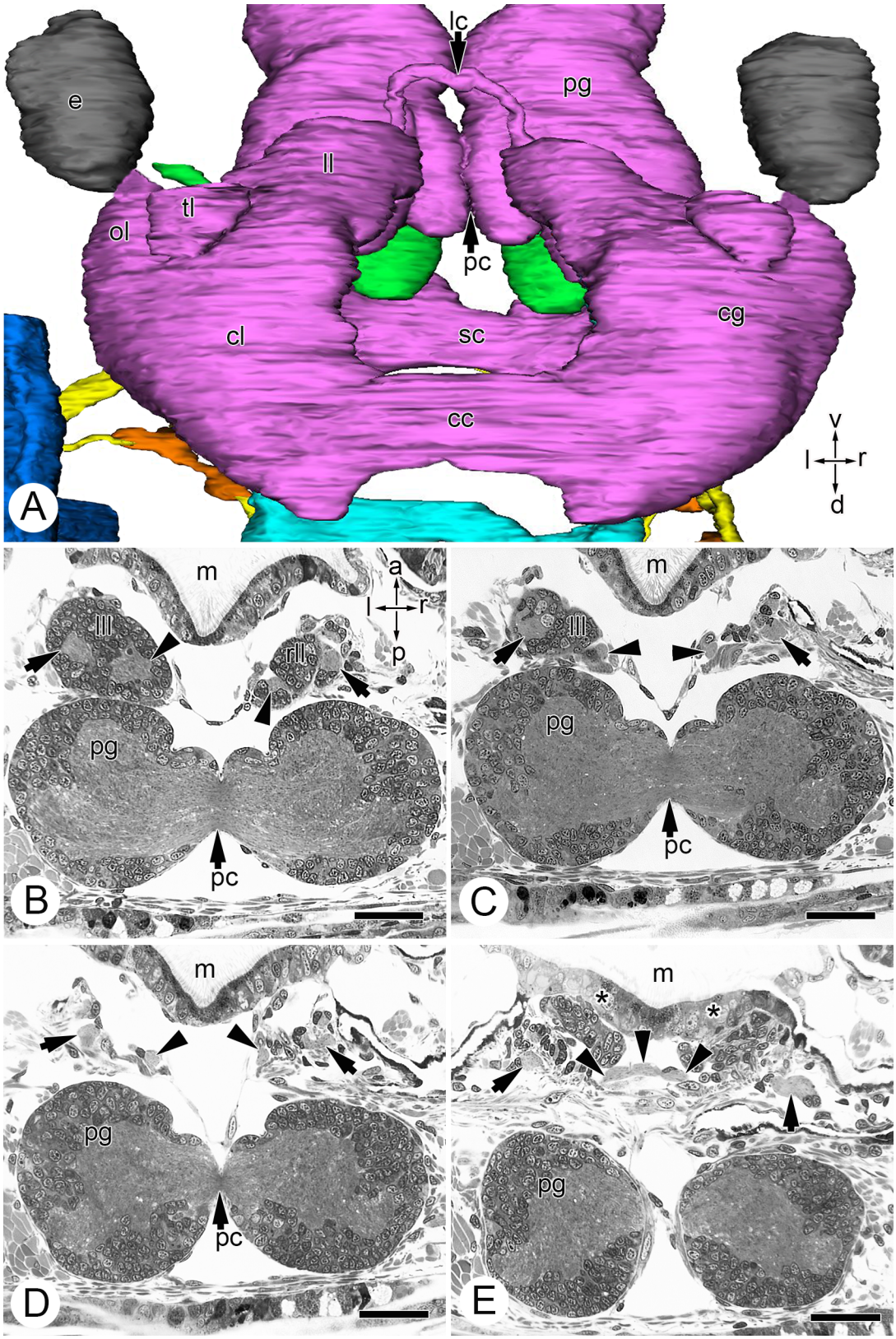

Figure 23. Surface rendered three-dimensional and histological representations of the labial commissure; reconstruction is displayed in anterior view; histological frontal-

sections are displayed in dorsal view; scale bars 25µm. **A.** Surface rendered three-dimensional reconstruction displaying the four lobes that make up the cerebral ganglia; the cerebral commissure extends between the cerebral lobes and the labial commissure extends ventrally and connects the two labial lobes; pallial nerves were omitted for clarity; the tentacles were not included in the reconstruction. **B.** Section through the ventral region of the left labial lobe and the ventral extreme of the right labial lobe; notice how the neuropil is divided into two distinct nerve bundles; the lateral nerve bundle (*arrows*) represents nerves that will innervate the lips of the mouth, the medial nerve bundle (*arrowheads*) represents nerves that will become the labial commissure; also note the pedal ganglia and the pedal commissure just posterior to the labial lobes. **C.** Section showing the left portion of the labial commissure (*left arrowhead*) emerging from the left labial lobe and the right portion of the labial commissure (*right arrowhead*) which has emerged from the right labial lobe; also note the ventral lip nerves (*arrows*). **D.** Section through the left and right portions of the labial commissure (*arrowheads*) as they extend ventrally; also note the ventral lip nerves (*arrows*) as they travel ventrally towards the lips of the mouth. **E.** Section through the point where the left and right portions of the labial commissure (*arrowheads*) loop medially and meet; also note the ventral lip nerves (*arrows*) as they continue to travel ventrally toward the lips; *asterisks* indicate the ventral lip. Abbreviations: cc= cerebral commissure, cg= cerebral ganglion, cl= cerebral lobe, e= eye, lc= labial commissure, ll= labial lobe, lll= left labial lobe. m= mouth, ol= ocular lobe, pc= pedal commissure, pg= pedal ganglion, rll= right labial lobe, sc= shortcut. Orientation axes: a= anterior, d= dorsal, l= left, p= posterior, r= right, v= ventral.

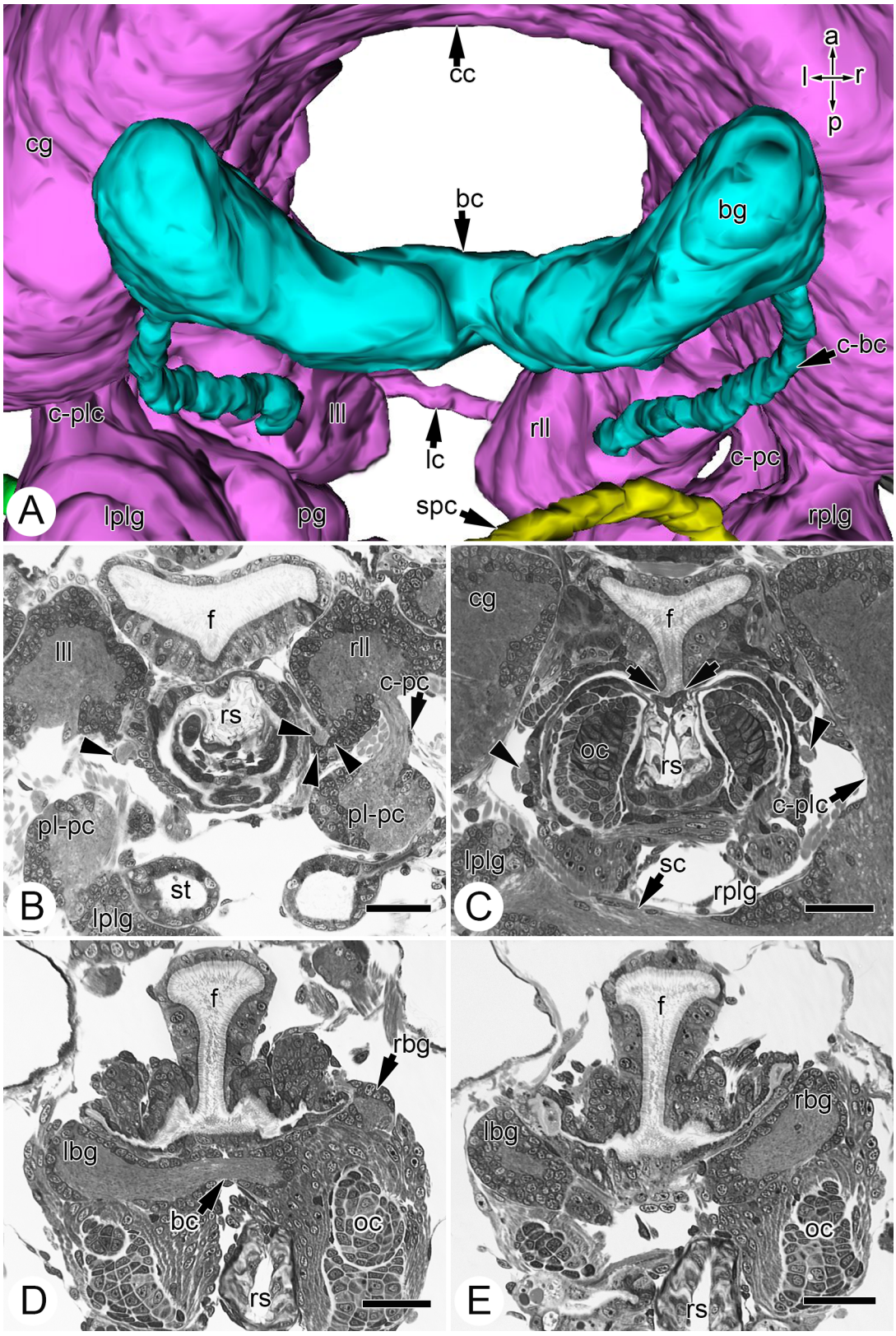

Figure 24. Surface rendered three-dimensional and histological representations of the cerebro-buccal connectives, buccal ganglia and buccal commissure; reconstruction and

histological frontal-sections displayed in dorsal view; scale bars 25µm. **A.** Enlarged surface rendered three dimensional reconstruction displaying the cerebro-buccal connectives emerging from the labial lobes of the cerebral ganglia, extending dorsally and connecting ventrolaterally to their respective buccal ganglion. **B.** Section through the point where the right cerebro-buccal connective (*right arrowheads*) is emerging from the right labial lobe and the left cerebro-buccal connective (*left arrowhead*) has emerged from the left labial lobe; notice the close association between the cerebro-buccal connectives and the radular sac. **C.** Section through the cerebro-buccal connectives (*arrowheads*) as they run dorsally along the lateral aspects of the definitive buccal mass; *arrows* indicate the point where the radular sac opens into the foregut. **D.** Section showing the buccal commissure connected to the left buccal ganglion and extending towards the right buccal ganglion; note the position of the buccal ganglia between the foregut and buccal mass. **E.** Section displaying the buccal ganglia as the buccal commissure is joining with the right buccal ganglion. Abbreviations: bc= buccal commissure, bg= buccal ganglion, cc= cerebral commissure, cg= cerebral ganglion, c-bc= cerebro-buccal connective, c-pc= cerebro-pedal connective, f= foregut, lbg= left buccal ganglion, lc= labial commissure, lll= left labial lobe, lplg= left pleural ganglion, oc= odontophoral cartilage, pg= pedal ganglion, pl-pc= pleuro-pedal connective, rbg= right buccal ganglion, rll= right labial lobe, rplg= right pleural ganglion, rs= radular sac, sc= shortcut, spc= supraintestinal connective, st= statocyst. Orientation axes: a= anterior, l= left, p=posterior, r= right.

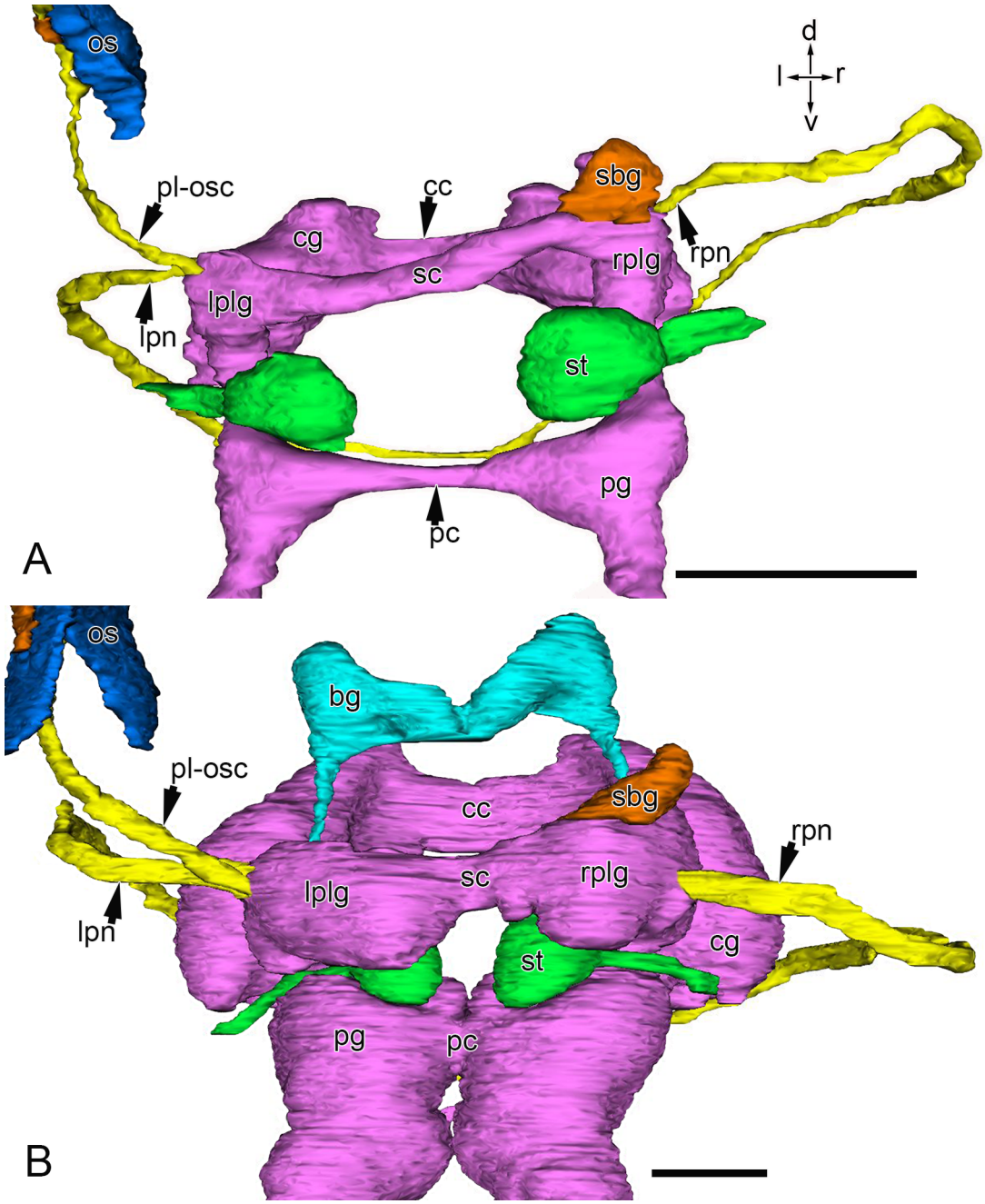

Figure 25. Surface rendered three-dimensional reconstructions of the central nervous system at 18 dph and 55 dph, comparing the trajectory of the shortcut and the emergence point of the right pallial nerve; both reconstructions are displayed in posterior view; the visceral loop has been omitted for clarity; scale bars 50µm. **A.** Reconstructions of the central nervous system at 18 dph; notice how the shortcut is directly connected to the right pleural ganglion, but remains very closely associated with the subintestinal ganglion; also notice how the right pallial nerve emerges from the right pleural ganglion,

but also remains very closely associated with the subintestinal ganglion. **B.** Reconstructions of the central nervous system at 55 dph; notice how the connection between shortcut and the right pleural ganglion has shifted ventrally so that it is no longer closely associated with the subintestinal ganglion; also notice how the pallial nerve emerges laterally from the middle of the right pleural ganglion and is also no longer closely associated with the subintestinal ganglion. Abbreviations: bg= buccal ganglion, cc= cerebral commissure, cg= cerebral ganglion, lplg= left pleural ganglion, lpn= left pallial nerve, os= osphradium, pc= pedal commissure, pg= pedal ganglion, pl-osc= pleuro-osphradial connective, rplg= right pleural ganglion, rpn= right pallial nerve, sbg= subintestinal ganglion, sc= shortcut, st= statocyst. Orientation axes: d= dorsal, l= left, r= right v= ventral.

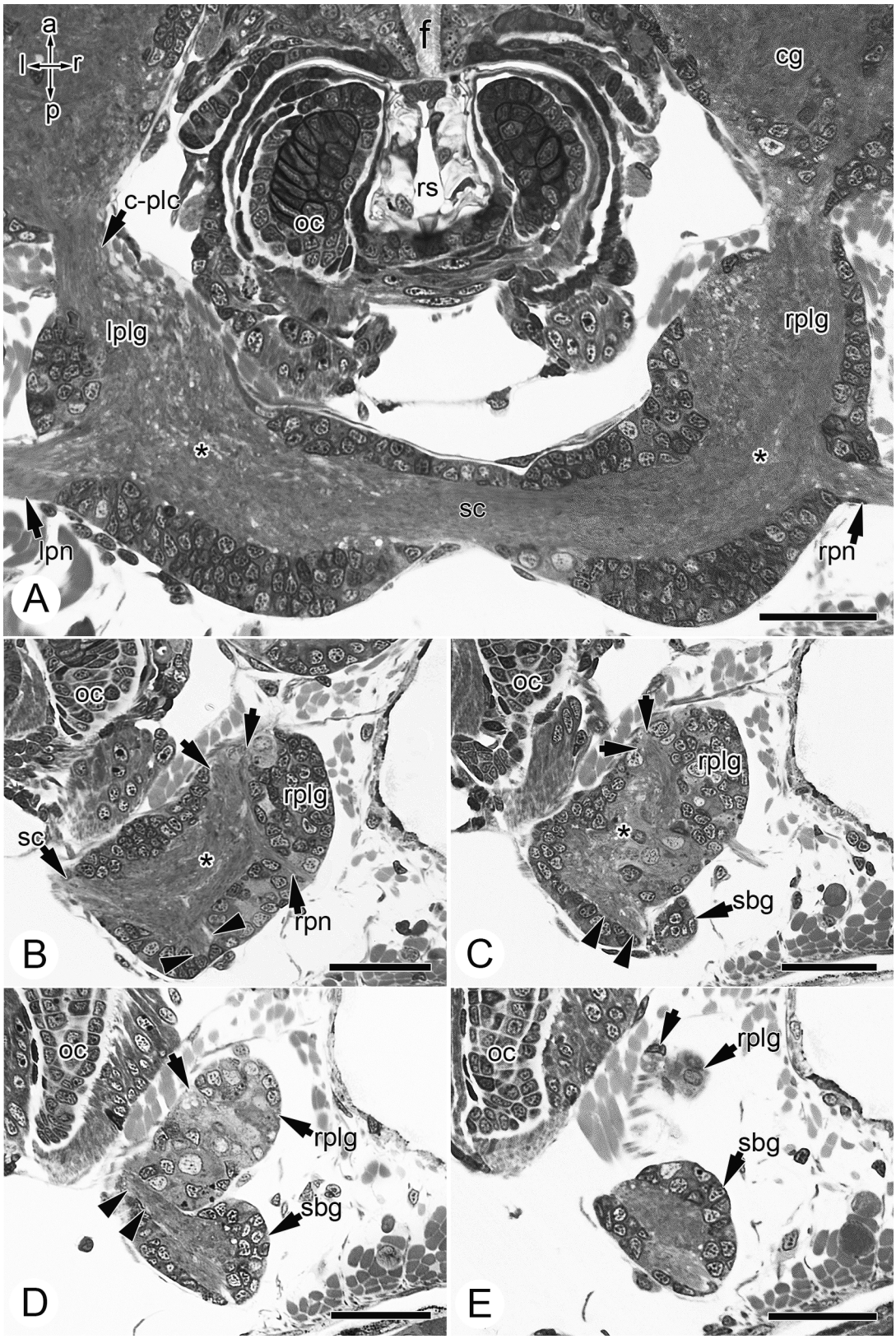

Figure 26. Histological frontal-sections displaying evidence for the disassociation between the shortcut and the subintestinal ganglion; all sections displayed in dorsal view;

scale bars 25µm. **A.** Section through the point where the neuropils of the left and right pleural ganglia (*asterisks*) are directly connected via the shortcut; also note that the left and right pallial nerves are emerging from their respective pleural ganglion within this same plane. **B.** Section through the right pleural ganglion at the right side of the shortcut and the right pallial nerve; *asterisk* indicates the center of the neuropil of the right pleural ganglion; *arrows* indicate the region of the right pleural neuropil that will give rise to the supraintestinal connective; *arrowheads* indicate region of the right pleural neuropil that will connect with the subintestinal ganglion. **C.** More dorsal section through the right pleural ganglion and the ventral origin of the subintestinal ganglion; notice the subset of the right pleural neuropil extending towards the subintestinal ganglion (*arrowheads*); *asterisk* indicates the center of the neuropil of the right pleural ganglion; *arrows* indicate the region of the right pleural neuropil that will give rise to the supraintestinal connective. **D.** More dorsal section through the connection between the right pleural ganglion and subintestinal ganglion (*arrowheads*); notice how the right pleural neuropil is now concentrated in the region where it connects with the subintestinal ganglion and where the supraintestinal connective will emerge (*arrow*). **E.** More dorsal section showing the subintestinal ganglion and the supraintestinal connective (*arrow*) emerging from extreme dorsum of the right pleural ganglion. Abbreviations: cg= cerebral ganglion, c-plc= cerebro-pleural connective, f= foregut, lplg= left pleural ganglion, lpn= left pallial nerve, oc= odontophoral cartilage, rplg= right pleural ganglion, rpn= right pallial nerve, rs= radular sac, sbg= subintestinal ganglion, spc= supraintestinal connective. Orientation axes: a= anterior, l= left, p=posterior, r= right.

3.1.4 Developmental stage 4: 6 days post metamorphosis (juvenile)

3.1.4.1 Esophageal nerve ring

There were no changes to the relative position of ganglia that made up the esophageal nerve ring between the 55 dph larval stage and the 6 days post-metamorphosis (dpm) juvenile stage (Figs. 27; 28). The configuration of the central nervous system observed at 55 dph was essentially what was carried through metamorphosis and into the juvenile, however several small changes occurred to the morphology of the esophageal nerve ring. For instance, the ganglia and the connectives of the esophageal nerve ring became more defined (Fig. 27). The cerebral commissure became noticeably longer and the labial commissure ran straight between the labial lobes of the cerebral ganglia at this stage (Fig. 27). The cerebro-pleural and cerebro-pedal connectives became more elongate as well (Fig. 27; 28C, D). These changes made the width of the esophageal nerve ring at the level of the cerebral ganglia greater relative to the width of the esophageal nerve ring at the level of the pleural ganglia (Fig. 27A; 28B, C; 30). The ratio between cerebral width and pleural width was greater in the juvenile than in the 55 dph larva being 1.7 and 1.4 respectively. Furthermore, the cerebral ganglia rotated anteriorly, as denoted by the position of the cerebral commissure (Fig. 28A). At 55 dph, the cerebral commissure was situated anterodorsally and sat above the dorsal portion of the subintestinal ganglion (Figs. 29A). In the post-metamorphic juvenile, however, the cerebral ganglia rotated anteriorly so that the cerebral commissure sat above the posterodorsal portion of the pleural ganglia (Figs. 29B). This likely occurs as a result of the substantial increase the size of the buccal mass during metamorphoses (compare Figs. 22D and 28D)

Metamorphosis marked the transition of a pelagic existence to one of crawling on the benthos. During the swimming larval stages, the foot was smaller and oriented ventrally; however, as the larvae approached metamorphosis the foot became posteriorly orientated, which is necessary for crawling. Consequently there was a posterior rotation of the pedal and pleural ganglia that occurred in correlation with the shift in the orientation of the foot (Fig. 29B). In pre-metamorphic stages the pedal ganglia projected ventrally and the pleural ganglia projected dorsally (Figs. 29A); however, in post-

metamorphic individuals, the pedal ganglia and the pleural ganglia essentially rotated towards each other like a folding piece of paper, so that they were both oriented more posteriorly (Fig. 29B). This was most noticeable in the orientation of the pedal ganglia, which essentially delineated the orientation of the foot (Figs. 27C; 29B).

The trajectory of the shortcut observed in 55 dph larvae was carried forward through metamorphosis and into the juvenile stage with essentially no changes (Figs. 27D; 30).

3.1.4.2 Visceral loop

The configuration of the ganglia and the connectives of the visceral loop, were carried through metamorphosis without any significant changes other than slight increases in width (~225μm) and length (~320μm)(Figs. 27). The trajectory of the visceral loop, however, became more posterodorsal in post-metamorphic juveniles, as opposed to a more directly posterior trajectory in pre-metamorphic larvae (Fig. 29).

3.1.4.3 Sensory organs

There were no major changes to the morphology or configuration of the osphradium and osphradial ganglion (Fig. 27), as well as no major changes to the trajectory of the osphradial nerve or the pleuro-osphradial connective (Figs. 27; 30).

The optic nerves increased in length and continued to point ventrally despite the anterior rotation of the cerebral ganglia (Figs. 27C; 29B; 30B).

3.1.4.4 Pallial nerves

The trajectory and morphology of the pallial nerves at 55 dph was carried through metamorphosis and is present within juveniles without any major changes (Figs. 27; 30).

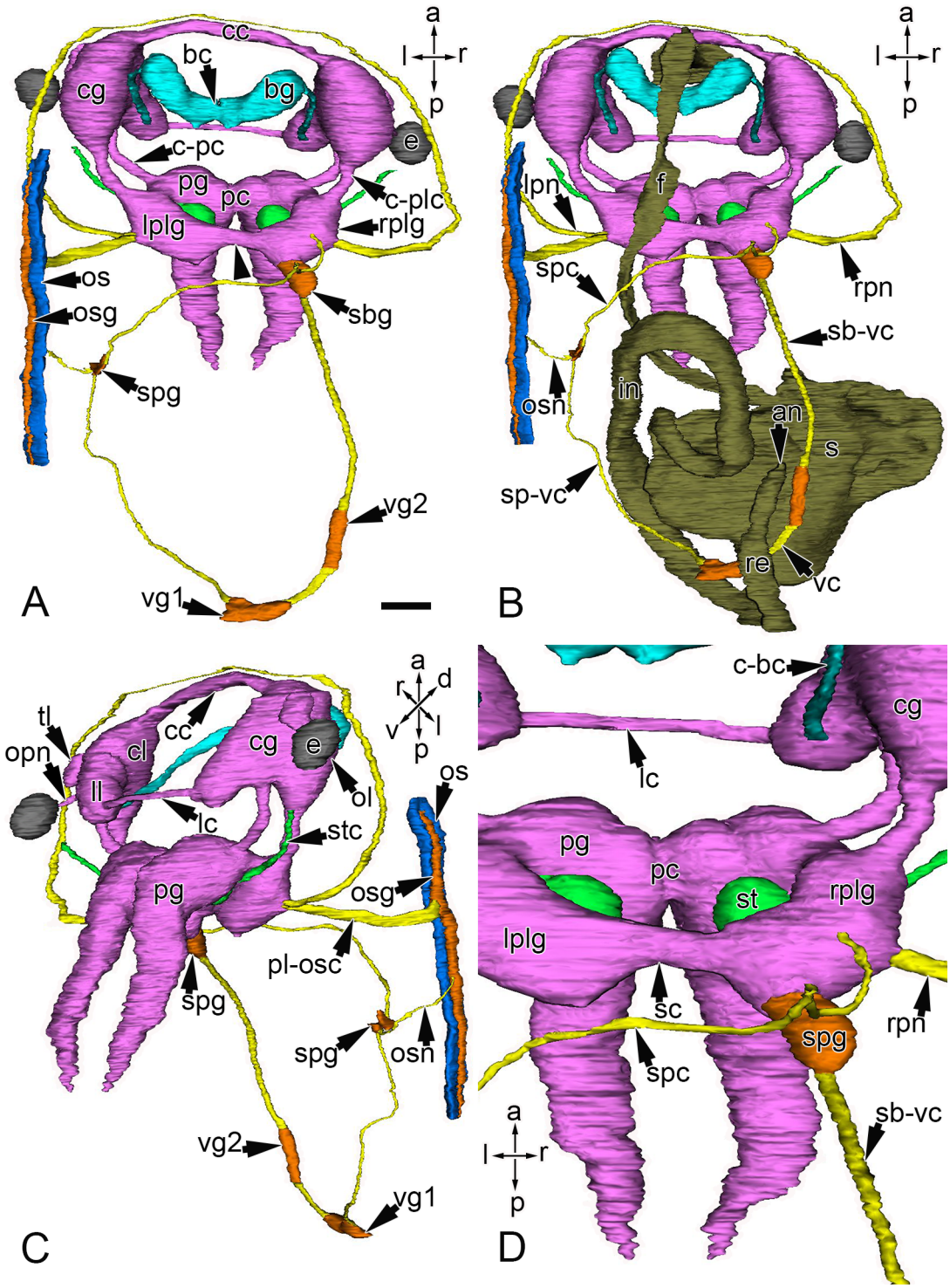

Figure 27. Surface rendered three-dimensional reconstructions showing the components of the central nervous system in a 6 dpm juvenile *N. melanotragus*. Notice the greater definition of the ganglia, commissures and connectives of the esophageal nerve ring, as well as the increased length of the commissures and connectives associated with the

cerebral ganglia. **A.** Dorsal view; note the more posterior orientation of the pedal and pleural ganglia; scale bar 50µm. **B.** Dorsal view of the central nervous system and gut (dark green). **C.** Left ventrolateral view showing posterior orientation of the pedal ganglia, as well as the osphradial nerve and pleuro-osphradial connective joining with the elongate osphradial ganglion. **D.** Enlarged, dorsal view of the neuroanatomical shortcut between the two pleural ganglia; note how the trajectory remains virtually unchanged from the 55 dph stage. Abbreviations: an= anus, bc= buccal commissure, bg= buccal ganglion, cc= cerebral commissure, cg= cerebral ganglion, cl= cerebral lobe, c-pc= cerebro-pedal connective, c-plc= cerebro-pleural connective, e= eye, f= foregut, in= intestine, lc= labial commissure, ll= labial lobe, lplg= left pleural ganglion, lpn= left pallial nerve, m= mouth, ol= ocular lobe, opn= optical nerve, os= osphradium, osg= osphradial ganglion, osn= osphradial nerve, pg= pedal ganglion, pl-osc= pleuro-osphradial connective, re= rectum, rplg= right pleural ganglion, rpn= right pallial nerve, sbg= subintestinal ganglion, sc= shortcut, sb-vc= subintestinal-visceral connective, s= stomach, spg= supraintestinal ganglion, spc= supraintestinal connective, sp-vc= supraintestinal-visceral connective, st= statocyst, vg1= first visceral ganglion, vg2= second visceral ganglion, vc= visceral commissure. Orientation axes: a= anterior, d= dorsal, l= left, p= posterior, r= right, v= ventral.

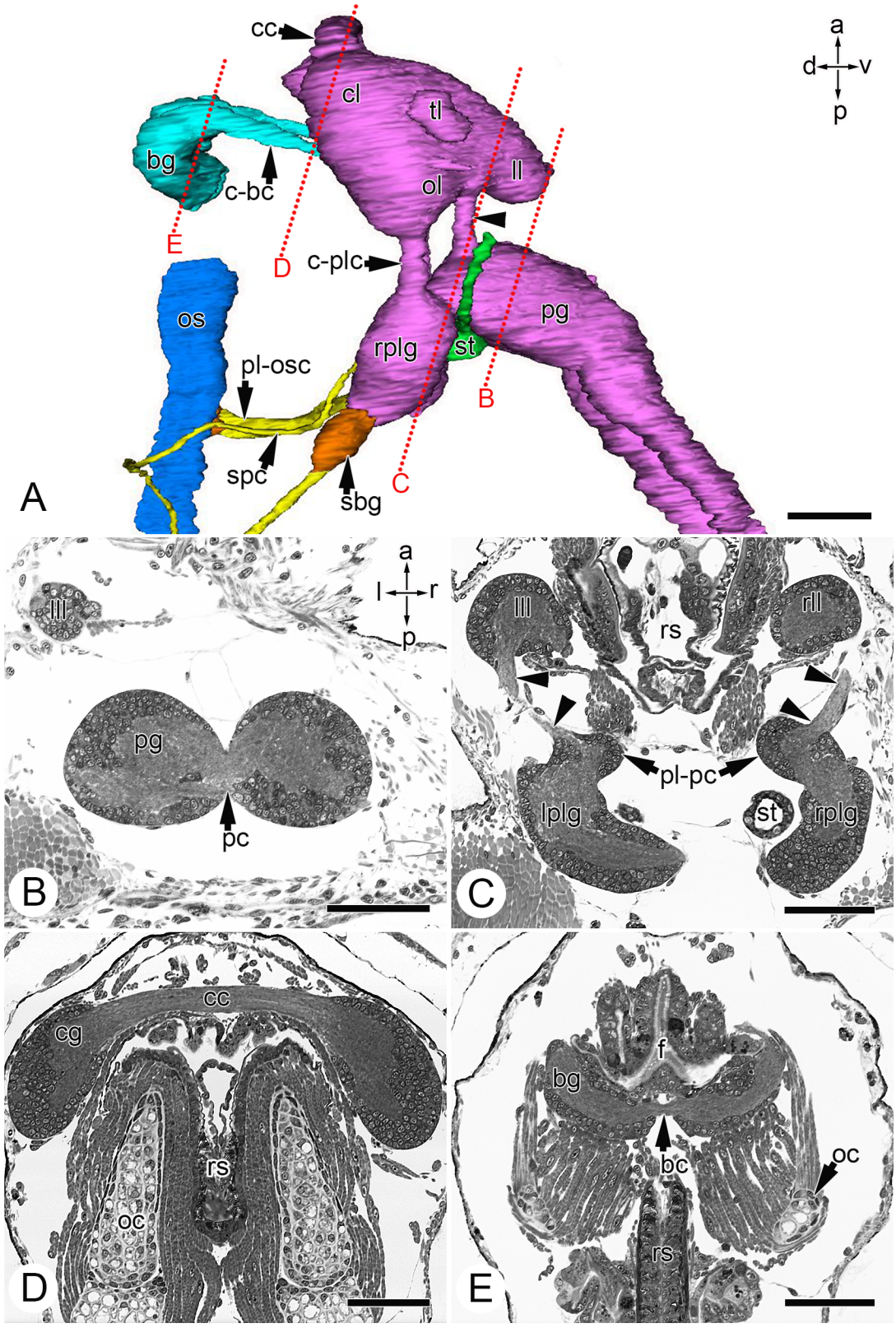

Figure 28. Histological frontal-sections through the ganglia of the central nervous system in 6 dpm *N. melanotragus* juveniles; all sections are displayed in dorsal view; scale bars

50µm. **A.** Surface rendered three-dimensional reconstruction of the ganglia of the esophageal nerve ring in right lateral view; the eyes and pallial nerves have been omitted for clarity; the red dotted lines indicate planes of section for B-D; *arrowhead* indicates the cerebro-pedal connective. **B.** Section through the pedal ganglia and pedal commissure; also note the increased width between the cerebral ganglia as the ventral origin of the left labial lobe is situated anterolateral to the left pedal ganglion, whereas the labial lobes are directly anterior to the pedal ganglia at 55 dph (see Fig. 23B). **C.** Section through a dorsal portion of the labial lobes, the elongated cerebral-pedal connectives (*arrowheads*), and the pleuro-pedal connectives joining with the pleural ganglia; note the noticeable increase in width between the cerebral ganglia (see Fig. 22B for comparison). **D.** Section through the elongated cerebral commissure; also note the size increase in the components of the buccal mass relative to the ganglia after metamorphosis (see Fig. 22D for comparison). **E.** Section through the buccal ganglia and buccal commissure; they maintain the same relative position between the foregut and the buccal mass (see Fig. 24D for comparison). Abbreviations: bc= buccal commissure, bg= buccal ganglion, cc= cerebral commissure, cl= cerebral lobe, c-plc= cerebro-pleural connective, f= foregut, ll= labial lobe, lll= left labial lobe, lplg= left pleural ganglion, oc= odontophoral cartilage, ol= ocular lobe, pc= pedal commissure, pg= pedal ganglion, pl-pc= pleuro-pedal connective, rplg, right pleural ganglion, rs= radular sac, sbg= subintestinal ganglion, spc= supraintestinal connective, st= statocyst. Orientation axes: a= anterior, d= dorsal, l= left, p=posterior, r= right, v= ventral.

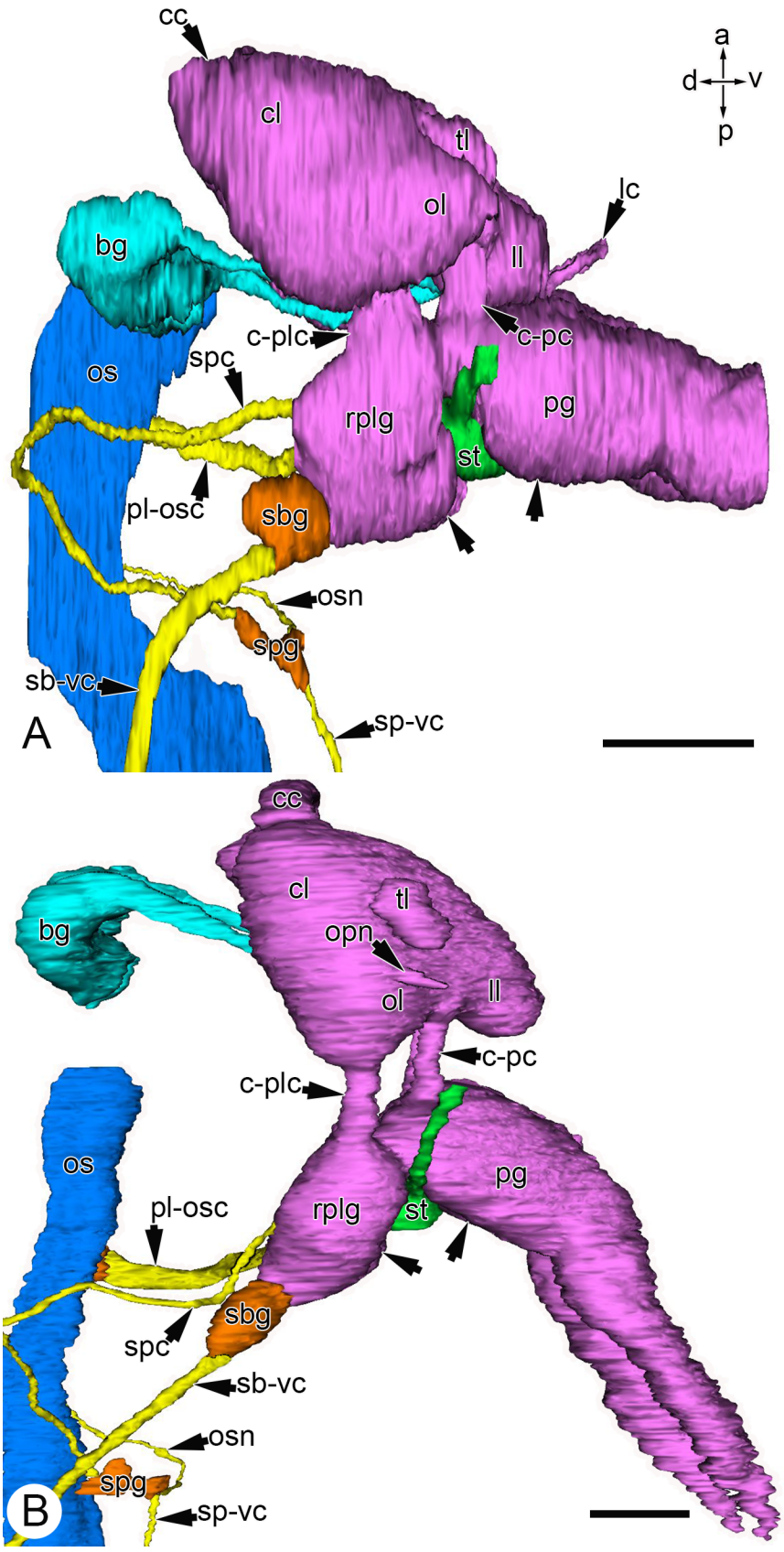
cc
a
d
v
p
cl
tl
ol
lc
bg
ll
c-plc
c-pc
spc
os
rplg
pg
st
pl-osc
sbg
osn
spg
sb-vc
sp-vc
A
cc
cl
tl
bg
opn
ol
ll
c-pc
c-plc
os
pg
pl-osc
rplg
st
sbg
spc
sb-vc
osn
spg
sp-vc
B

Figure 29. Surface rendered three-dimensional reconstructions of the central nervous system at 55 dph and 6 dpm, comparing the orientation of the cerebral, pleural and pedal ganglia, as well as the trajectory of the visceral loop; both reconstructions are displayed in right-lateral view; the eyes and pallial nerves have been omitted for clarity; scale bars 50μm. **A.** Reconstructions of the central nervous system in 55 dph larvae; notice the anterodorsal location of the cerebral commissure; also notice how the pedal ganglia essentially run straight in the ventral direction, and the pleural ganglia run slightly posterodorsally, so that the posterior surfaces of the pleural ganglia (*left arrow*) and the pedal ganglia (*right arrow*) run almost straight along the dorso-ventral axis with a slight angle between them at the point of the statocysts; note how the subintestinal-visceral connective and the supraintestinal-visceral connective of the visceral loop extend almost directly posteriorly. **B.** Reconstructions of the central nervous system in 6 dpm juveniles; notice the anterior rotation of the cerebral ganglia as denoted by the more anteroventral position of the cerebral commissure; also notice that the pedal and pleural ganglia have rotated towards each other so that pedal ganglia run more posteroventrally at this stage and the pleural ganglia run more posterodorsally, creating a more acute angle between their posterior surfaces (*arrows*) at the point of the statocysts; note the more posterodorsal trajectory of the subintestinal-visceral and the supraintestinal-visceral connectives of the visceral loop. Abbreviations: bg= buccal ganglion, cc= cerebral commissure, cl= cerebral lobe, lc= labial commissure, ll= labial lobe, ol= ocular lobe, opn= optical nerve, os= osphradium, osn= osphradial nerve, pg= pedal ganglion, pl-osc= pleural osphradial connective, sbg= subintestinal ganglion, sb-vc= subintestinal-visceral connective, spc= supraintestinal connective, spg= supraintestinal ganglion, sp-vc= supraintestinal-visceral connective, st= statocyst . Orientation axes: a= anterior, d= dorsal, p= posterior, v= ventral.

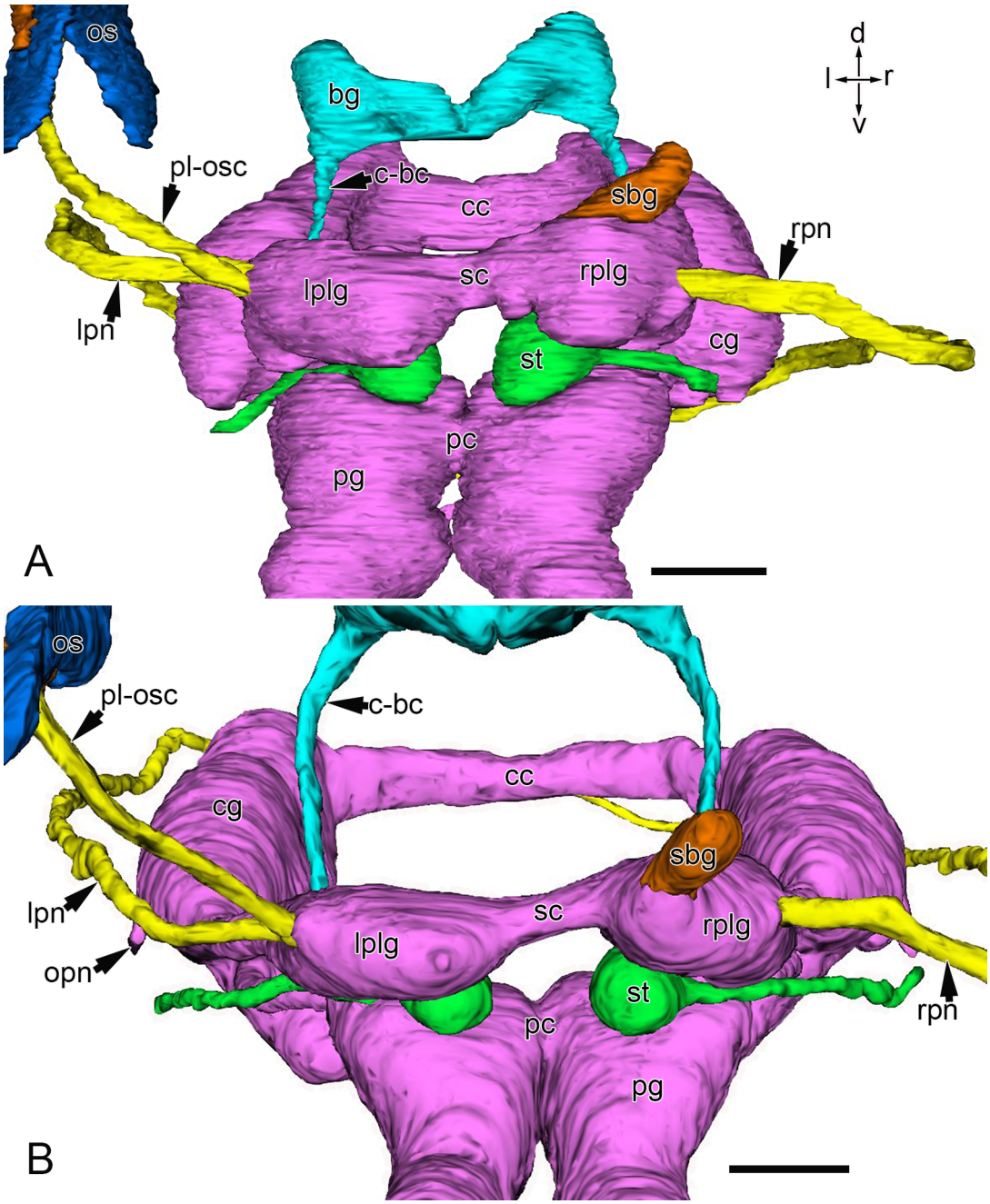

Figure 30. Surface rendered three-dimensional reconstructions of the central nervous system at 55 dph and 6 dpm, comparing the trajectory of the shortcut and the emergence point of the right pallial nerve; both reconstructions are displayed in posterior view; the eyes and visceral loop have been omitted for clarity; scale bars 50µm. **A.** Reconstruction of the central nervous system at 55 dph; notice how the connection between shortcut and the right pleural ganglion is no longer closely associated with the subintestinal ganglion; also notice how the pallial nerve emerges laterally from the middle of the right pleural

ganglion and is no longer closely associated with the subintestinal ganglion. **B.** Reconstruction of the central nervous system at 6 dpm; notice how the trajectory of the shortcut and the emergence point of the right pallial nerve remains virtually unchanged in post-metamorphic juveniles; also notice how the width of the esophageal nerve ring has increased slightly at the level of the pleural ganglia and to a much greater extent at the level of the cerebral ganglia in the 6 dpm juvenile in comparison to the 55 dph larva. Abbreviations: bg= buccal ganglion, cc= cerebral commissure, cg= cerebral ganglion, lplg= left pleural ganglion, lpn= left pallial nerve, opn= optical nerve, os= osphradium, pc= pedal commissure, pg= pedal ganglion, pl-osc= pleuro-osphradial connective, rplg= right pleural ganglion, rpn= right pallial nerve, sbg= subintestinal ganglion, sc= shortcut, st= statocyst. Orientation axes: d= dorsal, l= left, r= right v= ventral.

3.2 Shell muscles in larvae of *N. melanotragus*

3.2.1 Description of the shell muscles

Larvae of *N. melanotragus* hatched with 2 pairs of shell-anchored muscles, the larval retractor muscles and the pedal muscles (Page and Ferguson, 2013). Although, the morphology of the shell anchored muscles of newly hatched *N. melanotragus* larvae have been described previously (Page and Ferguson, 2013), figure 31 showcases the morphology of these muscles in context with the central nervous system in newly-hatched larvae.

The left larval retractor muscle possessed more muscle fibres than the right larval retractor muscle, however, both muscles originated on the inner postero-lateral walls of either side of the shell and possessed distally branched muscle fibres (Fig. 31A) (Page and Ferguson, 2013). The left larval retractor muscle inserted within the mantle fold, the apical plate, the left and right velar lobes and anterior aspects of the larval foregut, whereas the distal branches of the right larval retractor muscle extended into the right velar lobe only (Fig. 31) (Page and Ferguson, 2013).

The ventral branches of the left larval retractor muscle, which inserted on the anterior foregut, the apical plate, as well as the muscle branches that inserted laterally and ventrally within the left velar lobe were embraced by the cerebro-visceral nerve ring (consisting of the cerebral commissure, cerebral ganglia and visceral loop) (Fig. 31A, B). Conversely, the dorsal branches of the left larval retractor muscle, which inserted dorsally within the left velar lobe, right velar lobe and the mantle fold extended outside this nerve ring (Fig. 31A). The entire right larval retractor muscle was embraced by the cerebro-visceral nerve ring (Fig. 31A, D).

The two pedal muscles were more symmetrical than the larval retractor muscles and originated adjacent to the larval retractor muscles on the posterolateral walls of the shell (Fig. 31) (Page and Ferguson, 2013). The right pedal muscle inserted on epithelium overlying the right side of the operculum (Fig. 31B), whereas the left pedal muscle inserted directly on the apophyses projecting from the inner, left side of the operculum (Fig. 31D) (Page and Ferguson, 2013). All of the pedal muscle fibres extended entirely outside of the cerebro-visceral nerve ring (Fig. 31) (Page and Ferguson, 2013).

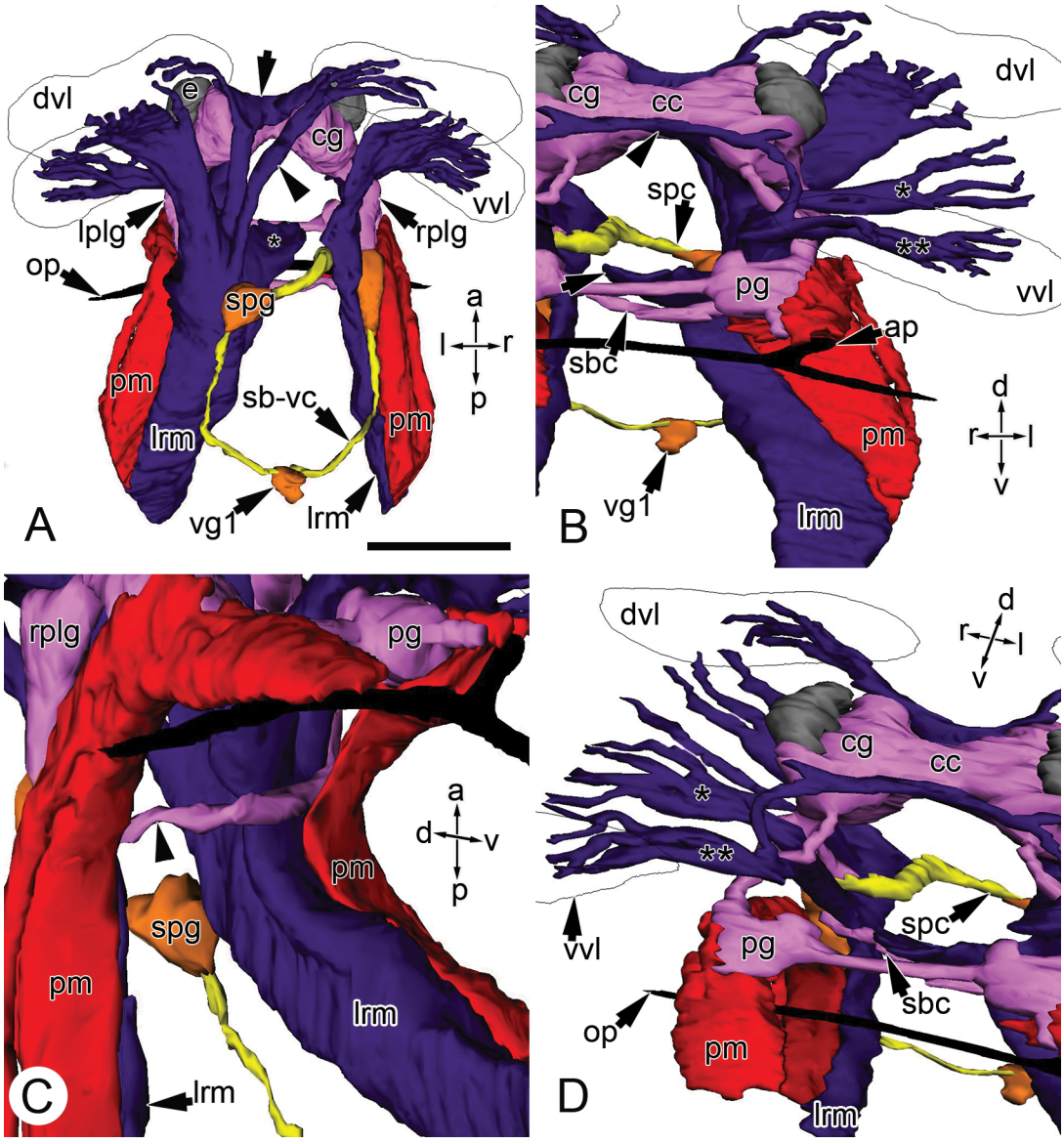

Figure 31. Surface rendered three-dimensional reconstruction showing the morphology of the two pairs of shell muscles present in newly hatched *N. melanotragus* in anatomical context with the central nervous system; the reconstructions include single section profiles through the left and right velar lobes and the operculum (blackened). **A.** Dorsal view of the shell muscles and central nervous system; *arrow* indicates branch of the left larval retractor muscle that inserts within the mantle fold; *arrowhead* indicates the branch of the left larval retractor muscle that insert within the right velar lobe; *asterisk* indicates the ventral muscle cells of the left larval retractor muscle that insert on the anterior

foregut; note that the entire right larval retractor muscle is embraced by the cerebro-visceral nerve ring; scale bar 50µm. **B.** Anteroventral view showing the ventral muscle tracts of the left larval retractor muscle that insert on the anterior foregut (*arrow*), apical plate (*arrowhead*), and the muscle tracts that insert ventrally (*double asterisk*) and laterally (*asterisk*) within the left velar lobe; these muscle tracts are embraced by the cerebro-visceral nerve ring; also note the left pedal muscle inserting on the apophyses on the left side of the operculum. **C.** Right-ventrolateral view showing that the left larval retractor muscle is contained ventrally by the subintestinal connective (*arrowhead*). **D.** Anteroventral view showing the ventral muscle tracts of the right larval retractor muscle that insert ventrally (*double asterisk*) and laterally (*asterisk*) within the right velar lobe; note that the entire right larval retractor muscle is embraced by the cerebro-visceral nerve ring. Abbreviations: ap= apophyses of the operculum cg= cerebral ganglion, dvl= dorsal velar lobe, e= eye, lplg= left pleural ganglion, lrm= larval retractor muscle, op= operculum, pg= pedal ganglion, pm= pedal muscle, rplg= right pleural ganglion, sbc= subintestinal connective, sb-vc= subintestinal-visceral connective, spc= supraintestinal connective, spg= supraintestinal ganglion, vg1= first visceral ganglion. Orientation axes: a= anterior, d= dorsal, l= left, p= posterior, r= right, v= ventral.

3.2.2 Innervation of the larval retractor muscles

Table 1 summarizes the point of origin and innervation site(s) for each of the nine nerves that innervate the larval retractor muscles. Each muscle was innervated by two nerves that emerged directly from the ipsilateral pleural ganglion and by two additional nerves that emerged from regions associated with that pleural ganglion (Fig. 32). Furthermore, a nerve that emanated from the left cerebral ganglion innervated the left larval retractor muscle (Fig. 32).

On the left side, the first left larval retractor nerve (ll1) emanated from the posterior extreme of the left pleural ganglion, just dorsal to where the subintestinal connective emerged (Fig. 32). This nerve initially extended posteriorly between the larval

retractor muscle and the pedal muscle, and then branched between the muscle cells of the larval retractor muscle, innervating lateral portions of the trunk of left larval retractor muscle (Figs. 32; 33). Individual neurites were observed synapsing directly on muscle cells (Fig. 33B-D, F) indicating that this nerve was involved in motor control of the left larval retractor muscle.

The second left larval retractor nerve (ll2) emanated from the dorsal surface of the left pleural ganglion, just anterior to where the first larval retractor nerve emerged (Fig. 32). This nerve initially extended medially before it branched, with one branch extending anteromedially and the other posteriorly (Fig. 32). The anteromedial nerve branch ran between myocytes of the muscle branch that inserted on the anterior foregut (Figs. 32; 34B), and the posterior nerve branch ran parallel to the first larval retractor nerve, and branched between several more muscle cells (Figs. 32; 34A, B). The first left larval retractor nerve and the posterior branches of the second left larval retractor nerve, collectively innervated the lateral portion of the trunk of the left larval retractor muscle (Figs. 32; 34A, B). Individual neurites were observed synapsing directly on muscle cells (not shown), indicating that the second left larval retractor nerve was also involved in motor control of the left larval retractor muscle.

The third left larval retractor nerve (ll3) emerged from the area where the cerebro-pleural connective entered the pleural ganglion on the left side (Fig. 34C). This nerve extended along the myocytes that inserted laterally within the left velar lobe (Fig. 34C). Individual neurites were observed synapsing directly on these muscle cells (not shown), indicating that this nerve was also involved in motor control of the left larval retractor muscle.

The fourth left larval retractor nerve (ll4) emerged from the pleuro-pedal connective just ventral to where the pleuro-pedal connective merged with the cerebro-pedal connective (Fig. 34B, C). This nerve extended anterolaterally along myocytes of the muscle branch that inserted ventrally within the left velar lobe (Fig. 34D). Individual neurites were observed synapsing directly on these muscle cells (not shown), indicating that this nerve was involved in motor control of the left larval retractor muscle as well.

The fifth left larval retractor nerve emanated posteriorly from a middle region of the left cerebral ganglion (Figs. 32; 34A). This nerve initially extended posteriorly and

then branched, with one branch extending anterolaterally and the other continuing posteriorly (Fig. 32). The anterolateral nerve branch ran between myocytes projecting dorsally into the velar lobes, whereas the posterior nerve branch traveled between muscle cells of the medial portion of the trunk of the left larval retractor muscle and branched several more times (Figs. 32; 34A,B). Individual neurites were observed synapsing directly on these muscle cells (not shown), indicating that this nerve was also involved in motor control of the left larval retractor muscle.

Similar to what was observed on the left, two nerves emerged from the right pleural ganglion at distinct posterior locations. The first right larval retractor nerve (rl1) emanated from the ventral surface of the right pleural ganglion, anterior to where the right pleural ganglion and subintestinal ganglion connected (Fig. 34B). This nerve extended posteriorly between the muscle cells, branching many times to cover the majority of the trunk of the right larval retractor muscle and is the only nerve that innervated this region (Figs. 32; 34A, B). Individual neurites were observed synapsing directly on these muscle cells (not shown), indicating that this nerve was involved in motor control of the right larval retractor muscle.

The second right larval retractor nerve (rl2) emanated dorsally from the posterior of the right pleural ganglion, just anterior to where the supraintestinal connective emerged from the right pleural ganglion (Figs. 32; 34A). This nerve initially extended dorsally and then looped anteriorly, running between the muscle cells of the dorsal branch of the right larval retractor muscle that inserted dorsally within the right velar lobe (Figs. 32; 34A). Individual neurites were observed synapsing directly on these muscle cells (not shown), indicating that this nerve was also involved in motor control of the right larval retractor muscle.

The third and fourth right larval retractor nerves (rl3, rl4) were almost symmetrical to the third and fourth left larval retractor nerves. The third right larval retractor nerve emanated from the point where the right cerebro-pleural connective and the right pleural ganglion met and the fourth right larval retractor nerve emerged from the pleuro-pedal connective, just ventral to where the pleuro-pedal and the cerebro-pedal connectives joined (Fig. 34B, D). The third right larval retractor nerve (rl3) ran along the muscle cells of the dorsal branch of the right larval retractor muscle that inserted laterally

within the right velar lobe (Fig. 34D); whereas, the fourth right larval retractor nerve (rl4) ran along the muscle cells of the ventral branch of the right larval retractor muscle that inserted ventrally within the right velar lobe (Fig. 34D). Individual neurites from both nerves were observed synapsing directly on muscle cells of the right larval retractor muscle associated with the right velar lobe (not shown), indicating that these nerves were also involved in motor control of this muscle.

Table 1. Summary of the origins and sites of innervation for the nine nerves that innervate the larval retractor muscles in newly hatched *N. melanotragus*; a 'left nerve' implies that this nerve innervates the left larval retractor muscle and a 'right nerve' implies that it innervates the right larval retractor muscle.

Larval Retractor Muscle Nerves	Origin of Nerve	Site(s) of Innervation
First left larval retractor nerve (ll1)	Left pleural ganglion	Lateral portions of the trunk
Second left larval retractor nerve (ll2)	Left pleural ganglion	Lateral portion of the trunk, myocytes that insert on the anterior foregut
Third left larval retractor nerve (ll3)	Left cerebro-pleural connective/left pleural ganglion	Myocytes that insert laterally within the left velar lobe
Fourth left larval retractor nerve (ll4)	Left pleuro-pedal connective	Myocytes that insert ventrally within the left velar lobe
Fifth left larval retractor nerve (ll5)	Left cerebral ganglion	Medial portions of the trunk, myocytes that insert dorsally within the left velar lobe
First right larval retractor nerve (rl1)	Right pleural ganglion	Entire trunk
Second right larval retractor nerve (rl2)	Right pleural ganglion	Myocytes that insert dorsally within the right velar lobe
Third right larval retractor nerve (rl3)	Right cerebro-pleural connective/right pleural ganglion	Myocytes that insert laterally within the right velar lobe
Fourth right larval retractor nerve (rl4)	Right pleuro-pedal connective	Myocytes that insert ventrally within the right velar lobe

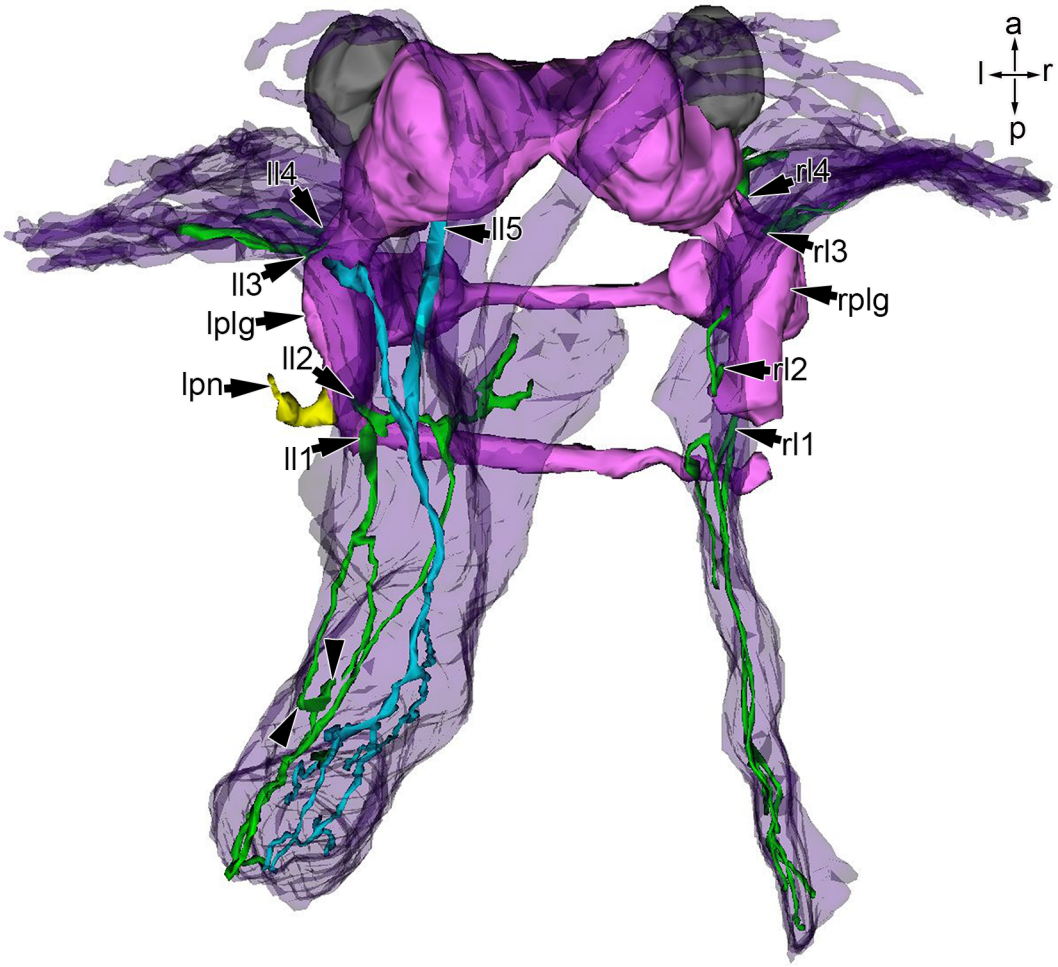

Figure 32. Surface rendered three-dimensional reconstruction of the morphology and trajectory of the nine nerves that innervate the larval retractor muscles; green nerves are associated with the pleural ganglia, the blue nerve is associated with the left cerebral ganglion; the larval retractor muscles have been rendered semi-transparent, the visceral loop omitted for clarity and the left pallial nerve included for anatomical context when viewing the transmission electron micrographs in figure 33; the nerves were reconstructed free-hand based on serial thin-sections through two newly hatched *N. melanotragus* specimens; the size of the nerves are not to scale but represent a close approximation of their morphology and trajectory; *arrowheads* indicate the portion of the first larval retractor nerve shown in the transmission electron micrographs of figure 33E and F. Abbreviations: ll1= left larval retractor nerve #1, ll2= left larval retractor nerve #2, ll3= left larval retractor nerve #3, ll4= left larval retractor nerve #4, ll5= left larval retractor nerve #5, lplg= left pleural ganglion, lpn= left pleural nerve, rl1= right larval

retractor nerve #1, rl2= right larval retractor nerve #2, rl3= right larval retractor nerve #3, right larval retractor nerve #4, rplg= right pleural ganglion. Orientation axes: a= anterior, l= left, p= posterior, r= right.

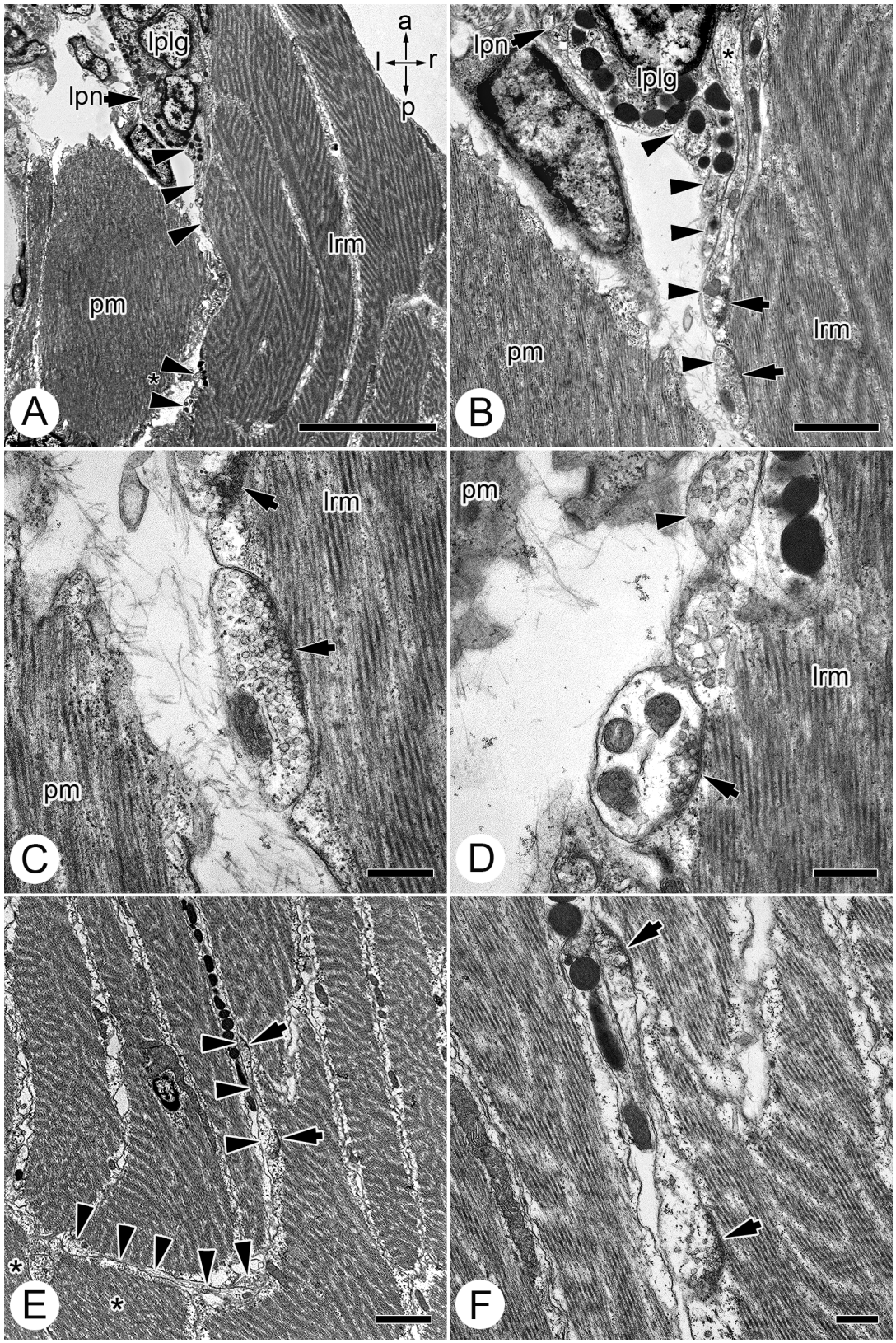
A
lplg
lpn
a
l
r
p
lrm
pm
*
B
lpn
lplg
*
lrm
pm
C
lrm
pm
D
pm
lrm
E
*
*
F

Figure 33. Transmission electron micrographs of frontal-sections showing the origin and trajectory of the first left larval retractor nerve, as well as five examples of neurites belonging to this nerve synapsing on larval retractor muscle cells; note the oblique striation characteristic of the larval retractor muscles and the lack of striation characteristic of the pedal muscles; all sections displayed in dorsal view. **A.** Low magnification micrograph of two portions of the first larval retractor nerve; the anterior portion (*arrowheads*) is emerging from the posterior of the left pleural ganglion and extending posteriorly between the left pedal muscle and the left larval retractor muscle; *asterisk* indicates a more posterior portion of the first larval retractor nerve (*arrowheads*); scale bar 10µm. **B.** Higher magnification of the first larval retractor nerve (*arrowheads*) emerging from the posterior of the left pleural ganglion; *asterisk* indicates an individual neurite; *arrows* indicate neurites synapsing on the larval retractor muscle; scale bar 2µm. **C.** Higher magnification of the synapsing neurons; note the synaptic vesicles binding to the intensely stained presynaptic membrane (*arrows*); scale bar 500nm. **D.** Higher magnification of the posterior portion of the first larval retractor nerve indicated by an *asterisk* in 'A'; *arrow* indicates a synapsing neurite; *arrowhead* points to non-synapsing neurite as a comparison; scale bar 500nm. **E.** Micrograph of a section that passes through two portions of the first larval retractor nerve (*arrowheads*) as it extends into the larval retractor muscle; the anterior portion of the nerve is synapsing on the larval retractor muscle (*arrows*); *asterisks* indicate pedal muscle cells, all other muscle cells belong to the left larval retractor muscle; note that this section passes through the point of the nerve indicated by *arrowheads* in figure 32; scale bar 2µm. **F.** Higher magnification of the anterior portion of the first larval retractor nerve in 'E'; *arrows* indicate synapses on the larval retractor muscle; scale bar 500nm. Abbreviations: lplg= left pleural ganglion, lpn= left pallial nerve, lrm= larval retractor muscle, pm= pedal muscle. Orientation axes: a= anterior, l= left, p= posterior, r= right.

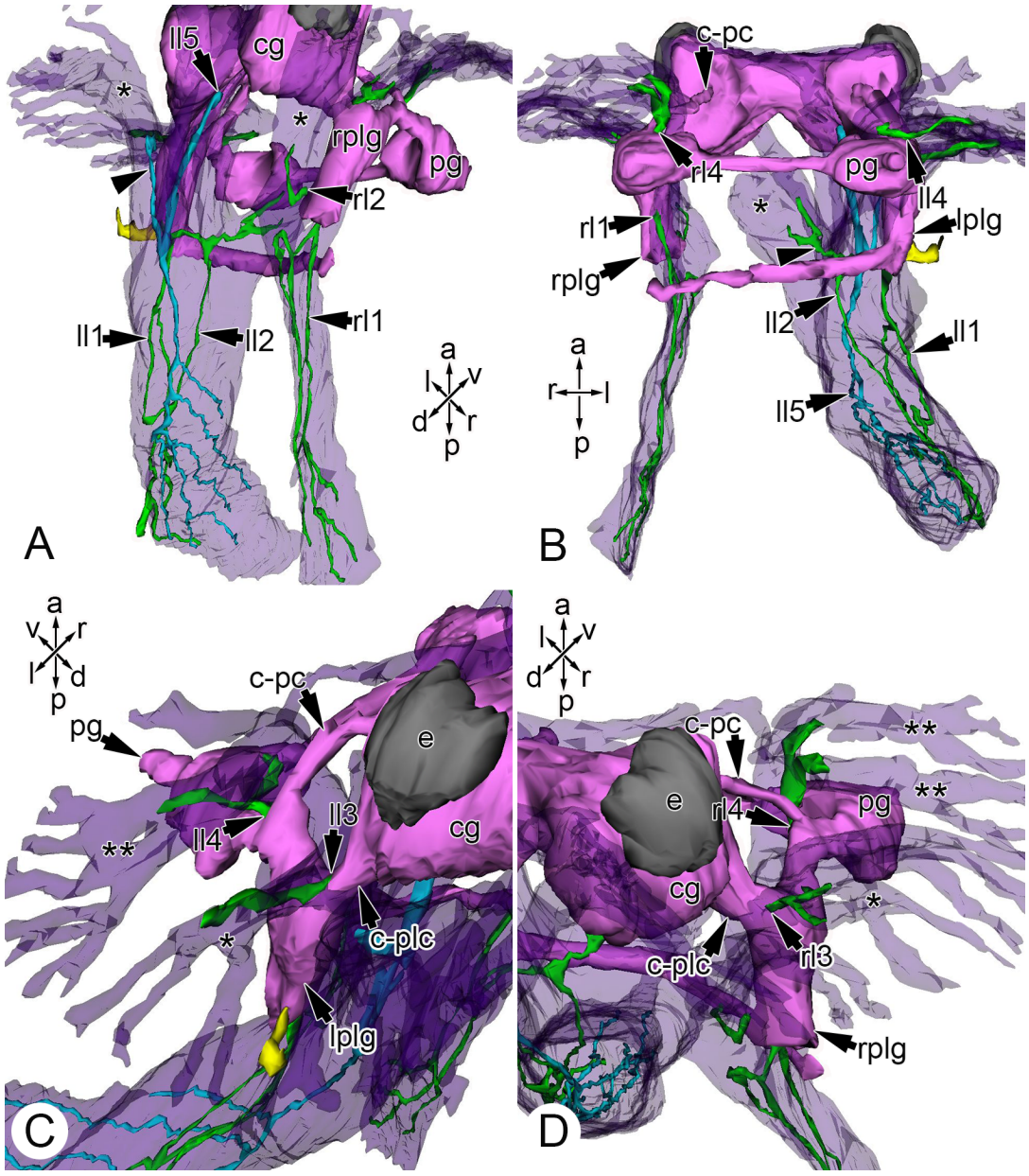

Figure 34. Surface rendered three-dimensional reconstructions showing the origin and trajectory of the nine nerves that innervate the larval retractor muscles. **A.** Dorsolateral view showing the left cerebral origin, as well as the trajectory of the fifth left larval retractor nerve and the right pleural origin, as well as the trajectory of the second right pleural nerve; *arrowhead* indicates the anterolateral branch of the fifth left larval retractor nerve that innervates the dorsal branch of the left larval retractor muscle (left *asterisk*); note that the second right pleural nerve innervates the dorsal branch of the right larval retractor muscle (right *asterisk*). **B.** Ventral view showing the first right larval retractor

nerve emerging from the ventral surface of the right pleural ganglion and extending posteriorly within the right larval retractor muscle; *arrowhead* indicates the anteromedial branch of the second left larval retractor nerve that extends into the branch of the left larval retractor muscle that inserts on the anterior foregut (*asterisk*). **C.** Left-anterolateral view showing the third left larval retractor nerve emerging from the point where the cerebro-pleural connective connects with the left pleural ganglion and innervates the muscle cells that insert laterally within the left velar lobe (*asterisk*); this view also shows the fourth left larval retractor nerve emerging from the pleuro-pedal connective, just ventral to where it connects with the cerebro-pedal connective and innervating the muscle cells that insert ventrally within the left velar lobe (*double asterisk*). **D.** Right-anterolateral view showing the third and fourth right larval retractor nerves emerging from symmetrical points to the nerves depicted in 'C' and innervating the muscle cells that insert laterally (*asterisk*) and ventrally (*double asterisk*) within the right velar lobe respectively. Abbreviations: cg=cerebral ganglion, c-pc= cerebro-pedal connective, c-plc= cerebro-pleural connective, e= eye, ll1= left larval retractor nerve #1, ll2= left larval retractor nerve #2, ll3= left larval retractor nerve #3, ll4= left larval retractor nerve #4, ll5= left larval retractor nerve #5, lplg= left pleural ganglion, pg= pedal ganglion, rl1= right larval retractor nerve #1, rl2= right larval retractor nerve #2, rl3= right larval retractor nerve #3, right larval retractor nerve #4, rplg= right pleural ganglion. Orientation axes: a= anterior, d= dorsal, l= left, p= posterior, r= right, v= ventral.

3.2.3 Innervation of the pedal muscles

Table 2 summarizes the point of origin and innervation sites for each pedal muscle nerve. In newly hatched *N. melanotragus* the left pedal muscle was innervated by a single nerve (lp) that emerged from the extreme posterior of the left pleural ganglion (Fig. 35), and neurites belonging to this nerve were observed synapsing directly on muscle cells of the left pedal muscle (not shown), suggesting it was directly involved in motor control of this muscle. A single nerve likewise innervated the entire right pedal muscle; however, it emerged from the posterior of the subintestinal ganglion (Figs. 35; 36A, B). Neurites that were a part of the right pedal nerve were observed synapsing on the muscle cells of the right pedal muscle (Fig. 36 C-F), indicating that the right pedal nerve was involved in the motor control of the right pedal muscle.

Bourne (1908) reported that the pedal muscles are innervated from single nerves extending from the ipsilateral pleural ganglion in adult neritimorphs. Indeed, upon histological analyses of serial sections through post-metamorphic juvenile *N. melanotragus*, the right pedal muscle nerve was observed to emerge dorsolaterally from the right pleural ganglion instead of from the subintestinal ganglion (Fig. 37). Transmission electron microscopy was not done to ensure that these nerves directly synapsed onto the muscle cells of the ipsilateral pedal muscle in the juvenile. However, they were the only nerves observed to innervate the pedal muscles, neither nerve was observed emerging from either pedal muscle and both the point of emergence and the trajectories of the pedal muscle nerves from their respective pleural ganglion matched the anatomical description of the pedal muscle nerves given by Bourne (1908) for adult neritimorphs. Furthermore, no nerves were observed emanating from the subintestinal ganglion in the juvenile. Thus, like the shortcut and the right pallial nerve, the right pedal muscle nerve was directly connected with the subintestinal ganglion at hatching, and then became associated with the right pleural ganglion later in development.

Table 2. Summary of the origin and site of innervation for the pedal muscle nerves in *N. melanotragus*; the site of origin for the right pedal muscle nerve changes over the course of development.

Pedal Muscle Nerve	Origin of Nerve	Site of Innervation
Left pedal muscle nerve	Left pleural ganglion	Entire left pedal muscle
Right pedal muscle nerve	Subintestinal Ganglion at hatching, right pleural ganglion later in development	Entire right pedal muscle

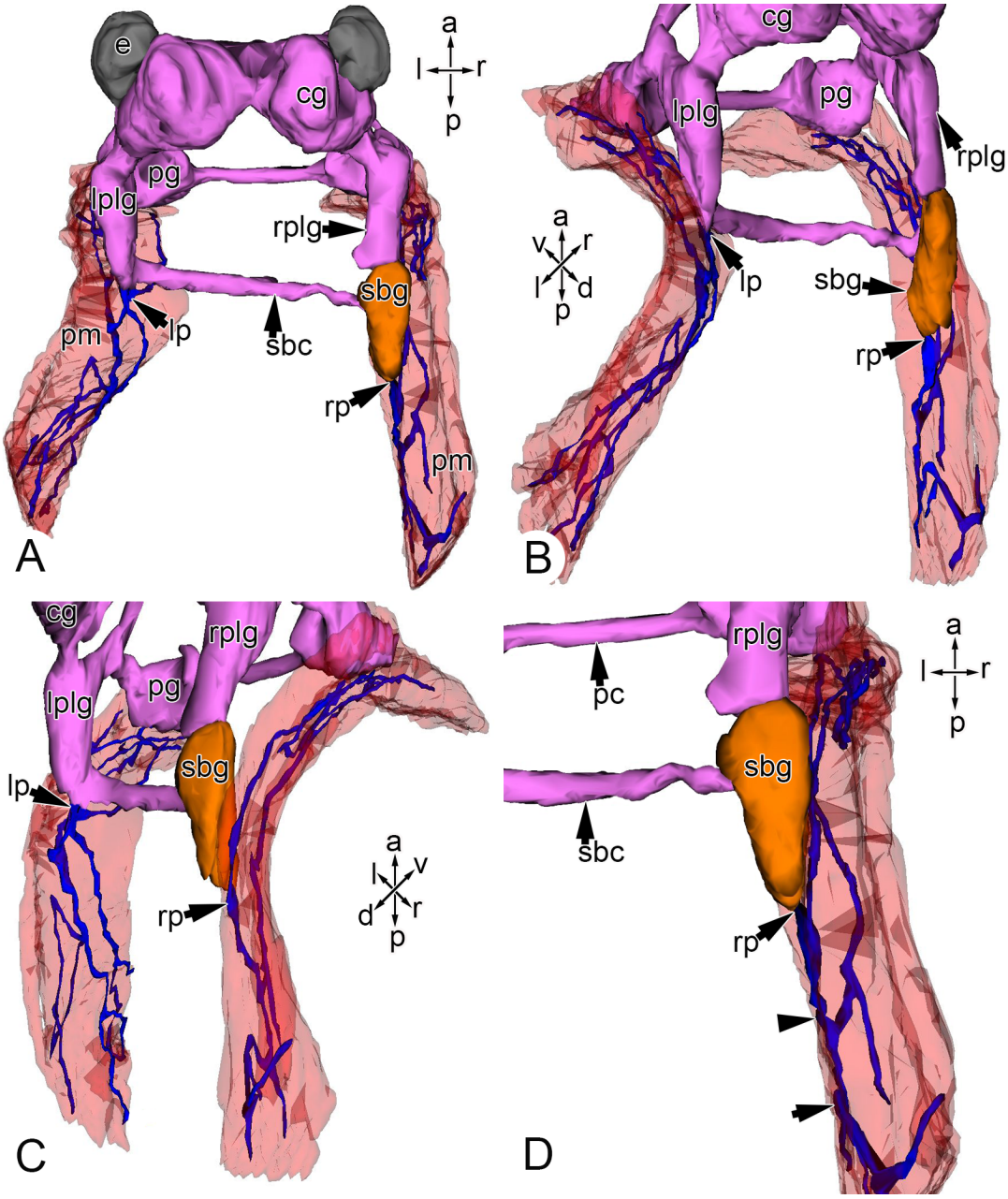

Figure 35. Surface rendered three-dimensional reconstructions of newly hatched *N. melanotragus*, showing the origin and trajectory of the nerves that innervate the pedal muscles. **A.** Dorsal view showing the single left pedal muscle nerve emerging from the posterior of the left pleural ganglion and the single right pedal muscle nerve emerging from the posterior of the subintestinal ganglion. **B.** Left-dorsolateral view showing that the left pedal muscle nerve innervates the entire left pedal muscle. **C.** Right-dorsolateral view showing that the right pedal muscle nerve innervates the entire right pedal muscle. **D.** Close up dorsal view of the right pedal muscle nerve emerging from the posterior of

the subintestinal ganglion; *arrowhead* indicates the position of the posterior neurites shown in figure 36B; *arrow* indicates the position along the right pedal muscle nerve that is shown in Figure 36E and F. Abbreviations: cg= cerebral ganglion, e= eye, lplg= left pleural ganglion, lp= left pedal muscle nerve, pc= pedal commissure, pg= pedal ganglion, pm= pedal muscle, rp= right pedal muscle nerve, rplg= right pleural ganglion, sbc= subintestinal connective, sbg= subintestinal ganglion. Orientation axes: a= anterior, d= dorsal, l= left, p= posterior, r= right, v= ventral.

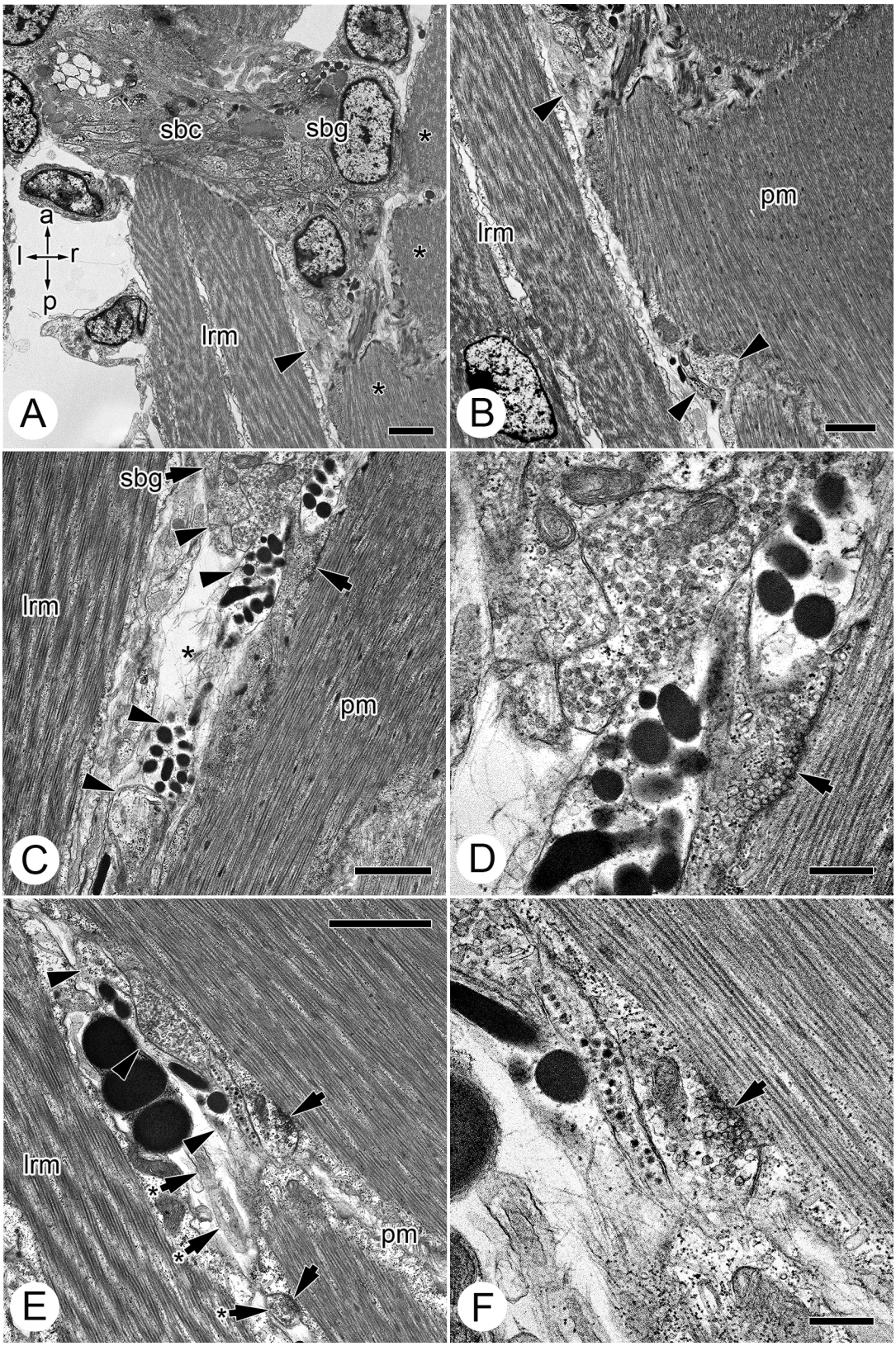
sbc
sbg
a
l
r
p
lrm
A
pm
lrm
B
sbg
lrm
pm
C
D
lrm
pm
E
F

Figure 36. Transmission electron micrographs of frontal-sections showing the origin and trajectory of the right pedal muscle nerve, as well as three examples of neurites belonging to this nerve synapsing on pedal muscle cells; all sections are displayed in dorsal view. **A.** Low magnification micrograph showing the subintestinal connective connecting with subintestinal ganglion and the pedal muscle nerve (*arrowhead*) about to emerge from the posterior of the subintestinal ganglion; *asterisks* indicate muscle cells of the right pedal muscle; scale bar 2µm. **B.** Higher magnification of the neurites of the pedal muscle nerve about to emerge from the posterior of the subintestinal ganglion (*upper arrowhead*) and more posterior section profiles through this nerve (*lower arrowheads*), the position of these neurites is indicated by the *arrowhead* in figure 35D; scale bar 2µm. **C.** Section showing the right pedal muscle nerve beginning to emerge from the posterior of the subintestinal ganglion (*upper arrowheads*) and connecting with the posterior portion of the nerve shown in 'B' (*lower arrowheads*); *asterisk* indicates where the two portions of the nerve are connecting; *arrow* indicates one of the neurites emerging from the subintestinal ganglion that is synapsing on the right pedal muscle; scale bar 2µm. **D.** Higher magnification of the neurite emerging from the subintestinal ganglion synapsing on the right pedal muscle; scale bar 500nm. **E.** Micrograph showing the portion of the right pedal muscle nerve indicated by the *arrow* in figure 35D; note how one branch is continuing posteriorly between the larval retractor muscle and the pedal muscle (*arrow + asterisk*), and the other branch is about to extend posterolaterally between the two muscle cells of the right pedal muscle (*arrowheads*); *arrows* indicate neurites that are synapsing on the pedal muscle; scale bar 2µm. **F.** Higher magnification micrograph of the neurite belonging to the posterolateral branch that is synapsing on the pedal muscle; scale bar 500nm. Abbreviations: lrm= larval retractor muscle, pm= pedal muscle, sbc= subintestinal connective, sbg= subintestinal ganglion. Orientation axes: a= anterior, l= left, p= posterior, r= right.

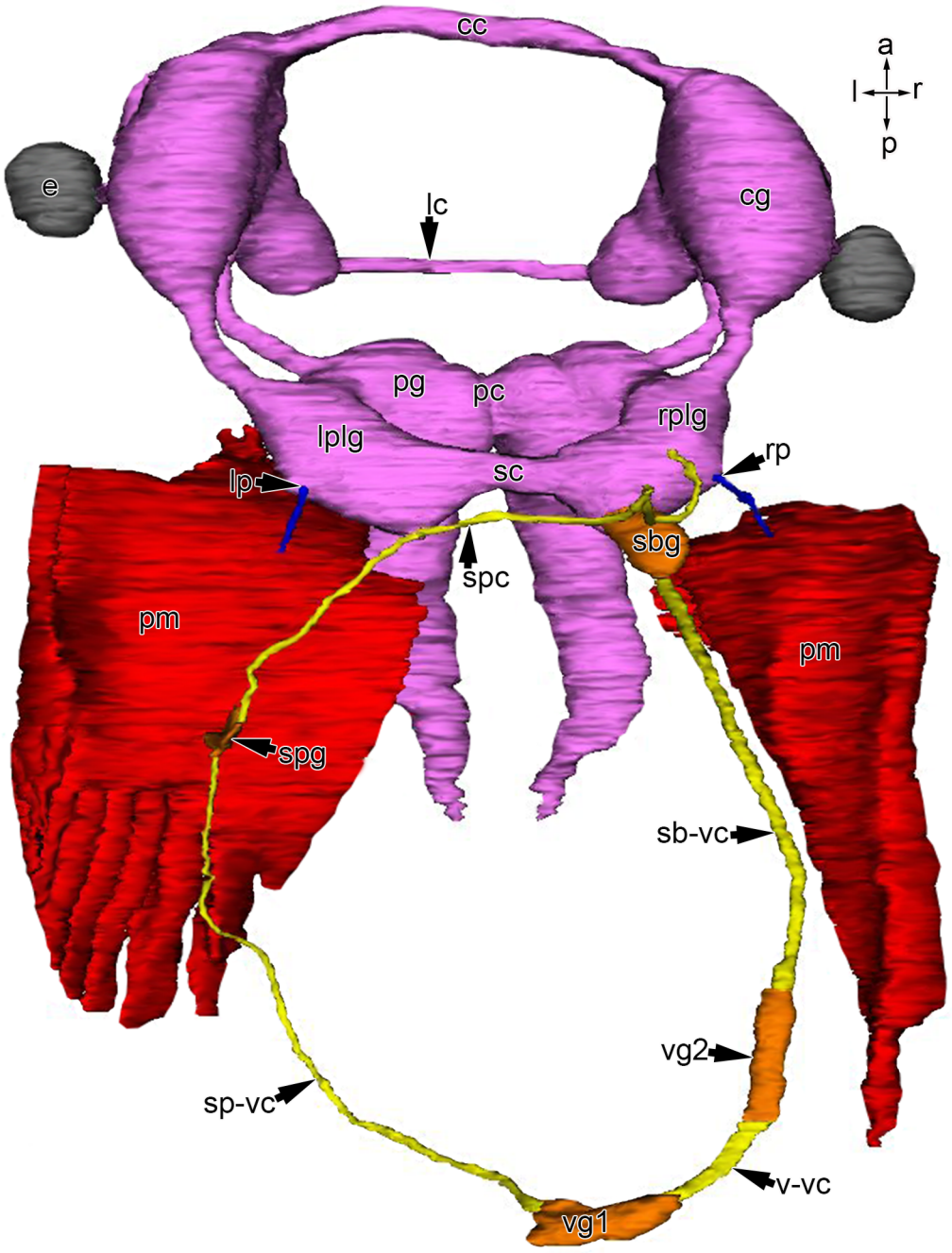

Figure 37. Surface rendered three-dimensional reconstruction of the central nervous system, pedal muscles and the innervation of the pedal muscles in juvenile *N. melanotragus*, shown in dorsal view; note how the right pedal muscle nerve no longer emanates from the subintestinal ganglion but emerges dorsolaterally from the right pleural ganglion and that the left pedal muscle nerve emanates from a symmetrical location out of the left pleural ganglion. Abbreviations: cc= cerebral commissure, cg=

cerebral ganglion, e= eye, lc= labial commissure, lp= left pedal muscle nerve, lplg= left pleural ganglion, pc= pedal commissure, pg= pedal ganglion, pm= pedal muscle, rp= right pedal muscle nerve, rplg= right pleural ganglion, sbg=subintestinal ganglion, sb-vc= subintestinal-visceral ganglion, sc= shortcut, spc= supraintestinal connective, spg= supraintestinal ganglion, sp-vc= supraintestinal-visceral connective, vg1= first visceral ganglion, vg2= second visceral ganglion, v-vc= visceral-visceral connective. Orientation axes: a= anterior, l= left, p= posterior, r= right.

4.0 Discussion

4.1 Evolutionary origins of the neuroanatomical shortcut

Evolutionary novelties can arise *de novo*, or from modifications to the developmental program of pre-existing structures (Panganiban *et al.,* 1997). A major objective of this study was to use development to try and gain insight into the evolutionary past of the novel connection in the nervous system of neritimorphs. Although the subintestinal ganglion is already fused to the right pleural ganglion at hatching, the neuroanatomical shortcut between the two pleural ganglia is not definitively present until 18 dph in *N. melanotragus* larvae (Figs. 14; 17). Before this point in development, it emerges from the left pleural ganglion and extends to the right**,** running ventrally beneath the esophagus and connecting to the subintestinal ganglion (Figs. 5; 10). This connective conforms to all the criteria that define a subintestinal connective of the visceral loop (Bullock and Horridge, 1965; Fretter and Graham, 1994). Thus, the observed development of the shortcut supports my hypothesis that the neuroanatomical shortcut between the two pleural ganglia is a derived construct of the ancestral subintestinal connective, and did not evolve *de novo*.

An evolutionary novelty can be defined as a characteristic that is neither homologous to any characteristic in the ancestral species nor homonomous to any other structure in the same organism (Müller and Wagner, 1991). A direct connection between the pleural ganglia represents a novel characteristic within the central nervous system of gastropods; however, the observed development of the neuroanatomical shortcut in the neritimorph nervous system suggests that it forms from a connective that is homologous to the subintestinal connective of other gastropods. Therefore, although a direct connection between the pleural ganglia represents a novel central nervous system characteristic, the shortcut itself represents a modified subintestinal connective and not a novel structure.

4.2 Function of the neuroanatomical shortcut

Morphological changes to components of the nervous system are functionally linked to changes in their target tissues. Bourne (1908) showed that the two pedal muscles present in adult neritimorphs were innervated by nerves from the ipsilateral pleural ganglia and thus hypothesized that the novel connection between the pleural ganglia may function in coordinating the two pedal muscles present in adult neritimorphs. However, the fact that similar modifications to the nervous system don't exist in the other gastropods with two pedal muscles that have been studied, and the recent discovery that *N. melanotragus* larvae hatch with both the adult pedal muscles and a pair of larval retractor muscles led me to extend Bourne's (1908) hypothesis to state that the neuroanatomical shortcut may function in coordinating the two pairs of shell muscles present within the larval stages. To test this hypothesis, I used the timing of development of the shortcut, as well as the innervation pattern of the two sets of ontogenetic shell muscles, to elucidate the function of the neuroanatomical shortcut in neritimorphs.

Despite the fact that the pattern of development revealed the evolutionary origins of the shortcut, it did not conform exactly to my predicted model of development (Fig. 38). According to my model, the shortcut between the two pleural ganglia should be present at hatching because I implicated the shortcut in the coordination of the two pairs of shell muscles that are present in hatching *N. melanotragus* larvae (Fig. 38A). However, the direct connection between the two pleural ganglia is not established until 18 dph (Fig. 38B). Furthermore, the right pedal muscle was innervated by the subintestinal ganglion in newly hatched larvae (Figs. 35; 36), and the right pedal muscle nerve became incorporated into the right pleural ganglion later in development (Fig. 37). Figure 39 depicts a diagram summarizing the data presented in Figures 35, 36, 37 and 38B that depict the ontogeny of the neuroanatomical shortcut and the ontogenic pattern of shell muscle innervation that was used to elucidate the function of the neuroanatomical shortcut.

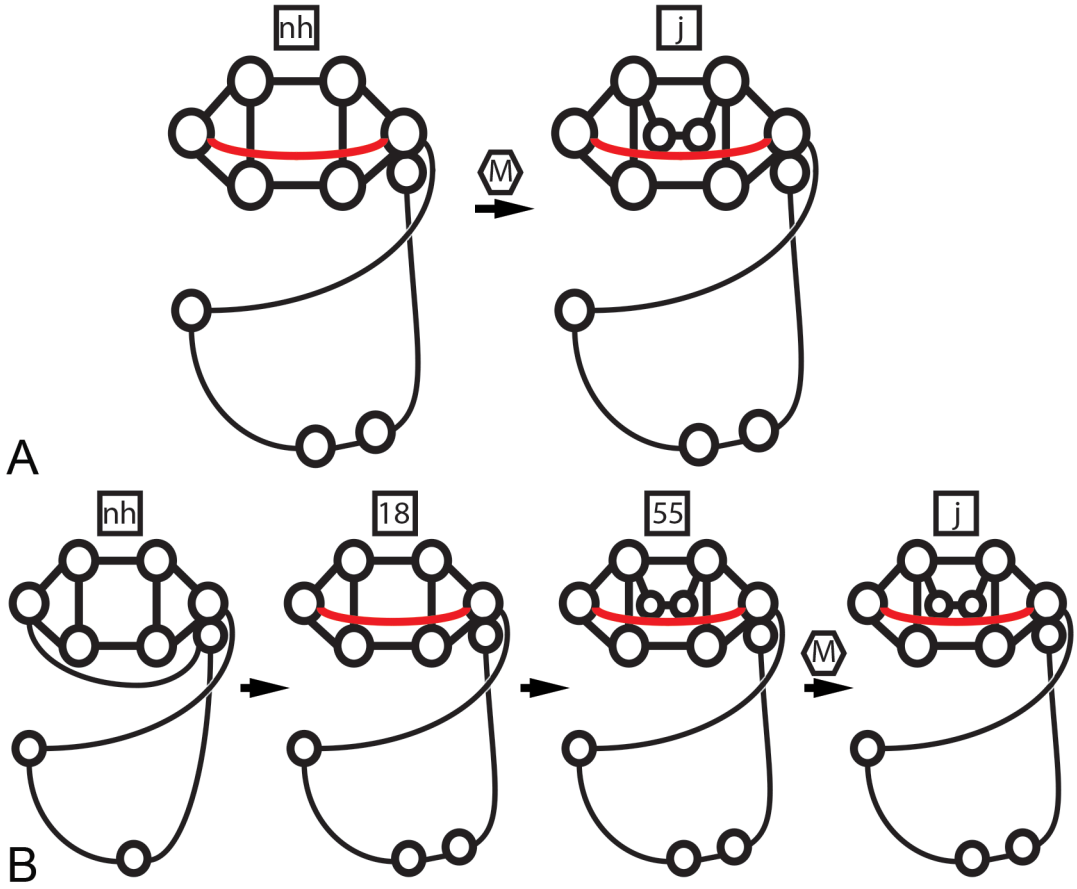

Figure 38. Diagrammatic illustrations of my hypothesized model of development of the nervous system in *N. melanotragus* (**A**) and the observed development of the nervous system (**B**); boxes above each diagram indicate the developmental stage, and the 'M' indicates metamorphosis; the neuroanatomical shortcut is drawn in red.

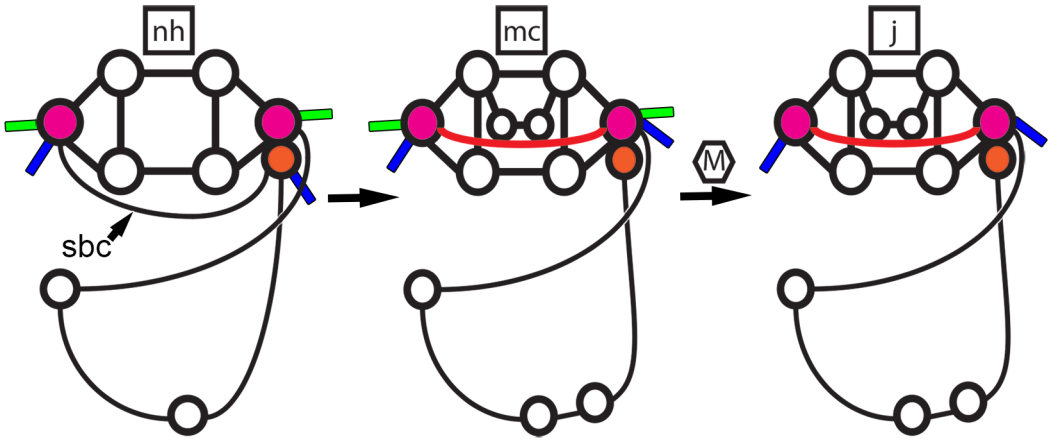

Figure 39. Diagram summarizing the data presented in Figures 35, 36, 37 and 38B that depict the ontogeny of the neuroanatomical shortcut and the ontogenic pattern of shell muscle innervation that was used to elucidate the function of the neuroanatomical shortcut. Boxes above each diagram indicate the developmental stage: nh= newly hatched, mc= metamorphic competence, M= metamorphosis, j= juvenile; pleural ganglia are drawn in pink, subintestinal ganglion is drawn in orange, pedal muscle nerves are drawn in blue, a summarized version of the larval retractor nerves are drawn in green, the shortcut is drawn in red. Abreviations: sbc= subintestinal connective.

The lack of developmental synchrony between time of differentiation of the two pedal muscles and time of formation of the neuroanatomical shortcut appeared to undermine the hypothesis that the function of the neuroanatomical shortcut was to coordinate the two pedal muscles. Yet the hypothesis was undermined to an even more serious extent by the surprising discovery that the right pedal muscle was innervated by the subintestinal ganglion at hatching because a direct connection between the left pleural ganglion, which innervates the left pedal muscle, and the subintestinal ganglion, which innervates the right pedal muscle is provided by the subintestinal connective (Fig. 39); no special additional connection should be required. In essence, if the exclusive purpose of the shortcut is to coordinate the pedal muscles, then the fusion between the subintestinal and right pleural ganglion, as well as the incorporation of neural components into the right pleural ganglion is superfluous because the connection between the ganglia that

innervate the pedal muscles is already established at hatching as the subintestinal connective.

Fusion between the subintestinal ganglion and right pleural ganglion must serve to coordinate some other set of structures innervated by both pleural ganglia, and the most likely candidate is the pair of larval retractor muscles. Larvae of *N. melanotragus* possess both a left and right larval retractor muscle; both are present in hatching larvae and the motor control of both originates primarily from the pleural ganglia (Figs. 32; 33; 34; 39). These observations support the hypothesis that the neuroanatomical shortcut functions in coordinating the left and right larval retractor muscles as well as the left and right pedal muscles, however these results further suggest that the shortcut did not strictly evolve to coordinate both sets of muscles. Instead, the subintestinal connective, which already coordinates the pedal muscles, was co-opted to additionally coordinate the left and right larval retractor muscles through fusion of the subintestinal and right pleural ganglia. Coordination of all four muscles becomes even more direct later in larval development as the subintestinal connective and right pedal muscle nerve become incorporated into the right pleural ganglion (Fig. 39). Finally, the presence of the shortcut in post-metamorphic juveniles and adults suggests that it represents, at least, a neutral overall modification to the nervous system, although it is likely that coordination of the pedal muscles remains beneficial after the destruction of the larval retractor muscles at metamorphosis (Fig. 39).

The present study emphasizes the importance of analyzing different life history stages when addressing the function of evolutionary novelties. The present study also illustrates that the presence of a novelty within a given developmental stage does not necessitate a primary function within that stage. The neuroanatomical shortcut is present within the central nervous system of adult neritimorphs, but including developmental stages in the functional analysis led to rejection of Bourne's (1908) adult-centric hypothesis and to its replacement with a hypothesis specific to the larval stages. Therefore, the stage at which one studies a novelty is critically important in determining its functional value.

4.3 Mechanism for the incorporation of the subintestinal connective, right pallial nerve and right pedal muscle nerve into the right pleural ganglion

The subintestinal connective, right pallial nerve and right pedal muscle nerve all emerge from the subintestinal ganglion at hatching and then emerge from the right pleural ganglion later in development (Figs. 5D; 25; 30; 35). Although this seems extraordinary, both the observed development of the neritimorph nervous system, as well as the process of gangliogenesis provide clues as to a potential mechanism for this ganglionic switch in innervation.

At the newly hatched stage, the pleural ganglia are elongate swellings along the cerebro-pleural connective (Fig. 5) and are very slender along the dorsoventral axis (Fig. 5B). Furthermore, the right pleural ganglion and the subintestinal ganglion are nearly equivalent in size at hatching (Fig. 5), and based on the relative sizes of the right pleural ganglion and subintestinal ganglion at later stages of development (Figs. 25; 30) it is clear that the right pleural ganglion increased in size to a much greater extent than the subintestinal ganglion. Thus, it is possible that the anterior portion of the subintestinal ganglion becomes incorporated into the right pleural ganglion as a result of disproportionate growth of the right pleural ganglion relative to the subintestinal ganglion. This mechanism can explain the incorporation of both the subintestinal connective and the right pallial nerve because they are both associated with the anterior of the subintestinal ganglion. However, this mechanism fails to explain the incorporation of the right pedal nerve, which emerges from the posterior tip of the subintestinal ganglion at hatching (Fig. 35).

It is possible that the incorporation of the pedal muscle nerve occurs as a result of differential growth of the portion of the subintestinal ganglion that is posterodorsal to where this nerve emerges. As discussed previously (see section 1.4.1), neurons within ganglia do not undergo mitosis, and increase in cell number is achieved by the ingression of cells from proliferative zones of ectodermal placodes (McAllister *et al.,* 1983; Jacob, 1984; Hickmott and Carew, 1991; Page, 1992a,b). If more of the ingressed cells were being incorporated into regions of the subintestinal ganglion that are posterodorsal to where the right pedal muscle nerve initially emerges than into regions anteroventral to

this nerve, then as the subintestinal ganglion grows, the pedal muscle nerve would seemingly be emerging from more and more anteroventral positions over time.

This proposed differential growth of the posterodorsal portion of the subintestinal ganglion in combination with the observed disproportionate growth of the right pleural ganglion relative to the subintestinal ganglion throughout development can explain the incorporation of the subintestinal connective, right pallial nerve and right pedal muscle nerve from the subintestinal ganglion at hatching, to the right pleural ganglion later in development.

I resolved the pedal muscle nerves at the newly hatched stage using transmission electron microscopy, however I did not use transmission electron microscopy to analyze muscle innervation in later stages. I could not resolve the pedal muscle nerves using light microscopy until 55 dph (not shown) and at this stage they exhibited the same point of emergence and trajectory from each of the pleural ganglia as in the 6 dpm juvenile (Fig. 37). Thus, I cannot report exactly when the pedal muscle nerve becomes incorporated into the right pleural ganglion, only that it does happen by metamorphic competence at 55 dph. Transmission electron microscopic analysis of the right pedal nerve in mid-larval stages is required to test the proposed mechanism of differential growth of the subintestinal ganglion.

4.4 Function of four ontogenetic shell muscles in neritimorph larvae

Adult gastropods that lack a columella, or possess a shell-coiling pattern that effectively reduces the columella, require a left and right pedal muscle to retract the entire body of the snail into the shell (Salvini-Plawen and Haszprunar, 1987; Haszprunar, 1988a; Fretter and Graham, 1994; Lindberg and Ponder, 2001). This on its own explains why two pedal muscles are present in adult neritimorphs, but does not explain why they are present so early within the larva. The single larval retractor muscle functions in bringing the entire cephalopodium into the shell within the earliest larval stages in other gastropods (Page, 1995, 1998). This is achieved because the foot is so small at these stages (Page, 1995, 1997, 1998; Wanninger, 1999a). Furthermore, the pedal muscle(s) develop in coordination with the growth of the foot that occurs later in larval

development in other gastropods (Page, 1995, 1997, 1998; Wanninger, 1999a; Evans *et al.,* 2009). *N. melanotragus* on the other hand possesses a relatively broad foot with the characteristically large operculum with an internal apophyses at hatching (Page and Ferguson, 2013). It seems reasonable to suggest that the pedal muscles, which insert entirely on either side of the operculum are required to help fully retract the cephalopodium and operculum into the shell at hatching.

The presence of left and right larval retractor muscles in *N. melanotragus* is much more perplexing because one larval retractor muscle is able to retract the entire cephalopodium into the shell of all other early veliger larvae that have been studied (Page, 1995, 1997, 1998; Degnan *et al.,* 1997, Wanninger *et al.,* 1999a, Wollesen *et al.*, 2008). It is made even more perplexing considering the distal insertion sites of the left larval retractor muscle in *N. melanotragus* are essentially the same as the distal insertion sites of the single larval retractor muscle in all other gastropods (see section 1.5) and the right larval retractor muscle in *N. melanotragus* only inserts within the right velar lobe (Page, 1995, 1997, 1998; Degnan *et al.,* 1997, Wanninger *et al.,* 1999a, Wollesen *et al.*, 2008; Page and Ferguson, 2013). However, neritimorph larvae are the only gastropod known to have a convolute protoconch (Bandel and Frýda, 1999; Bandel 2007; Nüzel *et al.* 2007; Page and Ferguson, 2013), and the neritoidean larvae are the only gastropod larvae observed to resorb the inner-whorls of their protoconch (Bandel and Frýda, 1999; Kaim and Sztajner, 2005; Nüzel *et al.* 2007; Page and Ferguson, 2013). Thus, it is possible that one of these changes in shell morphology was significant enough to require an additional larval retractor muscle on the right side in order to help retract the entire cephalopodium into the shell.

4.5 Which came first- the shell or the shortcut?

Analysis of ontogeny suggests that the evolution of the novel connection in the neritimorph nervous system is functionally linked to the presence of four shell muscles in hatching stage larva, which in turn is correlated with convolute protoconchs and dissolution of internal shell walls. The fossil record provides clues to the evolutionary timeline for these derived morphologies of the neritimorph protoconch. It is therefore

possible to map the emergence of these characteristics in order to make legitimate hypotheses on the evolutionary history of this integrated functional unit (Fig. 39).

The extant Nertimorpha with convolute protoconchs are likely descendants of naticopsid gastropods that possessed low-spired, non-convolute protoconchs, and coiled teleoconchs with a columella (Knight, 1933; Knight *et al.,* 1960; Squires, 1976; Yoo, 1994; Nüzel and Mapes, 2001; Squires, 1976; Bandel *et al.,* 2002; Kaim and Sztajner, 2005; Bandel, 2007; Nüzel *et al.,* 2007). The protoconchs of these ancient snails did not undergo dissolution of the inner shell whorls, which is an apomorphy of the Neritoidea (Nüzel *et al.,* 2007). Furthermore, all pre-Mesozoic opercula of naticopsids exhibit only one pedal muscle scar on the operculum, indicating that they only possessed one pedal muscle (Kaim and Sztajner, 2005).

Existing information on living members of the Neritopsidae indicates that these neritimorphs do not resorb the inner whorls of their shell. However, an analysis on opercular muscle scars from both fossil and Recent neritopsids suggests that like neritoideans, neritopsids possess two pedal muscles (Kaim and Sztajner, 2005). This suggests that the shell-coiling pattern exhibited by members of Neritopsidae-in which there is a high whorl expansion rate-reduces the columella enough to require left and right pedal muscles.

The pre-metamorphic stages of members of the Neritopsidae have never been studied and thus it remains unknown whether the paired condition of the larval retractor muscles is present within members of the Neritopsidae. As such, it remains unknown whether the emergence of the paired larval retractor muscles coincided with the emergence of a convolutely coiled protoconch, as exhibited by all extant neritimorphs, or with the emergence of the hollow shell exhibited by the Neritoidea. Nevertheless, the development of the shortcut and the pattern of shell muscle innervation observed in this study provide some clues.

The ganglionic switch in muscle innervation observed in development suggests that the paired condition of the larval retractor muscles and pedal muscles arose separately. If both pairs of muscles arose concurrently you would expect that they would be innervated by the same ganglionic pair throughout development, and most likely by a pair with a pre-established commissure (i.e. cerebrals or pedals). The fact that both larval

retractor muscles are innervated primarily by nerves associated with the pleural ganglia at hatching and that the right pedal muscle is initially innervated by the subintestinal ganglion at hatching and then innervated by the right pleural ganglion subsequently suggests that the paired condition of the pedal muscles arose first. Furthermore, as mentioned above, all members of the extant Neritimorpha possess paired pedal muscles and convolutely coiled protoconchs. Therefore, I propose that the paired condition of the pedal muscles occurred around the time that the columella became reduced in the convolutely coiled shells of all post-Palaeozoic neritimorphs around the Palaeozoic-Mesozoic transition, 250 million years ago (Fig. 39) (Bandel, 2007; Nüzel *et al.,* 2007). I further propose that at this time, the right pedal muscle was innervated by the subintestinal ganglion. The notion that the paired condition of the larval retractor muscles evolved after the pedal muscles as indicated by the pattern of innervation observed in the ontogeny of *N. melanotragus* suggests that the paired larval retractor muscles may have co-evolved with dissolution of the inner-whorls of the protoconch (Fig. 39). Hollow, convolute protoconchs of the Neritoidea appear in the fossil record within the early-Triassic, 250-245million years ago (Fig. 39) (Bandel and Frýda, 1999; Kaim and Sztajner, 2005; Kano, 2006; Bandel, 2008).

The need for neural coordination between the pleural ganglia likely occurred when the paired condition of the larval retractor muscle emerged as a result of the evolution of the right larval retractor muscle. The required coordination between the pleural ganglia could have initially been achieved via a zygoneury between the right pleural ganglion and the subintestinal ganglion, and then over time, this coordination could have become more direct through shortening of the zygoneury and eventual fusion of the subintestinal ganglion to the right pleural ganglion. Thus, evolution of the neuroanatomical shortcut likely arose in coordination with the evolution of the right larval retractor muscle and dissolution of the inner walls of the protoconch (Fig. 39).

Evidence supporting this hypothesis on the evolutionary history of the derived characteristics of the shell, shell muscles and the neuroanatomical shortcut lies within the partial recapitulation of this process during the development of the shortcut in *N. melanotragus*. Further evidence for this hypothesis is that various members of the Helicinidae (Bourne, 1911) and the one studied member of the Phenacolepadidae

(Fretter, 1984) possess visceral loops that are seemingly more derived than members of the Neritidae (see section 1.3.1), yet the fusion between the subintestinal and the right pleural ganglia, as well as the neuroanatomical shortcut between the pleural ganglia remains present within their central nervous systems. The presence of these attributes of the central nervous system in three families of the Neritoidea suggests that they are plesiomorphic for this superfamily. The specializations of the visceral loop observed in Helicinidae (Bourne, 1911) and Phenacolepadidae (Fretter, 1984) could represent further derivations of the plesiomorphic neritoidean nervous system.

If my hypothesis on the evolutionary history of the derived aspects of the shell, shell muscles and nervous system is correct, the larvae of members of the Neritopsidae should possess paired pedal muscles, but lack the paired condition of the larval retractor muscles and the neuroanatomical shortcut in their visceral loop. Moreover, the larvae of other representatives of the Neritoidea should possess all of the derived larval characteristics observed in *N. melanotragus*. Morphological analyses on pre-metamorphic developmental stages of other Neritoideans, as well as on *Neritopsis* or *Titiscania*, the only living members of the Neritopsidae, are necessary to test the legitimacy of this evolutionary hypothesis.

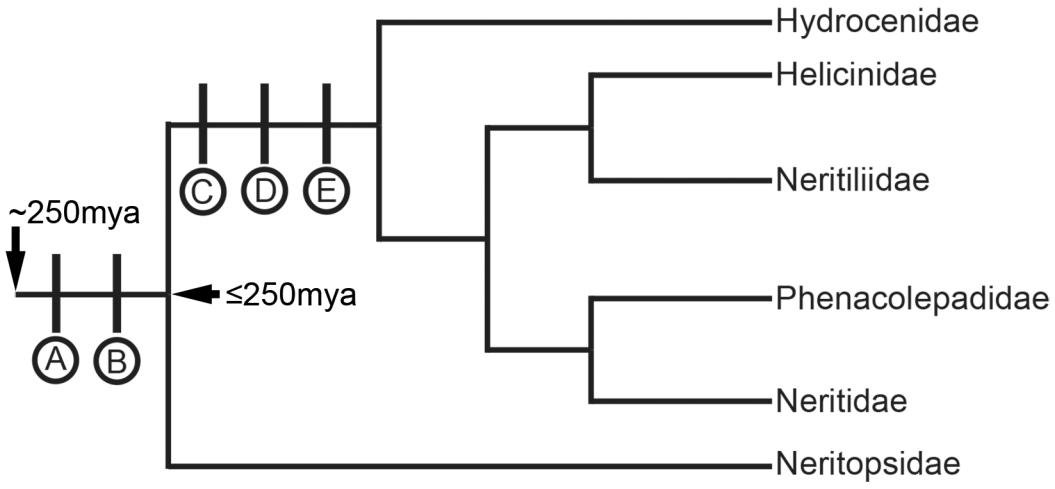

Figure 40. Diagrammatic illustration of my hypothesis on the evolutionary history of derived aspects of the shell, shell muscles and nervous system via a character map superimposed on a current phylogeny of the Neritimorpha adapted from Kano *et al.,*

(2002). **A.** Convolutely coiled protoconch. **B.** Paired pedal muscles. **C.** Dissolution of the inner-whorls of the protoconch. **D.** Paired larval retractor muscles. **E.** Neuroanatomical shortcut between the two pleural ganglia.

4.6 Comparisons with other gastropods

4.6.1 Homology of the pedal muscles

All extant neritimorphs posses two pedal muscles, and paired structures are usually interpreted as being plesiomorphies among gastropods (Thiele, 1925; Fretter, 1965; Haszprunar, 1988a; Salvini-Plawen and Haszprunar, 1987). Indeed, the majority of the members of the two subclasses (Patellogastropoda and Vetigastropoda) that are thought to form a clade sister to the rest of the Gastropoda (Aktipis *et al.,* 2008) possess two pedal muscles. However, evidence from the fossil record suggests that post-Palaeozoic neritimorphs are descendants of an extinct clade that possessed a coiled shell with a single pedal muscle (Kaim and Stajner, 2005). This suggests that the paired pedal muscles are an apomorphy of extant neritimorphs (Neritoidea and Neritopsidae), and that these muscles are not homologous to the paired plesiomorphic muscles of the Gastropoda. Comparing pedal muscle innervation in other gastropods with two pedal muscles further supports this notion.

Despite some variation, the majority of anatomical descriptions of gastropod adult nervous systems suggest that the pedal muscle nerve(s) arise from the pleural ganglia (Bourne, 1908; Bullock and Horridge, 1965; Fretter, 1984; Bouvier, 1887; Berthold, 1990, 1991). Indeed, Haszprunar (1985c) states that pedal muscle innervation occurs almost exclusively via the pleural ganglia in the Gastropoda. Haszprunar's (1985c) analysis suggests that if the pedal muscle nerves emerged from alternate locations such as the subintestinal ganglion, partway along the visceral loop, or from a parietal ganglion, the nerves could be traced back through various connectives to soma within one of the pleural ganglia. Such a consistent pattern of innervation is appealing, however these observations should be considered with caution as the methods employed in this study could not have provided the resolution required to accurately trace individual neurite

bundles through ganglia and nerve connectives and the author only provides sketches as evidence for these observations (Haszprunar, 1985c).

It has become clear that one cannot definitively assign homology or novelty to components of the nervous system based simply on their position within the adult nervous system. More analyses on the development of peripheral nerves is required in order to understand the variation of peripheral innervation in adult gastropod nervous systems. As it stands, very little is known about the ontogeny of pedal muscle nerves in other gastropods. Nevertheless, fusion between the subintestinal ganglion and right pleural ganglion is uncommon. The only other documented occurrences of this fusion are within three members of the Ampullariidae (Ceanogastropoda) (Honegger, 1974; Demian and Yousif, 1975; Brown and Berthold, 1990) and a species of *Crepidula* (Caenogastropoda) (Moritz, 1939). Thus, it seems unlikely that the 're-wiring' pattern of development exhibited by the right pedal muscle nerve in *N. melanotragus* is representative of other gastropods. Ontogeny of the pedal muscle nerve in *N. melanotragus* suggests that the pleural origin of this nerve in post-metamorphic juveniles and adults is a secondarily derived characteristic. Therefore, the right pedal muscle nerve in neritimorphs is not homologous with the pedal muscle nerves that originate from the pleural ganglia in other gastropods with two pedal muscles.

More analyses on the development of peripheral nerves across gastropod taxa are required to confirm or reject any hypotheses on the homology of the pedal muscle nerve. Nevertheless, the observations presented here suggest that the paired pedal muscles in the Neritimorpha are a secondarily derived characteristic, and are therefore not homologous with the paired plesiomorphic pedal muscles of the Gastropoda.

4.6.2 Homology of the larval retractor muscles

The right larval retractor muscle originates on the inner postero-lateral wall of the right side of the shell, the distal branches insert exclusively within the right velar lobe and the entire muscle is embraced by the cerebro-visceral nerve ring (Page and Ferguson, 2013; Fig. 31A, D). A right ontogenetic shell muscle that conforms to all the defining criteria of a larval retractor muscle has never been observed in any other gastropod

veliger larva. This suggests that the right larval retractor muscle in *N. melanotragus* represents a novel gastropod structure. Analysis of myogenesis in embryonic stages is required to determine whether the right larval retractor muscle is a *de novo* innovation, or a derived construct of a pre-existing muscle.

The left larval retractor muscle originates on the inner postero-lateral wall of the left side of the shell and gives rise to distal branches that insert within the mantle fold, apical plate, left and right velar lobes and the anterior foregut in patellogastropods (Degnan *et al.,* 1997; Wanninger *et al.*, 1999a), vetigastropods (Degnan *et al.*, 1997; Page, 1997), caenogastropods (Page, 1998), heterobranchs (Page, 1995; Wollesen *et al.*, 2008) and neritimorphs (Page and Ferguson, 2013; present study). Furthermore, ventral muscle tracts that insert on the anterior foregut, apical plate and within the ventral portion of the left velar lobe are embraced by the cerebro-visceral nerve ring in five species of nudibranch (Page, 1995), *Euspira lewisii* (Caenogastropoda)(Page, 1998) and *Haliotis kamtschatkana* (Vetigastropoda)(Page, 1997). Page and Ferguson (2013) reported that the left larval retractor muscle in *N. melanotragus* was embraced by the visceral loop. However, this study revealed that although the left larval retractor muscle is contained within the visceral loop ventrally (Fig. 31C), it is not embraced by the visceral loop (Fig. 31A, C). Similar to what was observed in other gastropods (Page, 1995,1997,1998), the ventral muscle tracts are embraced by the cerebro-visceral nerve ring in *N. melanotragus* (Fig. 31A, B), as well as an additional muscle tract that inserts laterally within the left velar lobe (Fig. 31B). The morphological and developmental similarities between the left larval retractor muscle in neritimorphs and the single left larval retractor muscle found in other gastropods suggests that they are homologous and that this muscle is a plesiomorphy of the Gastropoda. However, differences in the innervation of the larval retractor muscles challenge this hypothesis.

Very few studies have looked at neural control of the larval retractor muscle, and only one has addressed it specifically (Page, 1995). A study analyzing myogenesis in multiple nudibranch species provides evidence that neurites emerging from the left and right cerebral ganglia synapse on the muscle cells of the single larval retractor muscle (Page, 1995).

I observed nine discrete nerves that directly synapse on the larval retractor muscles in *N. melanotragus* (Table 1; Fig. 32). Interestingly, the fifth left larval retractor nerve was the only one that did not have a corresponding nerve on the right side that innervated the right larval retractor muscle, and was also the only nerve that was not associated with a pleural ganglion. The fifth left larval retractor nerve emerged from the posterior of the left cerebral ganglion and innervated the dorsal velar branch and the entire medial portion of the trunk of the left larval retractor muscle (Figs. 32; 34A). Furthermore, unlike what was observed in nudibranchs (Page, 1995), I did not observe any ganglia on the right of the nervous system innervate the left larval retractor muscle or vice-versa (Fig. 32). The fifth left larval retractor nerve in *N. melanotragus* and the neurites from the left cerebral ganglion that synapse on the larval retractor muscle in nudibranchs both emerge from the posterior of the left cerebral ganglion, however, assigning these nerves as homologous would be presumptuous. Indeed, comparing the character states of these two groups is particularly challenging because the phylogenetic placement of the Neritimorpha remains volatile, and the Nudibranchia are regarded as a highly derived clade within the Heterobranchia, which is regarded as the most derived gastropod subclass (Fig. 1) (Aktipis *et al.,* 2008). Until more studies look at larval retractor muscle innervation, it remains unknown as to which pattern of innervation represents an apomorphy of the clade, and which, if any, is a characteristic of gastropod larvae in general. As such, these differences in innervation of the larval retractor muscles are not enough to reject the hypothesis on homology between the left larval retractor muscle in neritimorphs and the single larval retractor muscle in other gastropods with indirect development.

4.6.3 Observed neurogenesis in *N. melanotragus*

Derived features aside, adult neritimorphs possess a streptoneurous-hypoathroid nervous system with elongate pedal ganglia (pedal cords), elongate buccal ganglia, a long cerebral commissure and a labial commissure- the secondary commissure between the labial lobes of the cerebral ganglia (Bourne, 1908; Fretter and Graham, 1962).

Adult *Aplysiids* possess a euthyneurous-hypoathroid nervous system, however upon analyses of neurogenesis it was discovered that the pleural ganglia begin development fused posterolaterally to the cerebral ganglia, and then subsequently migrate to associate closely with the pedal ganglia (Kriegstein, 1977). Thus, hypoathroidy has been secondarily acquired in aplysiids and epiathroidy represents the plesiomorphic nervous system configuration (Kriegstein, 1977). On the contrary, *N. melanotragus* hatched with a streptoneurous-hypoathroid nervous system (Fig. 5) suggesting this is the plesiomorphic state of the nervous system for neritimorphs.

Other than possessing the general configuration of the adult nervous system at hatching, none of the other adult features listed above were present in newly hatched larvae. *N. melanotragus* hatched from their egg capsules with all of the ganglia, connectives and commissures of the esophageal nerve ring and visceral loop, except for the components related to-and including the buccal ganglia, and the second visceral ganglion (Fig. 5). The pedal ganglia had begun tapering ventrally into cords by 18 dph (Fig. 14). This coincides with the thickening and lengthening of the foot that occurs in *N. melanotragus* after 2 weeks of development (Page and Ferguson, 2013). The second visceral ganglion also formed by 18 dph (Fig. 14). Bourne (1908), reported that this ganglion innervated the oviduct and ovarian follicle, as well as various aspects of the genitalia. The development of these organs was not documented but it seems reasonable to suggest that the appearance of this ganglion coincided with the development of these organs. The cerebral commissure was under a constant process of elongation throughout development, but had not become noticeably longer than the pedal commissure or the shortcut between the two pleural ganglia until 55 dph (Fig. 21), and the elongation became even more apparent after metamorphosis (Fig. 27). Finally, the labial lobes, the associated labial commissure and buccal ganglia formed by 55 dph (Figs. 21; 23; 24), and their emergence coincides with the development of the definitive buccal mass and lips (Page and Ferguson, 2013).

4.6.4 Phylogenetic significance of neurogenesis in *N. melanotragus*

I did not observe initial gangliogenesis and can only provide the time of development for the second visceral ganglion and the buccal ganglia. However, the remaining ganglia, the eyes and osphradium are all present at hatching. This is consistent with observations of morphogenesis in caenogastropods with planktotrophic larvae, which develop most components of the central nervous system and sensory organs before, or around the time of hatching (Bedford, 1966; D'Asaro, 1966, 1969; Demian and Yousif, 1975; Lin and Leise, 1996; Dickinson *et al.*, 1999; Dickinson and Croll, 2003). On the contrary, the cerebral, and often the pedal ganglia are the only well-developed ganglia present in hatching stage planktotrophic heterobranch veligers (Kriegstein, 1977; Bickell and Chia, 1979; Page, 1992a,b; Dickinson *et al.*, 1999; Ruthstensteiner, 1999; Nagy and Elekes, 2000). The pleural ganglia appear later in the veliger stage and the visceral loop ganglia do not fully form until mid- to late-larval development in members of the Heterobranchia (Kriegstein, 1977, Page, 1992a,b; Ruthsteiner, 1999; Nagy and Elekes, 2000).

Page (1994) suggested that hatching planktotrophic larvae of opisthobranchs (Heterobranchia) are equivalent to pre-hatching stage caenogastropod planktotrophic larvae in terms of the relative development of various anatomical components. More specifically, caenogastropods hatch with many structures of the definitive body plan that do not develop until the latter half of larval development or at metamorphosis in opisthobranchs (Page, 1994). The temporal pattern of gangliogenesis relative to hatching described here for planktotrophic larvae of *N. melanotragus* is similar to that described for caenogastropods, rather than heterobranchs. This adds support to phylogenetic analyses that suggest a closer relationship between the Neritimorpha and Caenogastropoda than between Neritimorpha and Heterobranchia (Bourne, 1908; Yonge, 1947; Harasewych *et al.,* 1998; van den Biggelaar and Haszprunar, 1996; Colgan *et al.,* 2003; Lindberg and Guralnick, 2003; McArthur and Harasewych, 2003; Aktipis *et al.,* 2008; Aktipis and Giribet, 2010; Castro and Colgan, 2010; Kocot *et al.,* 2011).

4.7 Summary

Development of the neuroanatomical shortcut was analyzed to make inferences on the evolutionary origin of this novel connection in the central nervous system of neritimorph gastropods. Histological sections for light, and transmission electron microscopy, as well as surface rendered three-dimensional reconstructions of the central nervous system at three pre-metamorphic larval stages (newly-hatched, 18 dph, 55 dph) and one post-metamorphic juvenile stage (6 dpm), revealed that the neuroanatomical shortcut between the two pleural ganglia is not present until 18 dph. Before this stage, this connective emerges from the left pleural ganglion, runs beneath the esophagus as it extends towards the right side of the body and connects with the subintestinal ganglion, and is thus, by definition, the subintestinal connective. This pattern of ontogeny suggests that the novel connection between the pleural ganglia in neritimorphs is a derived construct of the ancestral subintestinal connective, and did not evolve *de novo*.

I used the timing of development of the shortcut, as well as analysis of the innervation pattern of the pedal muscles and larval retractor muscles, to test the hypothesis that the shortcut functions in coordinating these 4 shell muscles present in *N. melanotragus* larvae. Although the neuroanatomical shortcut between the two pleural ganglia was not present until 18 dph, the subintestinal ganglion is fused to right pleural ganglion at hatching. Furthermore, serial sections for transmission electron microscopy through newly-hatched specimens revealed that the right pedal muscle nerve emerges from the subintestinal ganglion at hatching. These observations reveal that the function of the neuroanatomical shortcut is not to coordinate the pedal muscles, as a direct connection between the two ganglia that innervate the pedal muscles (left pleural and subintestinal ganglia)-and thus coordinate the pedal muscles-is already established via the subintestinal connective at hatching. My discovery that the motor control of the left and right larval retractor muscles originates primarily from nerves associated with the left and right pleural ganglion, respectively, suggests that the fusion between the subintestinal ganglion and right pleural ganglion may serve to coordinate activity of the two larval retractor muscles. Therefore, the subintestinal connective, a pre-established connection that already coordinated the pedal muscles was co-opted to additionally coordinate the

left and right larval retractor muscles through fusion of the subintestinal and right pleural ganglia.

I also explored how the evolution of the neuroanatomical shortcut coincided with the evolution of the unique characteristics of the protoconch and shell-anchored retractor muscles among neritimorph gastropods. The observed ganglionic switch in pedal muscle innervation that occurs in the ontogeny of *N. melanotragus,* suggests that the paired condition of the pedal muscles and larval retractor muscles arose separately and that the paired condition of the pedal muscles arose first. Furthermore, previous research has shown that the presence of paired pedal muscles in adult gastropods is tightly correlated with reduction of the columella. Therefore the paired pedal muscle condition likely arose with the convolutely coiled protoconch that emerged sometime within the Palaezoic-Mesozoic transition (Bandel and Frýda, 1999; Bandel 2007) and the paired condition of the larval retractor muscles likely arose with resorption of the inner-whorls of the convolutely coiled protoconch that first appear in Early Triassic strata (Bandel and Frýda, 1999; Kaim and Sztajner, 2005; Kano, 2006; Bandel, 2008). The larval retractor muscles are innervated primarily by nerves associated with the pleural ganglia and so the neuroanatomical shortcut between these two ganglia likely coincided with the evolution of the paired condition of the larval retractor muscles.

Finally, fossil record data indicating that the extant Neritimorpha (superfamilies Neritopsoidea and Neritoidea) evolved from a coiled ancestor with one pedal muscle, together with the developmental pattern of pedal muscle innervation observed in *N. melanotragus,* suggests that the paired pedal muscles are an apomorphy of extant neritimorphs, and that these muscles are not homologous to the paired plesiomorphic muscles of the Gastropoda. The morphology and development of the left larval retractor muscle in *N. melanotragus* suggests that it is a homologue of the single larval retractor muscle found in all other gastropod larvae, however the right larval retractor muscle seems to be unique to the neritimorphs. Therefore, the unique characteristics of the shell, shell muscles and nervous system in *N. melanotragus* represent a suite of derived characteristics that co-evolved as an integrated functional unit.

5.0 Literature Cited

Aktipis, S.W., Giribet, G. 2010. A phylogeny of Vetigastropoda and other "archaeogastropods": re-organizing old gastropod clades. Invertebrate Biology. **129**: 220-240.

Aktipis, S.W., Giribet, G., Lindberg, D.R., Ponder, W.F. 2008. Gastropod phylogeny: an overview and analysis in W.F. Ponder, and D.R. Lindberg (Eds.), Phylogeny and Evolution of the Mollusca (pp. 201-237). University of California Press, Ltd. Berkeley and Los Angeles, California.

Bandel, K. 1982. Morphologie und bildung der frühontogenetischen gehäuse bei conchiferen mollusken. Facies (Erlagen). **7**: 1-198.

Bandel, K. 2000. The new family Cortinellidae (Gastropoda, Mollusca) connected to a review of the evolutionary history of the subclass Neritimorpha. Neues Jahrbuch für Geologie und Palaontologie, Abhandlungen. **217**: 111-129.

Bandel, K. 2007. Description and classification of late Triassic Neritimorpha (Gastropoda, Mollusca) from the St. Cassian formation, italian alps. Bulletin of Geosciences. **82**: 215-274.

Bandel, K. 2008. Operculum shape and construction of some fossil Neritimorpha (Gastropoda) compared to those of modern species of the subclass. Vita Malacologica. **7**: 19-36.

Bandel, K., Frýda, J. 1999. Notes on the evolution and higher classification of the subclass Neritimorpha (Gastropoda) with the description of some new taxa. Geologica Et Palaeontologica. **33**: 219-235.

Bandel, K. Nüzel, A., Yancey, T.E. 2002. Larval shells and shell microstructures of exceptionally well-preserved late Carboniferous gastropods from the buckhorn asphalt deposit (Oklahoma, USA). Senckenbergiana lethea. **82**: 639-689.

Batten, R.L. 1984. *Neopilina*, *Neomphalus*, and *Neritopsis*, living fossil molluscs. Living Fossils (pp. 218-224). Springer New York. New York, N.Y.

Bedford, L. 1966. The electron microscopy and cytochemistry of oogenesis and the cytochemistry of embryonic development of the prosobranch gastropod *Bembicium nanum* L. Journal of Embryology and Experimental Morphology. **15**: 15-37.

Benjamin, P.R., Kemenes, G., Kemenes, I. 2008. Non-synaptic neuronal mechanisms of

learning and memory in gastropod molluscs. Frontiers in Bioscience. **13**: 4051-4057.

Berthold, T. 1990. Phylogenetic relationships, adaptations and biogeographic origin of the Ampullariidae (Mollusca, Gastropoda) endemic to Lake Malawi, Africa. Abhandlungen des Naturwissenschaftlichen Vereins in Hamburg. **31/32**: 47-84.

Berthold, T. 1991. Vergleichende anatomie, phylogenie und historisches biogeographie der Ampullariidae (Mollusca, Gastropoda). Abhandlungen des Naturwissenschaftlichen Vereins in Hamburg. **29**: 1-256.

Bickell, L.R., Chia, F.S. 1979. Organogenesis and histogenesis in the planktotrophic veliger of *Doridella steinbergae* (Opisthobranchia: Nudibranchia). Marine Biology. **52**: 291-313.

Bonar, D.B., Hadfield, M.G. 1974. Metamorphosis of the marine gastropod *Phestilla sibogae* Bergh (Nudibranchia: Aeolidacea). I. Light and electron microscope analysis of larval and metamorphic stages. Journal of Experimental Marine Biology and Ecology. **16**: 227-255.

Bourne, G.C. 1908**.** Contributions to the morphology of the group Neritacea of aspidobranch gastropods. Part I. The Neritidae. Proceedings of the Zoological Society of London*.* **1908:** 810-887.

Bourne, G.C. 1911. Contributions to the morphology of the group Neritacea of the aspidobranch gastropods. Part II. The Helicinidae. Proceedings of the Zoological Society of London. **1911**: 759-809.

Boutan, L. 1892. Sur le systeme nerveux de la *Nerita polita*. Académies des Sciences. **114**: 1133.

Bouvier, E.L. 1887. System nerveux, morphologie général et classification des gastéropodes prosobranches. Annales Des Sciences Naturelles-Zoologique et Biologie Animale. **3**(7): 1-510.

Brown, D.S., Berthold, T. 1990. *Lanistes neritoides* sp.n. (Gastropoda, Ampullariidae) from west central Africa: description, comparative anatomy and phylogeny. Abhandlungen Des Naturwissenschaftlichen Vereins in Hamburg, NF. **32-32**: 119-152.

Bullock, T.H., Horridge, G.A. 1965. Structure and Function in the Nervous Systems of Invertebrates (pp. 1283-1386). W.H. Feeman and Company. San Francisco, California.

Carroll, D.J., Kempf, S.C. 1994. Changes occur in the central nervous system of the nudibranch *Berghia verrucicornis* (Mollusca: Opisthobranchia) during metamorphosis. Biological Bulletin. **186**: 202-212.

Castro, L.R., Colgan, D.J. 2010. The phylogenetic position of Neritimorpha based on the mitochondrial genome of *Nerita melanotragus*. Molecular Phylogenetics and Evolution. **57**: 918-923.

Chase, R. 2002. Behaviour and its Neural Control in Gastropod Molluscs. Oxford University Press, New York, N.Y.

Cloney, R.A., Florey. E. 1968. Ultrastructure of cephalopod chromatophore organs. Zeitschrift fur Zellforschung und Mikroskopische Anatomie. **89**: 250-280.

Colgan, D.J., Ponder, W.F., Beacham, E., Macaranas, J.M. 2003. Gastropod phylogeny based on six segments from four genes representing coding or non-coding and mitochondrial or nuclear DNA. Molluscan Research. **23**: 123-148.

Collin, R. 2001. The effects of mode of development on phylogeography and population structure of north Atlantic *Crepidula* (Gastropoda: Calyptraeidae). Molecular Ecology. **10**: 2249-2262.

Crofts, D.R. 1937. The development of *Haliotis tuberculata*, with special reference to organogenesis during torsion. Philosophical Transactions of the Royal Society of London B. **228**: 219-268.

Crofts, D.R. 1955. Muscle morphogenesis in primitive gastropods and its relation to torsion. Proceedings of the Zoological Society of London. **125**: 711-750.

Croll, R.P., Voronezhskaya, E.E. 1996. Early elements in gastropod neurogenesis. Developmental Biology. **173**: 344-347.

Croll, R.P., Dickinson, A.J.G. 2004. Form and function of the larval nervous system in molluscs. Invertebrate Reproduction and Development. **46**: 173-187.

D'Asaro. C.N. 1966. The egg capsules, embryogenesis, and early organogenesis of a common oyster predator, *Thais haemastoma floridana* (Gastropoda: Prosobranchia). Bulletin of Marine Science. **16**: 884-914.

D'Asaro, C.N. 1969. The comparative embryogenesis and early organogenesis of *Bursa corrugata* Perry and *Distorsio clathrata* Lamarck (Gastropoda, Prosobranchia). Malacologia. **9**: 349-389.

Darwin, C. 1859. On the Origin of Species by Means of Natural Selection. John Murray., Alberdale Street, London, U.K.

Degnan, B.M., Degnan, S.M., Morse, D.E. 1997. Muscle-specific regulation of tropomyosin gene expression and myofibrillogenesis differs among muscle

systems examined at metamorphosis of the gastropod *Haliotis rufescens*. Developmental Genes and Evolution. **206**: 464-471.

Demian, E.S., Yousif, F. 1973. Embryonic development and organogenesis in the snail *Marisa cornuarietis* (Mesogastropoda: Ampullariidae). I. General outlines of development. Malacologia. **12**: 123-150.

Demian, E.S., Yousif, F. 1975. Embryonic development and organogenesis in the snail *Marisa cornuarietis* (Mesogastropoda: Ampullariidae). V. Development of the nervous system. Malacologia. **15**: 29-42.

Dickinson, A.J.G., Croll, R.P. 2003. Development of the larval nervous system of the gastropod *Ilyanassa obsoleta*. Journal of Comparative Neurology. **466**: 197-218.

Dickinson, A.J.G., Nason, J., Croll, R.P. 1999. Histochemical localization of FMRFamide, serotonin and catecholamines in embryonic *Crepidula fornicata* (Gastropoda, Prosobranchia). Zoomorphology. **119**: 49-62.

Dickinson, A.J.G., Croll, R.P., Voronezhskaya, E.E. 2000. Development of embryonic cells containing serotonin, catecholamines, and FMRFamide-related peptides in *Aplysia californica*. Biological Bulletin. **199**: 305-315.

Evans, C.C.E., Dickinson, A.J.G., Croll, R.P. 2009. Major muscle systems in the larval caenogastropod *Ilyanassa obsoleta*, display different patterns of development. Journal of Morphology. **270**: 1219-1231.

Fiala, J.C. 2005. Reconstruct: a free editor for serial section microscopy. Journal of Microscopy. **218**(pt. 1): 52-61.

Fretter, V. 1965. Functional studies of the anatomy of some neritid prosobranchs. Proceedings of the Zoological Society of London. **147**: 46-74.

Fretter, V. 1969. Aspects of metamorphosis in prosobranch gastropods. Proceedings of the Malacological Society of London. **38**: 375-386.

Fretter, V. 1984. The functional anatomy of the neritacean limpet *Phenacolepas omanensis* Biggs and some comparison with *Septaria*. Journal of Molluscan Studies. **50**: 8-18.

Fretter, V., Graham, A. 1962. British Prosobranch Molluscs: Their Functional Anatomy and Ecology. The Ray Society. London. UK.

Fretter, V., Graham, A. 1994. British Prosobranch Molluscs: Their Functional Anatomy and Ecology (2nd ed). The Ray Society. London. UK.

Frýda, J., Racheboeuf, P.R., Frydova, B., Ferrova, L., Mergl, M., Berkyova, S. 2009. Platyceratid gastropods – stem group of Patellogastropoda, Neritimorpha or

something else? Bulletin of Geosciences. **84**(1): 107-120.

Garstang, W. 1929. The origin and evolution of larval forms. Report of the British Association for the Advancement of Science section d. pp-77-98.

Haller, B. 1884. Untersuchungen uber marine rhipidoglossen. Morphologisches Jahrbüch **9**: 1.

Harasewych, M.G., McArthur, A.G. 2000. A molecular phylogeny of the Patellogastropoda (Mollusca: Gastropoda). Marine Biology. **137**: 183-194.

Harasewych, M.G., Adamkewicz, S.L., Plassmeyer, M., Gillevet, P.M. 1998. Phylogenetic relationships of the lower Caenogastropoda (Mollusca, Gastropoda, Architaenioglossa, Campaniloidea, Cerithioidea) as determined by partial 18S rDNA sequences. Zoologica Scripta. **27**: 361-372.

Haszprunar, G. 1985a. The fine morphology of the osphradium sense organs of the Mollusca. I. Gastropoda, Prosobranchia. Philosophical Transactions of the Royal Society B. **307**: 457-496.

Haszprunar, G. 1985b. The Heterobranchia: a new concept of the phylogeny and evolution of the higher Gastropoda. Zeitschrift fur Zoologische Systematik und Evolutionsforschung. **23**: 15-37.

Haszprunar, G. 1985c. On the innervation of gastropod shell muscles. Journal of Molluscan Studies. **51**: 309-314.

Haszprunar, G. 1987a. Anatomy and affinities of cocculinid limpets (Mollusca, Achaeogastropoda). Zoologica Scritpa. **16**: 305-324.

Haszprunar, G. 1987b. The fine structure of the ctenidal sense organs (bursicles) of Vetigastropoda (Zeugobranchia, Trochoidea) and their functional and phylogenetic significance. Journal of Molluscan Studies. **53**: 46-51.

Haszprunar, G. 1988a. On the origin and evolution of major gastropod groups, with special reference to the Streptoneura (Mollusca). Journal of Molluscan Studies. **54**: 367-441.

Haszprunar, G. 1988b. A preliminary phylogenetic analysis of the streptroneurous gastropods. In W.F. Ponder, (Ed), Prosobranch Phylogeny. Malacological Review, Supplement. **4**: 64-84.

Haszprunar, G. 1993. The Archaeogastropoda a clade, a grade or what else? American Malacolological Bulletin. **10**: 165-177.

Haszprunar, G., Salvini-Plawen, L.V., Reinhard, M.R. 1995. Larval planktotrophy: a primitive trait in the bilateria? Acta Zoologica. **76**: 141-154.

Healy, J.M. 1988. Sperm morphology and its systematic importance in the Gastropoda. In W.F. Ponder (Ed), Prosobranch Phylogeny. Malacological Review Supplement. **4**: 251-266.

Hickman, C.S. 1988. Archaeogastropod evolution, phylogeny and systematics: a re-evaluation. In Ponder, W.F. (Ed.), Prosobranch Phylogeny. Malacological Review Supplement. **4**: 17-34.

Hickmott, P.W., Carew, T.J. 1991. An autoradiographic analysis of neuronal proliferation in juvenile *Aplysia*. Journal of Neurobiology. **22**: 313-326.

Honegger, V.T. 1974. The embryonic development of *Ampullarius* (Gastropoda, Prosobranchia). Zool. Jb. Anat. Bd. **93**: 1-76.

Jacob, M.H. 1984. Neurogenesis in *Aplysia californica* resembles nervous system formation in vertebrates. Journal of Neuroscience. **4**: 1225-1239.

Jhering, H.v. 1877. Vergleichende Anatomie des Nervensystems und Phylogenie der Mollusken. Leipzig, Germany.

Kaim, A., Sztajner, P. 2005. The opercula of neritopsid gastropods and their phylogenetic importance. Journal of Molluscan Studies. **71**: 211-219.

Kandel, E.R. 1976. Cellular basis of behavior: an introduction to behavioral neurobiology. W.H. Freeman and Company, San Fransisco, C.A.

Kandel, E.R., Kriegstein, A., Schacher, S. 1980. Development of the central nervous system of *Aplysia* in terms of the differentiation of its specific identifiable cells. Neuroscience. **5**: 2033-2063.

Kano, Y. 2006. Usefulness of the opercular nucleus for inferring early development in neritimorph gastropods. Journal of Morphology. **267**: 1120-1136.

Kano, Y., Chiba, S., Kase, T. 2002. Major adaptive radiation in neritopsine gastropods estimated from 28S rRNA sequences and fossil records. Proceedings of the Royal Society of London B. **269**: 2457-2465.

Kase, T., Hayami, I. 1992. Unique submarine cave mollusc fauna: composition, origin, and adaptation. Journal of Molluscan Studies. **58**: 446-449.

Knight, J.B. 1933. The gastropods of the St. Louis, Missouri, Pennsylvanian outlier: VI. The Neritidae. Journal of Paleontology. **7**: 359–392.

Knight, J.B., Cox, L.R., Keen, A.M., Batten, R.L., Yochelson, E.L, Robertson, R. 1960. Systematic descriptions. In R.C. Moore (Ed.), Treatise on Invertebrate

Paleontology, part I, Mollusca 1 (pp.I169–I310). Lawrence Geological Society of America and University of Kansas Press.

Kocot, K.M., Cannon, J.T., Todt, C., Ditarella, M.R., Kohn, A.B., Meyer, A., Santos, S.R., Schander, C., Moroz, L.L., Lieb, B., Halanych, K.M. 2011. Phylogenomics reveals deep molluscan relationships. Nature. **477**: 452-456.

Kovac, M.P., Davis, W.J., Matera, E.M., Morielli, A., Croll, R.P. 1985. Learning: neural mechanisms analyzed in the isolated brain of a previously trained mollusc, *Pleurobranchaea californica*. Brain Research. **331**: 275-284.

Kriegstein, A.R. 1977. Stages in the post-hatching development of *Aplysia californica*. Journal of Experimental Zoology. **199**: 275-288.

Kristof, A., Klussmann-Kolb, A. 2010. Neuromuscular development of *Aeolidiella stephanieae* Valdez, 2005 (Mollusca, Gastropoda, Nudibranchia). Frontiers in Zoology. **7**: 5-29.

Lenssen, J. 1899. Systeme digestif et systeme genital de la *Neritina fluviatilis*. La Cellule. 20: 177.

Lin, M., Leise, E.M. 1996. Gangliogenesis in the prosobranch gastropod Il*yanassa obsoleta.* Journal of Comparative Neurology. **374**: 180-193.

Lindberg, D.R. 2008. Patellogastropoda, Neritimorpha, and Cocculinoidea in W.F. Ponder, and D.R. Lindberg (Eds.), Phylogeny and Evolution of the Mollusca (pp. 271-291). University of California Press, Ltd. Berkeley and Los Angeles, California.

Lindberg, D.R., Ponder, W.F. 2001. The influence of classification on the evolutionary interpretation of structure - a re-evaluation of the evolution of the pallial cavity of gastropod molluscs. Organisms Diversity & Evolution. **1**: 273-299.

Lindberg, D.R., Guralnick, R.P. 2003. Phyletic patterns of early development in gastropod molluscs. Evolution and Development. **5**: 494-507.

Lindberg, D.R., Ponder, W.F., Haszprunar, G. 2004. The Mollusca: relationships and patterns from their first half-billion years in J. Cracraft, and M.J. Donoghue (Eds.), Assembling the Tree of Life (pp. 252-278). Oxford University Press. New York, New York.

Lorenzetti, F.D., Mozzachiodi, R., Baxter, D.A., Byrne, J.H. 2006. Classical and operant conditioning differentially modify the intrinsic properties of an identified neuron. Nature Neuroscience. **9**: 17-19.

Marois, R., Carew, T.J. 1990. The gastropod nervous system in metamorphosis. Journal

of Neurobiology. **21**: 1053-1071.

McAllister, L.B., Scheller, R.H., Kandel, E.R., Axel, R. 1983. *In situ* hybridization to study the origin and fate of identified neurons. Science. **222**: 800-808.

McArthur, A.G., Harasewych, M.G. 2003. Molecular systematics of the major lineages of the Gastropoda in C. Lydeard and D.R. Lindberg (Eds.), Molecular Systematics and Phylogeography of Mollusks (pp. 140-160). Smithsonian Books, Washington, D.C., U.S.A.

Moritz, C.E. 1939. Organogenesis in the gastropod *Crepidula adunca* Sowerby. University of California Publications. Zoology. **43**: 217-248.

Müller, G.B., Wagner, G.P. 1991. Novelty in evolution: restructuring the concept. Annual Review of Ecology, Evolution and Systematics. **22**: 229-256.

Nagy, T., Elekes, K. 2000. Embryogenesis of the central nervous system of the pond snail *Lymnea stagnalis* L. an ultrastructural study. Journal of Neurocytology. **29**: 43-60.

Nützel, A., Mapes, R.H. 2001. Larval and juvenile gastropods from a Carboniferous black shale: palaeoecology and implications for the evolution of the Gastropoda. Lethaia. **34**: 143-162.

Nützel, A., Fryda, J., Yancey, T.E., Anderson, J.R. 2007. Larval shells of Late Palaeozoic naticopsid gastropods (Neritopsoidea: Neritimorpha) with a discussion of the early neritimorph evolution. Paläontologische Zeitschrift. **81**: 213-228.

Page, L.R. 1992a. New interpretation of a nudibranch central nervous system based on ultrastructural analysis of neurodevelopment in *Melibe leonina*. I. Cerebral and visceral loop ganglia. Biologial Bulletin. **182**: 348-365.

Page, L.R. 1992b. New interpretation of a nudibranch central nervous system based on ultrastructural analysis of neurodevelopment in *Melibe leonina*. II. Pedal, pleural and labial ganglia. Biological Bulletin. **182**: 366-381.

Page, L.R. 1994. The ancestral gastropod larval form is best approximated by hatching-stage opisthobranch larvae: evidence from comparative developmental studies in W.H. Wilson, S.T. Stricker, and G.I. Shin (Eds.), Reproduction and Development of Marine Invertebrates (pp. 206-223). John Hopkins University Press, Baltimore, Maryland, USA.

Page, L.R. 1995. Similarities in form and developmental sequence for three larval shell muscles in nudibranch gastropods. Acta Zoologica. **76**: 177-191.

Page, L.R. 1997. Larval shell muscles in the abalone *Haliotis kamtschatkana*. Biological Bulletin. **193**: 30-46.

Page, L.R. 1998. Sequential developmental programmes for retractor muscles of a

caenogastropod: reappraisal of evolutionary homologues. Proceedings of the Royal Society of London B. **265**: 2243-3350.

Page, L.R. 2002. Larval and metamorphic development of the foregut and proboscis in the caenogastropod *Marsenina (Lamellaria) stearnsii*. Journal of Morphology. **216**: 202-217.

Page, L.R. 2006. Early differentiating neuron in larval abalone (*Haliotis kamtschatkana*) reveals the relationship between ontogenetic torsion and crossing of the pleurovisceral nerve cords. Evolution and Development. **8**: 458-467.

Page, L.R. 2009. Molluscan larvae: pelagic juveniles or slowly metamorphosing larvae? Biological Bulletin. **216**: 216-225.

Page, L.R., Kempf, S.C. 2009. Larval apical sensory organ in a neritimorph gastropod, an ancient gastropod lineage with feeding larvae. Zoomorphology. **128**: 327-338.

Page, L.R., Ferguson, S.J. 2013. The other gastropod larvae: larval morphogenesis in a marine neritimorph. Journal of Morphology. **274**: 412-428.

Panganiban, G., Irvine, S.M., Lowe, C., Roehl, H., Corley, L.S., Sherbon, B., Grenier, J.K., Fallon, J.F., Kimble, J., Walker, M., Wray, G.A., Swalla, B.J., Martindale, W.Q., Carrol, S.B. 1997. The origin and evolution of animal appendages. Proceedings of the National Academy of Science. **94**: 5162-5166.

Plaut, I., Borut, A., Spira, M.E. 1995. Growth and metamorphosis of *Aplysia oculifera* larvae in laboratory culture. Marine Biology. **122**: 425-430.

Ponder, W.F. 1998. Superorder Neritopsina in P.L. Beesley, G.J.B. Ross and A. Wells (Eds.), Mollusca: The Southern Synthesis. Fauna of Australia, vol. 5 (pp. 693–702). Melbourne, Australia: CSIRO.

Ponder, W.F., Lindberg, D.R. 1997. Towards a phylogeny of gastropod molluscs: an analysis using morphological characters. Zoological Journal of the Linnean Society. **119**: 83-265.

Przeslawski, R. 2011. Notes on the egg capsule and variable embryonic development of *Nerita melanotragus* (Gastropoda: Neritidae). Molluscan Research. **31**: 152-158.

Raven, C.P. 1958. Morphogenesis: The analysis of molluscan development. Pergamon Press, New York.

Richardson, K.C., Jarrett, L., Finke, E.H. 1960. Embedding in resins for ultrathin sectioning in electron microscopy. Stain Technology. **35**: 313-323.

Ruthensteiner, B. 1999. Nervous system development of a primitive pulmonate (Mollusca: Gastropoda) and its bearing on comparative embryology of the gastropod nervous system. Bollettino Malacologico Roma. **34**: 1 -22.

Salvini-Plawen, L.V., Haszprunar. 1987. The Vetigastropoda and the systematics of streptoneurous Gastropoda (Mollusca). Journal of Zoology. **211**: 747-770.

Sasaki, T. 1998. Comparative anatomy and phylogeny of the recent Archaeogastropoda. University of Tokyo Bulletin. **38**: 1-224.

Schacher, S., Kandel, E.R., Woolley, R. 1979. Development of neurons in the abdominal ganglion of *Aplysia californica* I. Axosomatic synaptic contacts. Developmental Biology. **71**: 176-190.

Solem, A. 1983. Lost or kept internal whorls: ordinal differences in land snails. Journal of Molluscan Studies. **12A**: 172-178.

Smith, F.G.W. 1935. The development of *Patella vulgata.* Philosophical Transactions of the Royal Society of London B. **225**: 95-125.

Smith, S.T. 1967. The development of *Retusa obtusa* (Montagu)(Gastropoda, Opisthobranchia). Canadian Journal of Zoology. **45**: 737-764.

Squires, R.L. 1976. Colour pattern of *Naticopsis* (*Naticopsis*) *wortheniana*, buckhorn asphalt deposit, Oklahoma. Journal of Paleontology. **50**: 349-350.

Strathmann, R.R. 1985. Feeding and nonfeeding larval development and life history evolution in marine invertebrates. Annual Review of Ecology and Systematics. **16**: 339-361.

Thiele, J. 1925. Prosobranchia in W. Kükenthal and T. Krumbach (Eds.), Handbuch der Zoologie 5 (pp. 40-90). Walter de Gruyter, Berlin, Germany.

Tompa, A.S., Watabe, N. 1976. Ultrastructural investigations of the mechanism of muscle attachment to the gastropod shell. Journal of Morphology. **149**: 339-352.

van den Biggelaar, J.A.M., Hasprunar, G. 1996. Cleavage patterns and mesentoblast formation in the Gastropoda: an evolutionary perspective. Evolution. **50**: 1520-1540.

Voronezhskaya, E.E., Elekes, K. 2003. Expression of FMRFamide gene encoded peptides by identified neurons in embryos and juveniles of the pulmonate snail *Lymnaea stagnalis*. Cell Tissue Research. **314**: 297-313.

Wanninger, A., Ruthensteiner, B., Lobenwein, S., Salvenmoser, W., Dictus, W.J.A.G.,

Haszprunar, G. 1999a. Development of the musculature in the limpet *Patella* (Mollusca, Patellogastropoda). Developmental Genes & Evolution. **209**: 226-238.

Wanninger, A., Ruthensteiner, B., Dictus, W.J.A.G., Haszprunar, G. 1999b. The development of the musculature in the limpet *Patella* with implications on its role in the process of ontogenetic torsion. Invertebrate Reproduction & Development. **36**: 211-215.

Wenz, W. 1938. Gastropoda, teil 1: allgemeiner teil und Prosobranchia in O.H. Schindewolf (ed.), Handbuch der paläozoologie 6 (pp. 1-204). Gebrüder Bornträger, Berlin, Germany.

Wollesen, T., Wanninger, A., Klussmann-Kolb, A. 2008. Myogenesis in *Aplysia californica* (Cooper, 1863)(Mollusca, Gastropoda, Opisthobranchia) with special focus on muscular remodeling during metamorphosis. Journal of Morphology. **269**: 776-789.

Yonge, C. 1947. The pallial organs in the aspidobranch Gastropoda and their evolution throughout the Mollusca. Philosophical Transactions of the Royal Society B. **232**: 443-518.

Yoo, E.K. 1994. Early Carboniferous Mollusca from the tamworth belt, New South Wales, Australia. Records of the Australian Museum. **46**: 63–120.